

Radiological aspects of sprained ankle syndrome

Elizabeth Sijtske Sijbrandij

Radiological aspects of sprained ankle syndrome

(with a summary in Dutch)

Radiologische aspecten van enkelverzwikking

(met een samenvatting in het Nederlands)

Proefschrift

ter verkrijging van de graad van doctor
aan de Universiteit Utrecht
op gezag van de Rector Magnificus, Prof. dr W.H. Gispen,
ingevolge het besluit van het College voor Promoties
in het openbaar te verdedigen op
dinsdag 29 mei 2001 des namiddags te 2.30 uur

door

Elizabeth Sijske Sijbrandij
geboren 15 april 1960 te Groningen

Promotor : Prof. Dr. P.F.G.M. van Waes
Co-promotor : Dr. A.P.G. van Gils

The production of this thesis was made possible by kind financial support of Isalaklinieken locatie Sophia, Schering.

© No part of this book may be reproduced in any form, by print or any other means without written permission of the author.

Lay-out : E. Tetteroo
Printing : Krips BV Meppel
ISBN : 90-393-2699-1



Aan mijn ouders

Table of Contents

CHAPTER 1

| | |
|---------------------------|---|
| Introduction | 1 |
| 1.1. General aspects | |
| 1.2. Purpose | |
| 1.3. Outline | |

CHAPTER 2

| | |
|--|---|
| Talocrural and subtalar joint | 5 |
| 2.1. Ankle sprain, clinical aspects | |
| 2.2. Developmental anatomy and embryology | |
| 2.3. Functional and clinical anatomy | |
| 2.4. Instability | |
| 2.5. Ligaments and sinus tarsi | |
| 2.6. Osteochondral plate and articular cartilage | |

CHAPTER 3

| | |
|---|----|
| Pathology | 15 |
| 3.1. Classifications of osteochondral lesions | |
| 3.2. Talar dome and tibia plafond | |
| 3.3. Vascularity | |
| 3.4. Bone edema | |

CHAPTER 4

| | |
|---|----|
| Imaging techniques | 23 |
| 4.1. Conventional radiographic findings | |
| 4.2. Ultrasound | |
| 4.3. Bone scintigraphy | |
| 4.4. Computed tomography | |
| 4.5. MR imaging | |

CHAPTER 5

| | |
|--|----|
| Stress radiography and stress examination of the talocrural and subtalar joint on helical computed tomography | 31 |
|--|----|

Foot & Ankle International 1997;18:480-488

| | |
|--|-----|
| _____ CHAPTER 6 _____ | |
| Assessing the subtalar joint: The Brodén view revisited | 45 |
| <i>Foot & Ankle International april 2001</i> | |
| _____ CHAPTER 7 _____ | |
| Posttraumatic subchondral fractures of the talotibial joint: | 57 |
| Occurrence of “kissing” contusions | |
| <i>American Journal of Roentgenology 2000;175:1707-1710</i> | |
| _____ CHAPTER 8 _____ | |
| Osteochondritis dissecans of the talar dome: Evaluation of bone | 67 |
| viability with dynamic gadolinium-enhanced MR imaging in | |
| comparison with dynamic bone scintigraphy | |
| <i>Submitted for publication</i> | |
| _____ CHAPTER 9 _____ | |
| Bone marrow hyperintensities with tarsal coalition: | 79 |
| Magnetic Resonance Imaging findings | |
| <i>Submitted for publication</i> | |
| _____ CHAPTER 10 _____ | |
| Overuse and sports-related injuries of the ankle and hindfoot: | 89 |
| MR imaging findings. | |
| <i>Submitted for publication</i> | |
| _____ CHAPTER 11 _____ | |
| General discussion, recommendations and conclusions | 103 |
| Samenvatting, aanbevelingen en conclusies | 110 |
| Dankwoord | 117 |
| Curriculum vitae | 119 |

List of abbreviations

| | |
|-----------------------|--|
| ATFL | anterior talofibular ligament |
| CFL | calcaneofibular ligament |
| CT | computed tomography |
| FOV | field of view |
| Gd-DTPA | gadolinium-DTPA MRI |
| MP-GRE | magnetization prepared gradient echo |
| MRI | magnetic resonance imaging |
| NA | number of acquisitions |
| OD | osteocondritis dissecans |
| PTFL | posterior talofibular ligament |
| RF | radiofrequency |
| ROI | region of interest |
| SAS | sprained ankle syndrome |
| SE | spin-echo |
| SI | signal intensity |
| STIR | short tau inversion recovery |
| T | tesla |
| TCC | talocalcaneal coalition |
| $^{99m}\text{Tc-hdp}$ | ^{99m}Tc Technetiumhydroxymethylene diphosphonate |
| 3D | three-dimensional |
| 3DFT | three-dimensional Fourier transform |
| TE | echo time |
| TI | inversion time |
| TIC | time intensity curve |
| TSE | turbo spin echo |
| TR | repetition time |
| TT | talar tilt |
| T2 | transverse relaxation time |
| T2* | T2 gradient echo |
| T2W | T2 weighted |
| 2D | two-dimensional |

———— CHAPTER 1 ————

General introduction

Introduction

1.1. General aspects

Lateral ankle sprain is an extremely common injury. With a large percentage of the population involved in sports participation it is not surprising that athletically related injuries to the foot and ankle have been increased. Approximately 40% of the patients suffer from residual symptoms such as pain and a feeling of instability after ankle sprain [1-3]. Despite extensive clinical treatment, the recurrence rate remains high [3]. After spraining, structural damage not only occurs to the ligamentous tissue, but also to the nervous and musculotendinous structures around the ankle complex [3]. Because the clinical syndrome consists of different and variable signs and symptoms, it would be more appropriate to call this condition the 'sprained ankle syndrome' (SAS) [4]. Treatment and rehabilitation goals must address restoration of neuromuscular function as well as mechanical stability of the injured joint [3]. Conventional radiography, tomography, arthrography and stress views have traditionally been used to image the ankle and hindfoot. The value of conventional radiography is limited to fractures, malalignment and degenerative ankle diseases. Inversion stress radiography for evaluating instability in the talocrural joint is commonly used. These techniques can suggest a specific diagnosis, but repeating damage and overuse injuries are hard to detect.

With the introduction of computed tomography (CT), providing cross-sectional images and therefore precise bony anatomic details, new opportunities for the examination of ankle and hindfoot have been given. The use of multiplanar reconstruction has become easier with the introduction of the helical CT [5].

In the subtalar joint the complex anatomy with multi-faceted surfaces makes evaluation with plain radiography and stress views difficult. Three-dimensional reconstruction of helical CT scan is particularly helpful in defining and clarifying anatomic arrangements and articular tilting.

Magnetic resonance (MR) imaging has allowed more subtle detection and precise characterization of soft tissue details than conventional imaging modalities. Common complications of inversion injuries such as ligamentous rupture, bone bruise and fractures, impingement syndromes and coalitions are easily diagnosed and with this non-invasive technique identification of the vascular status of bone tissue is possible [6,7].

1.2. Purpose of the thesis

The purpose of this thesis is to evaluate some imaging features of sprained ankles, found on these new modalities, and to assess the additional diagnostic understanding and treatment planning of helical CT as well as MR imaging compared with conventional radiographic imaging in patients with ankle and hindfoot problems. In addition recommendations for prudent / optimal use of both new modalities are proposed.

This thesis addresses several problems related to sprained ankle syndrome.

The objectives of this thesis are:

1. Review and evaluation of the use of the Brodén view in subtalar joint instability.
2. Study of MR images after ankle sprains, focused on osteochondral lesions in talar dome and tibia plafond.
3. To report some MR imaging characteristics in detecting talocalcaneal coalitions.
4. To investigate the accuracy of dynamic gadolinium-enhanced MR imaging in determining the viability of osteochondral lesions in the talar dome after inversion injury.
5. To give an overview of some common sports-related injuries.

1.3. Outline of the thesis

Introductory chapters 1-4

Chapter 1 represents this introduction.

Chapter 2 a review is given of clinical symptomatology, developmental embryology and anatomy, instability, ligaments, osteochondral plate and articular cartilage.

Chapter 3 describes the classification systems of osteochondral lesions with conventional radiography, helical CT and MR imaging. Osteochondral lesions in relation with the talar dome and tibia plafond. The complex vascularisation of the talar dome is described and the nutrition of the articular cartilage. Etiology of bone edema in relation with (repetitive) trauma is reported.

Chapter 4 discusses the imaging techniques used after ankle spraining. Conventional radiography, tomography, stress radiology, ultrasound, bone scintigraphy and arthrography. The imaging protocols of helical CT and MR imaging in specific ankle and hindfoot problems are evaluated.

Scientific studies performed in chapter 5-11

- Chapter 5** reports a study of stress radiography and stress examination of the talocrural and subtalar joint on helical CT in 15 patients with unilateral instability. With stress radiography a variable amount of subtalar tilt was demonstrated in all feet.
- Chapter 6** evaluates the use of the Brodén view in subtalar joint instability. Helical CT didn't show tilting in the subtalar joint, except in the subluxated posteromedial part.
- Chapter 7** includes the results of posttraumatic osteochondral fractures of the talotibial joint in the relation with the tibia plafond. The high occurrence of "kissing" contusions is described.
- Chapter 8** viability of osteochondral fragments is an important parameter for healing. In this study dynamic gadolinium-enhanced MR imaging is compared with dynamic bone scintigraphy in OD lesions of the talar dome for evaluating the viability of the OD fragment.
- Chapter 9** concerns the MR imaging findings around the subtalar joint in 10 patients with talocalcaneal coalitions. A typical pattern of bone marrow hyperintensities in T2-weighted and STIR images is described.
- Chapter 10** discusses some common traumatic and overuse syndromes of the foot and ankle seen with MR imaging.
- Chapter 11** contains a general discussion on helical CT as well as MR imaging in patients with ankle and hindfoot problems. Conclusion of the thesis and general directions for proper use of both techniques are given.

References

1. Bosien WR, Staples OS, Russel SW. Residual disability following acute ankle sprains. *J Bone Joint Surg* 1955;37(A):1237-1243.
2. Zwipp H, Hoffman F, Thermann H, Wippermann BW. Rupture of the ankle ligaments. *Int Orthop* 1991;15:245-249.
3. Hertel J. Functional instability following lateral ankle sprain. *Sports Med* 2000;29:361-371.
4. Fallat L. Sprained ankle syndrome: prevalence and analysis of 639 acute injuries. *J Foot Ankle Surgery* 1998;37:280-285.
5. Pathria MN, Issacs P. Magnetic resonance imaging of bone marrow. *Curr Opin Radiol* 1992;4:21-31.
6. Cerezal L, Abascal F, Canga A, Bustamanre M, del Pinal F. Usefulness of Gadolinium-enhanced MR imaging in the evaluation of the vascularity of scaphoid nonunions. *AJR* 2000;174:141-149.
7. Munk PL, Lee MJ, Logan M, Connell DG, et al. Scaphoid bone waist fractures, acute and chronic: imaging with different techniques. *AJR* 1997;168:779-786.

———— CHAPTER 2 ————

Talocrural and subtalar joint

2.1. Ankle sprain, clinical aspects

Ankle sprain is a common injury [1]. Many simple ankle sprains resolve with conservative treatment while others linger on with persistent pain, weakness, "giving way sensation" and symptoms of functional instability [2]. Most patients could relate the onset of the symptoms to an acute or recurrent sprain of the ankle and persistent symptoms will exist after the injury such as stiffness, swelling and pain aggravated by weightbearing or activity [3].

Despite adequate treatment, approximately 40% of the patients suffer from residual symptoms after sustaining this injury [4]. Often there are more factors to the sprained ankle than only injury to the lateral collateral ligaments [5]. After a sprain, structural damage not only occurs to the ligamentous tissue, but also to the musculotendinous, nervous and vascular structures around the ankle complex. They manifest clinically as impaired balance, reduced joint position sense, musculotendinous disbalance, slowed nerve conduction velocity, strength deficits and decreased dorsiflexion.

Additionally the formation of scar tissue after injury may lead to sinus tarsi syndrome or impingement syndromes [1]. Assessment of patients with ankle sprain must address not only joint laxity and swelling but should include examination for neuromuscular deficits as well. The treatment and rehabilitation goals must be directed to restoration of mechanical stability to the injured joint, as well as restoration of neuromuscular function [1].

2.2. Developmental anatomy and embryology

The development of ankle and hindfoot originates from a solitary block of tissue at the age of 7 weeks and begins to separate into its components by 10 weeks [6]. The adult-like shapes of the tarsal bones develop before the formation of the actual joint clefts [7]. Tarsal coalitions are assumed to be congenital in origin. It is believed that the coalition results from a failure of differentiation and segmentation of primitive mesenchyme, with resultant lack of joint formation [8,9]. During the embryonic stage, the fibula undergoes rapid growth and brings the foot in marked adducto-equinovarus position. During the fetal stage, tibial growth corrects this position. Ossification of the ankle bones occurs in sequence, beginning with the talus, followed by the fibula and ending with the tibia. The talus ossifies in 3 to 8 months of intrauterine life. The horizontal portion of the distal epiphysis of the tibia appears between 6 and 10 months of age. The distal fibular epiphysis ossifies between 11 to 18 months. The talus shows a torsion of the neck from fetal to adult life, creating a long axis of the foot, and rotation of the forepart (Fig. 1 and 2) [9]. During development the ankle joint is subjected to stresses that may have a profound influence on its formation and function [6]. These stresses may be abnormal in situations in which

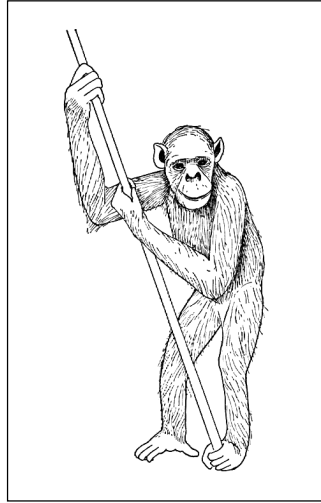


Figure 1. An ape supporting itself in an erect position. Its left foot is in grasping position. Its right foot, supporting part of its weight, shows the wide abduction of the hallux. Adapted from ref [9].

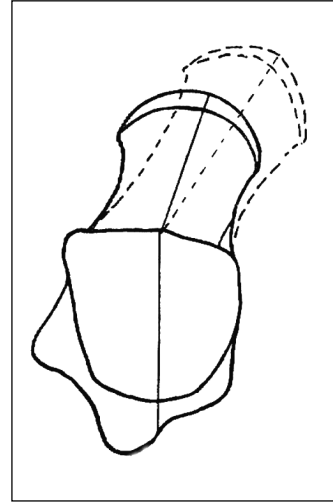


Figure 2. Diagram to show the alteration in the neck of the talus from fetal to adult life. The broken outline is of the longer and more angulated neck of the fetus. Adapted from ref [9].

there are alterations in mobility, due to intrinsic or extrinsic factors. Tarsal coalition is an intrinsic condition with an abnormal fusion of two or more independent bones of the hindfoot. Due to the rigidity of the “abnormal fused joints” the gliding motion of the joint is hampered, causing abnormal stress on the articular surfaces and the subchondral bone of the joint adjacent to the fusion. Immobility of the hindfoot can cause compensatory excessive mobility in the ankle joint [6]. Extrinsic factors causing restricted motion of the limb are hydramnion and casting for a long time.

2.3. Functional and clinical anatomy; a few characteristics of the ankle and hindfoot

The ankle joint is formed by three bones: the tibia, fibula and talus. The foot has been divided traditionally into the hindfoot (talus and calcaneus), midfoot and forefoot (Fig. 3). The ankle or talocrural joint consists of the mortise (tibia and fibula) and the trochlea tali (Fig. 4). High congruity between the articular surfaces, together with the close relationship created by the ligamentous complexes gives the talocrural joint a high degree of stability (Fig. 4) [10]. The subtalar joint is formed by talus and calcaneus and is divided in two

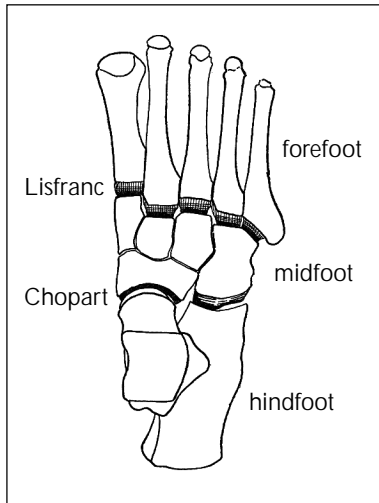


Figure 3. Hindfoot and midfoot divided by Chopart articulation. Midfoot and forefoot divided by Lisfranc articulation. Adapted from ref [9].

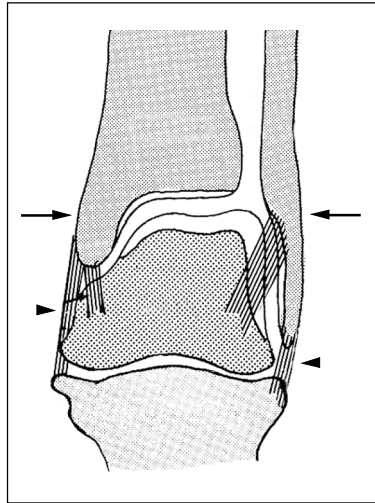


Figure 4. Coronal view of left ankle mortise (arrows). The ankle joint receives its strongest support from the collateral ligaments (arrowheads). Adapted from ref [36].

synovial lined independent joints: the anterior and posterior subtalar articulations (Fig. 5). These are separated by the sinus tarsi and the tarsal canal. The posterior talocalcaneal articulation is formed by the posterior facet of the inferior surface of the talus and the corresponding posterior facet of the calcaneus. These facets are convex-concave, thus increasing the stability of the joint. The anterior subtalar articulation is formed by anterior part of the talus, the posterior surface of the navicular, and the anterior portion of the calcaneus. The very complex multifaceted surfaces of these joints make evaluation clinically and radiologically difficult.

Movements of the ankle and hindfoot

Sideways tilting of the ankle joint is prevented by the cone shaped talar trochlea which is wider anterior than posterior (Fig. 6A), and a concave shaped distal tibial (Fig. 6B) [11]. The talus neither has tendinous attachments nor muscular origins and relies for its stability on a system of opposed articulating surfaces together with strong ligamentous attachments. Movements of the talus in relation to the leg and foot are exceedingly complex and never consist solely of one-plane movements. Plantarflexion and dorsiflexion are the main

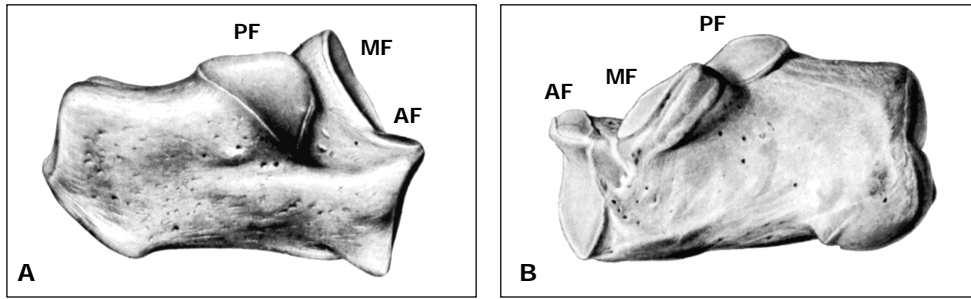


Figure 5.

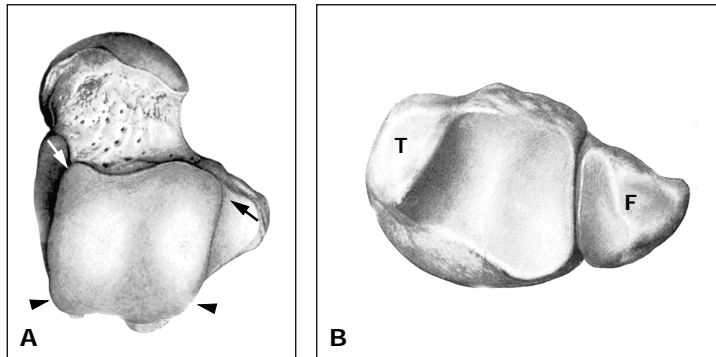
Right calcaneus. The talus and calcaneus are joined by three facets: posterior facet (PF), middle facet (MF) and anterior facet (AF). Adapted from ref [38].

A, Lateral view of calcaneus. **B**, Medial view of calcaneus.

Figure 6. Left ankle mortise and talus relationship.

A, Superior view of the talus. Viewed from above the talus is wedge shaped being wider anteriorly (arrows) than posteriorly (arrowheads).

B, Ankle mortise from below: lateral (fibular, F) and medial (tibial, T) malleoli that form the ankle mortise.



functions of the ankle joint. However, in internal rotation of the leg the talocrural joint is one of the major regions in which motion takes place [11,12]. Movements in the subtalar joint, are mainly inversion and eversion, occurring by moving of the ovoid surfaces of the talus over the ovoid surfaces of the calcaneus [13].

2.4. Instability

The etiology of chronic functional ankle instability is fairly well understood [14]. Pathophysiological factors such as mechanical instability, proprioceptive deficit and peroneal muscle weakness have been demonstrated [14]. The major source of instability is thought to be located at the talocrural level [14]. Often a tear or sprain of the anterior talofibular ligament (ATFL) alone can lead to widening of the mortise, greatly reducing articular stability of the ankle [15].

The role of the subtalar joint in instability of ankle and hindfoot is less well understood. Both the articular surface and bony configuration of the talus and calcaneus and the stabilizing role of the ligamentous anatomy are believed to play an important role in subtalar stability. Subtalar instability must be considered after a sprain, if other causes have been excluded [16,17].

Acute injury to the subtalar joint rarely warrants invasive intervention. Chronic instability symptoms can require surgical stabilization [18].

2.5. Ligaments and sinus tarsi

Each of the ligaments has a role in stabilizing the ankle and subtalar joint, depending on the position of the foot and ankle. There are three main ligamentous structures in the ankle:

- the **medial collateral ligament complex** (deltoideus), rarely involved in ankle sprains,
- the **distal tibiofibular syndesmotic complex**, and
- the **lateral ligamentous complex**, most frequently involved in ankle sprains.

The lateral ligamentous complex consist of three ligaments: the anterior talofibular ligament (ATFL), the calcaneofibular ligament (CFL) and the posterior talofibular ligament (PTFL) (Fig. 7).

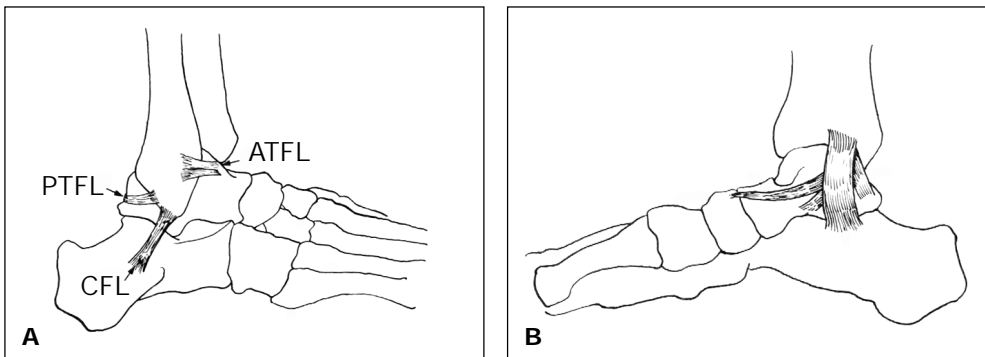


Figure 7.

The collateral ligaments of the ankle joint.

A, The lateral collateral ligaments support the lateral aspect of the ankle. Lateral view: ATFL: anterior talofibular ligament, CFL: calcaneofibular ligament and PTFL: posterior talofibular ligament.

B, The medial aspect of the ankle is supported by the deltoid ligament, composed of four bands. Adapted from ref [36].

The ATFL is a thickening in the anterolateral joint capsule and limits internal rotation and inversion of the talus [19,20]. This ligament plays a crucial role in external rotation of the talus, which results into inversion of the foot [21].

The CFL primarily inhibits inversion of the calcaneus [19]. When torn, it is often associated with ATFL tears in more severe injuries [22].

The PTFL is the strongest ligament of the lateral ligament complex and rarely injured. The PTFL primarily inhibits external rotation and dorsiflexion [19].

The clinical diagnosis of rupture of these ligaments has been based on instability of the joint. Inversion and anterior stress radiography of the ankle have been commonly used to show instability of the joint due to rupture of these lateral ligaments [23]. Values for a normal range of talar tilt and anterior displacement of the talus in relation to the tibia have been difficult to determine [24].

Sinus tarsi

The tarsal canal and sinus tarsi form the space between talus and calcaneus. It contains the ligamentous complex of the sinus tarsi, composed of the interosseous talocalcaneal ligament and the cervical ligament. The main function of these ligaments is stabilization of the hindfoot. The inferior extensor retinaculum is composed of three groups of very lax fibers only indirectly contributing to talocalcaneal stability [25,26]. The subtalar ligaments may be injured during inversion. The major complaints of such patients are a feeling of instability and weakness [20]. Acute ankle sprain is associated with acute abnormalities of the sinus tarsi in 43% of the patients and correlates with the extent of lateral ligament tears [27].

2.6. Osteochondral plate and articular cartilage

The articular surfaces of the bones are covered with hyaline cartilage. Articular cartilage is a highly ordered structure. Four distinct layers have been described within it: the superficial, the transitional, the deep zones, and the calcified zone.

The deep and calcified zone are divided by a line called the *tidemark* (Fig. 8) [28]. In traumatic separation of cartilage and bone the separation takes place at the junction between the calcified and noncalcified cartilage [29]. Hyaline cartilage deforms under pressure but recovers its original shape when pressure is removed, when damaged it has virtually no intrinsic repair capacity [28].

Acute injuries can produce damage to the cartilage (pure chondral component), damage to the subchondral bone with preservation of the overlying cartilage, or a combined damage: cartilage together with underlying subchondral bone forming an osteochondral fragment [29].

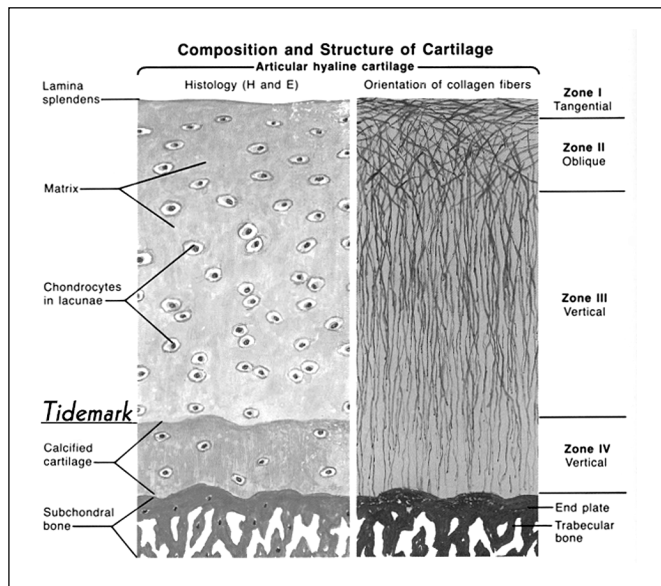


Figure 8. Composition and structure of articular cartilage. Four zones can be recognized, with differences in cell size and matrix. Adapted from ref [37].

The dome of the talus is part of the weightbearing bone. Direct weightbearing forces through the ankle are transmitted to the subchondral plate which is supported by the trabecular meshwork in the metaphysis and epiphysis [30]. When impactational forces occur during injury, a bone contusion or bone bruise can arise. This bone bruise is formed by trabecular microfractures associated with hemorrhage, edema and hyperemia [31]. MR imaging findings in ankle injury do not depend on direct visualization of this fractured trabeculae (either at the time of injury or during repair), but depend on imaging the marrow and its behaviour in response to acute injury. In osteochondral fractures, rotational high energy forces, extending to the underlying bone are responsible for the classic osteochondral fracture (see classification of osteochondral talar injury, chapter three). Comminution of the articular surface may occur with variable degrees of surface depression [28].

An intact subchondral plate is of critical importance in avoiding posttraumatic sequelae. Without the smooth support of the intact subchondral bone, the articular cartilage can break down, leading to degenerative joint disease [30]. Current treatment of osteochondritis dissecans (OD) lesions is aimed at preservation of the integrity of the joint. If MR imaging identifies a bony injury, there are clinical implications: injuries to bone require reduced weightbearing during an extended period for proper healing [32]. Cancellous bone is the

weightbearing structure that suffers most in acute traumatic injuries of the ankle [32]. A period of non-weightbearing may be sufficient to induce healing [32,33]. When there is no healing response, a surgical option is percutaneous drilling of the subchondral bone in an attempt to facilitate revascularization of the compromised subchondral tissues. Therefore MR investigation is recommended to all patients after ankle sprain if a painful condition is maintained after conservative treatment [34,35].

References

1. Hertel J. Functional instability following lateral ankle sprain. *Sports Med* 2000;29:361-371.
2. Freeman M. Instability of the foot after injuries to the lateral ligament of the ankle. *J Bone Joint Surg* 1965;47(B):669-667.
3. Zwipp H, Hoffman F, Thermann H, Wippermann BW. Rupture of the ankle ligaments. *Int Orthop* 1991;15:245-249.
4. Louwerens JWK. Chronic lateral instability of the foot. Thesis, University of Rotterdam, Rotterdam, The Netherlands. 1996.
5. Fallat L. Sprained ankle syndrome: prevalence and analysis of 639 acute injuries. *J Foot Ankle Surg* 1998;37:280-285.
6. Schon LC, Ouzounian TJ. The ankle. In: Jahss MH, ed. *Disorders of the foot and ankle*. 2nd ed. Philadelphia: WB Saunders, 1991:1417-1460.
7. Pistoia F, Ozonoff MB, Wintz P. Ball-and-socket ankle joint. *Skelet Radiol* 1987;16:447-451.
8. Herzenberg JE, Goldner JL, Martinez S, Silverman P. Computerized tomography of talocalcaneal tarsal coalition: a clinical and anatomic study. *Foot Ankle Int* 1986;6:273-288.
9. Wood Jones F. *Structure and function as seen in the foot*. London: Bailliere, Tindall and Cox, 1949.
10. Erickson SJ, Quinn SF, Kneeland JB, et al. MR imaging of the tarsal tunnel and related spaces. Normal and abnormal findings with anatomic correlations. *AJR* 1990;155:323-328.
11. Goldie I, Lundberg A, Svensson OK. Biomechanics of the ankle joint. In: Jahss MH, ed. *Disorders of the foot and ankle*. 2nd ed. Philadelphia, WB Saunders, 1991:520-531.
12. Bonnin JG. The hypermobile ankle. *Proc R Soc Med* 1944;37:282-286.
13. Siegler S, Chen J, Schneck CD. The three-dimensional kinematics and flexibility characteristics of the human ankle and subtalar joints Part I: Kinematics. *J Biomech Eng* 1988;110:364-373.
14. Karlsson J, Eriksson BI, Renström PA. Subtalar Ankle Instability. *Sports Med* 1997;24:337-346.
15. Passariello R, Mastantuono M. Instability of the tibiotalar joint. In: Masciocchi, ed. *Radiological imaging of sports injuries*. Berlin: Springer-Verlag, 1998:141-149.
16. Brantigan JW, Pedegana LR, Lippert FG. Instability of the subtalar joint: diagnosis by stress tomography in three cases. *J Bone Joint Surg* 1977;59(A):321-324.
17. Clanton TO. Athletic injuries to the soft tissues of the foot and ankle. In: Coughlin MJ, Mann RA, eds. *Surgery of the foot and ankle*. 7th ed. St Louis: Mosby, 1999:1090-1209.
18. Rasmussen O. Stability of the ankle joint: analysis of the function and traumatology of the ankle ligaments. *Acta Orthop Scand Suppl* 1985;211:1-75.
19. Mink JH. Ligaments of the ankle. In: Deutsch AL, Mink JH, Kerr R, eds. *MRI of the foot and ankle*. 1st ed. Philadelphia: Lippincott-Raven, 1992:173-197.
21. Huson A. Functional anatomy of the foot. In: Jahss MH, ed. *Disorders of the foot and ankle*. 2nd ed. Philadelphia: W.B. Saunders, 1991:409-432.

22. Prins JG. Diagnosis and treatment of injury to the lateral ligament of the ankle. *Acta Chir Scand* 1978;486.
23. Grace DL. Lateral ankle ligament injuries. *Clin Orthop* 1984;183:153-159.
24. Rubin G, Witten M. The talar tilt angle and the fibular collateral ligaments. *J Bone Joint Surg* 1960;42(A):311-326.
25. Beltran J. Sinus tarsi syndrome. *Magn Reson Imaging Clin North Am* 1994;2:59-65.
26. Klein M, Spreitzer AM. MR imaging of the tarsal sinus and canal: normal anatomy, pathologic findings, and features of the sinus tarsi syndrome. *Radiology* 1993;186:233-240.
27. Breitenseher MJ, Trattnig S, Kukla C, et al. MRI versus lateral stress radiography in acute lateral ankle ligament injuries. *J Comput Assist Tomogr* 1997;21(2):280-285.
28. Bohndorf K. Imaging of acute injuries of the articular surfaces (chondral, osteochondral and subchondral fractures). *Skeletal Radiol* 1999;28:545-560.
29. Deutsch AL. Osteochondral injuries of the talar dome In: Deutsch AL, Mink JH, Kerr R, eds. *MRI of the foot and ankle*. 1st ed. Philadelphia: Lippincott-Raven,1992:111-134.
30. Blum GM, Tirman PFJ, Crues III JV. Osseous and cartilaginous trauma. In: Mink JH, Reicher MA, Crues III JV, Deutsch A, eds. *MRI of the knee*. 2nd ed. New York: Raven Press,1993:295-332.
31. Kaplan PA, Craig WW, Kilcoyne RF, et al. Occult fracture patterns of the knee associated with anterior cruciate ligament tears: assessment with MR imaging. *Radiology* 1992;183:835-838.
32. Newberg AH, Wetzner SM. Bone bruises: their patterns and significance. *Semin Ultrasound CT MR* 1994;15:396-409.
33. Canale ST, Belding RH. Osteochondral lesions of the talus. *J Bone Joint Surg* 1980;62(A):97-102.
34. Dann K, Wahler G, Neubauer N, et al. Concomitant injuries after upper ankle joint dislocations. *Sportverletz Sportschaden* 1996;10:67-69.
35. McDermott EP. Basketball injuries of the foot and ankle. *Clin Sports Med* 1993;165:775-780.
36. Cailliet R. Structural anatomy. In: Challiet R, ed. *Foot and ankle pain*. Philadelphia: FA Davis company,1968:1-28.
37. Netter FH. Physiology. In: Netter FH, ed. *The Ciba collection of medical illustrations. Musculoskeletal system*. 2nd ed. New Jersey: Ciba-Geigy corporation,1991:168.
38. Sobotta J, Becher H. *Atlas of human anatomy*. Ferner H, Staubesand J, eds. Munchen: Urban & Schwarzenberg,1975.

———— CHAPTER 3 ————

Pathology

3.1. Classifications of osteochondral lesions

The most widely accepted radiological classification of osteochondral talar injury, introduced by Berndt and Harty (Fig. 1) [1] in 1959 and based on research on the position of the fractured bone fragment in cadavers, is as follows:

Stage 1 - localized area of subchondral trabecular compression

Stage 2 - incomplete separation of transchondral fragment

Stage 3 - fragment is completely separated but not displaced

Stage 4 - fragment is displaced or inverted in its fracture bed.

The first two stages are difficult to visualize by conventional radiography and the lesions may go undetected when only radiographs are obtained for evaluation. Standard radiographs are generally reliable in diagnosing late stage 3 and 4 lesions.

MR imaging has been shown to demonstrate this osteochondral lesions with high sensitivity, allowing early detection (stages 1 and 2) and treatment of the abnormalities [2]. Using MR imaging, hemorrhage and edema are visualized as ill-defined semi-circular areas of abnormal signal intensity in the subcortical bone. Especially short tau inversion recovery (STIR) images appeared to be helpful.

The classification system of Berndt and Harty modified by Loomer, is based on computed tomography, and adds a radiolucent defect staged as type V (77% of the cases) [3]. The radiolucent defect seen on CT scan is fibrous at surgery. It originated as an undisplaced

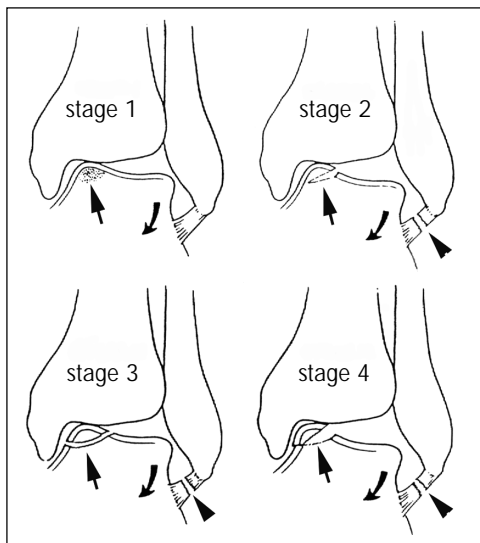


Figure 1.

Berndt and Harty classification of osteochondral talar injury after inversion injury (curved arrows) [1].

Stage 1 localized area of subchondral trabecular compression (arrow).

Stage 2 incomplete separation of transchondral fragment (arrow) with lateral ligament rupture (arrowhead).

Stage 3 fragment is completely separated but not displaced (arrow) with lateral ligament rupture (arrowhead).

Stage 4 fragment is displaced or inverted in its fracture bed (arrow) with lateral ligament rupture (arrowhead). Adapted from ref [16].

bony fragment or compression fracture that has become avascular secondary to the trauma and disruption of its intra-osseous blood supply. It is unable to revascularize because of the repeated microtrauma of walking. The bone is resorbed and the defect fills in with fibrous tissue that ossifies very slowly. The surrounding trabeculae thicken in response to increased stress, forming a thick shell of sclerotic bone (Fig. 2) [3].

Another classification system based on MR imaging and arthroscopy was proposed by Nelson [4].

Stage 0 - normal situation

Stage 1 - signal changes consistent with articular cartilage injury

Stage 2 - shows a high signal breach of articular cartilage with a stable subchondral fragment

Stage 3 - a partial chondral attachment is associated with a thin high signal rim behind the osteochondral fragment, probably representing synovial fluid around the fragment

Stage 4 - represents a loose body within the center of the osteochondral bed or free in the joint space.

Osteochondral injuries of the talus are relatively common articular lesions and more frequent in men than in women. Bone bruises together with ligamental damage are not unusual after ankle sprains, and with recurrent trauma can lead to more severe osteochondral pathology which in turn may result in progressive disability [5]. Although the exact cause of OD is unknown, it is thought that in mild cases microfractures, hemorrhage and edema occur. When these subside, the disease may be reversible. However, in more severe instances the subchondral fractures together with the vascular insufficiency can eventually lead to necrosis of the bone fragment [3,6]. Currently, in order to examine the status of the subchondral bone, diagnostic arthroscopy is performed, whereby the articular cartilage is inspected and, when intact, the stability of the underlying subchondral layer containing the OD lesion is determined by palpating the overlying cartilage [7]. Motion of the cartilage is associated with lack of underlying subchondral osseous support [7,8].

Healing of the OD depends on the viability of the injured bone. Lesions with viable bone are likely to heal spontaneously with conservative treatment, whereas necrotic bone may collapse, leading to destruction of the joint [3].

Current treatment of OD is aimed at the prevention of a necrotic section in order to maintain the integrity of the joint. Such treatment includes percutaneous drilling of the

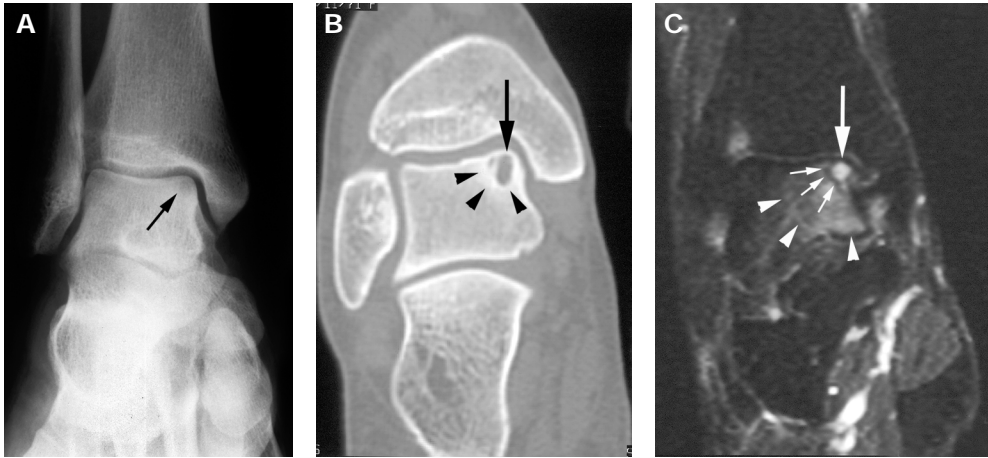


Figure 2.

Type V (classification of Loomer) radiolucent defect in medial talar dome.

A, AP radiograph with radiolucent defect in medial talar dome (arrow).

B, Coronal CT of clearly defined radiolucent defect (arrow) with sharp margins surrounded by sclerotic bone (arrowheads).

C, Coronal STIR T2-weighted MR image obtained at the same level as B demonstrates the defect (arrow), sclerotic rim (small arrows) and surrounding edema (arrowheads).

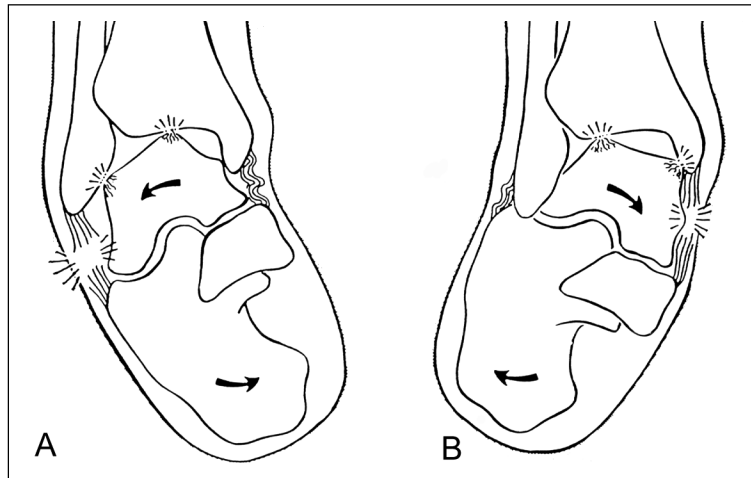
subchondral bone in an attempt to facilitate revascularization of the compromised subchondral tissues, reduction and fixation with drilling or excision of the unstable fragment [7].

When the cartilage is unstable and gives way, it suggests the presence of a loose fragment which in turn would be indicative of necrosis of the bone fragment [6]. However, since arthroscopic palpation is relatively unspecific in diagnosing necrosis of the underlying bone, and there is currently no other diagnostic test to determine the vascular status in OD, drilling is usually done empirically, even when there is no evidence of necrosis [7].

3.2. Talar dome and tibia plafond

It has been noted that in an above-average number of patients with traumatic osteochondral lesions of the talar dome, similar lesions can be seen on the opposite side of the joint, the tibia plafond (Fig. 3). In the literature there is a strong relation between ankle sprains and talar dome lesions [1,3-5]. However, tibia plafond lesions which are part of the trauma mechanism are hardly mentioned. A few reports notice osteochondral lesions in the talus with associated lesions in the tibia plafond in relation to lateral ligamentous damage [9,10].

Figure 3.
Trauma mechanism.
A, Inversion of the ankle (curved arrows).
B, Eversion of the ankle (curved arrows).
Adapted from ref [17].



3.3. Vascularity

Blood supply to the ankle joint provides insight into the etiology of ankle pathology. Talar blood supply is the most complex of the three osseous components of the ankle joint [11]. Since cartilage takes up 60% of the surface of the entire talus and 73% of the surface area of the body of the talus, blood supply to the talus is limited, as there are only a few areas where arteries can enter the bone. The surrounding capsular and ligamentous attachments play a vital role in providing a conduit for vessels entering the talus [11]. Primary blood supply to the talus comes in the first place from the dorsalis pedis and posterior tibial artery and secondary from branches of the peroneal and small periosteal vessels. A branch of the posterior tibial artery enters the bone under the deltoid ligament and supplies the medial surface of the talus, the artery of the tarsal canal is the most important blood supply to the body of the talus (Fig. 4). The talar dome is fed by small end-arteries, extending from the artery of the tarsal canal [6]. Because there are no collaterals, the vascular supply to the dome is vulnerable, and can easily be compromised. Orientation of osteochondral lesion to these arterioles determines the likelihood of complications in healing and increases the incidence of delayed or non-union and avascular necrosis [12]. Articular cartilage receives much of its nutrients from synovial fluid, a feature that excludes this area from ischemic processes [12].

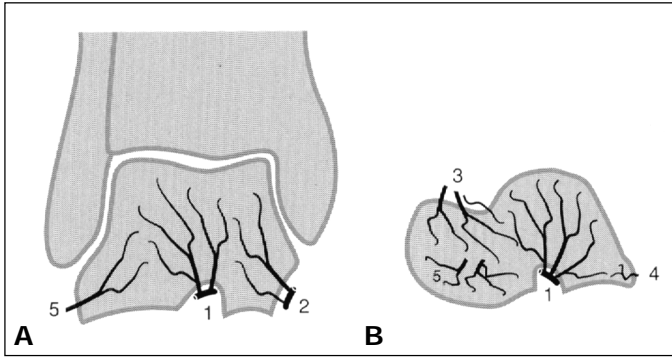


Figure 4.

Blood supply of the talus.

A, Coronal plane.

B, Sagittal plane.

1. artery of the tarsal canal.

2. deltoid branch. 3. dorsalis

pedis artery branches. 4.

posterior tubercle branches.

5. tarsal sinus branches.

Adapted from ref [18].

3.4. Bone edema

Stress response and stress fractures.

Micro-damage related to daily activity is necessary for physiological bone remodeling. Altered biomechanics in the foot or ankle can result in bone marrow edema [13]. Runners have an increased prevalence of marrow edema in the foot and ankle compared with non-runners [14]. Stress response occurs when abnormal repetitive forces on the bone cause an imbalance of bone resorption over bone formation [14]. This in turn leads to focal trabecular microfractures associated with edema and hemorrhage. Under repetitive stress, focal trabecular microfractures can progress into a linear stress fracture with periosteal or endosteal response. At the onset, radiographs are normal, but after 2 to 3 weeks a cortical lucency representing the fracture may be seen [14].

In tarsal coalition, where abnormal fusion of two or more independent bones of the hindfoot occurred, edema around the coalition is often seen. Due to the rigidity of abnormally fused joints the gliding motion of the joint is hampered, causing abnormal stress on articular surfaces and subchondral bone of the joint adjacent to the fusion.

Considering the foot and ankle, runners are by far the most affected group with tibial and tarsal stress fractures [14]. Calcaneal stress fractures, caused by jumping, are commonly seen in military recruits and basketball players.

MR imaging is far more sensitive than radiography in detecting stress response in bone at an early stage [15].

When stress response progresses into a fracture, a band-like area of low-signal intensity in the intramedullary space is seen, extending to the cortex (see chapter 10 Fig. 3B, 4). The fracture is usually surrounded by edema and hemorrhage [15].

References

1. Berndt AL, Harty M. Transchondral contusion (osteochondritis dissecans) of the talus. *J Bone and Joint Surg* 1959;41(A):988-1020.
2. Anderson IA, Crichton MB, Grattan-Smith T, Cooper RA, Brazier D. Osteochondral fractures of the dome of the talus. *J Bone Joint Surg* 1989;71(A):1143-1152.
3. Loomer R, Fisher C, Lloyd-Smith R, Sisler J, Cooney T. Osteochondral lesions of the talus. *Am J Sports Medicine* 1993;21:13-19.
4. Nelson DW, DiPoala J, Colville M, et al. Osteochondritis dissecans of the talus and knee: prospective comparison of MR and arthroscopic classifications. *J Comput Assist Tomogr* 1990;14:804-808.
5. Schweitzer ME. Magnetic resonance imaging of the foot and ankle. *Magn Reson Q* 1993;9:214-234.
6. Schenck RC, Goodnight JM. Current concepts review osteochondritis dissecans. *J Bone Joint Surg* 1996;78(A):439-456.
7. Kumai T, Takakura Y, Higashiyama I, Tamai S. Arthroscopic drilling for the treatment of osteochondral lesions of the talus. *J Bone Joint Surg* 1999;81(A):1229-1235.
8. Pappas AM. Osteochondritis dissecans. *Clin Orthop* 1981;158:59-69.
9. Nishimura G, Yamato M, Togawa M. Trabecular trauma of the talus and medial malleolus concurrent with lateral collateral ligamentous injuries of the ankle: evaluation with MR imaging. *Skeletal Radiol* 1996;25:49-54.
10. Labovitz JM, Schweitzer ME. Occult osseous injuries after ankle sprains: incidence, location, pattern, and age. *Foot Ankle Int* 1998;19:661-667.
11. Schon LC, Ouzounian TJ. The ankle. In: Jahss MH, ed. *Disorders of the foot and ankle*. 2nd ed. Philadelphia: WB Saunders, 1991:1417-1460.
12. Berquist TH, Williams HJ, Oldenburg WA. Bone and soft tissue ischemia. In: Berquist TH, ed. *Radiology of the foot and ankle*, 2nd ed. Philadelphia: Lippincott Williams & Wilkins, 2000:405-445.
13. Lazzarini KM, Troiano RN, Smith RC. Can running cause the appearance of marrow edema on MR images of the foot and ankle. *Radiology* 1997;202:540-542.
14. Rasmussen O. Stability of the ankle joint: analysis of the function and traumatology of the ankle ligaments. *Acta Orthop Scand* 1985;211:1-75.
15. Kier R, Mc Carthy S, Dietz M, et al. MR appearance of painful conditions of the ankle. *Radiographics* 1991;11:401-414.
16. Staufner RN. Intra-articular ankle problems. In: McCollister Everts C, ed. *Surgery of the musculoskeletal system*. 2nd. ed. New York: Churchill Livingstone, 1990:3861-3867.
17. Smith GR, Winqvist RA, Allan NK, Northrop CH, et al. Subtle transchondral fractures of the talar dome: a radiological perspective. *Radiology* 1977;124:667-673.
18. Mulfinger GL, Trueta JC. The blood supply of the talus. *J Bone Joint Surg* 1970;52(B):150-167.

———— CHAPTER 4 ————

Imaging techniques

4.1. Conventional radiographic findings

Conventional radiography, tomography, arthrography and stress views have traditionally been used for imaging the ankle and hindfoot. Although these techniques have been used for years, especially for the subtalar joint, they lack anatomic detail. Several supplemental radiographic techniques were developed and new procedures were introduced to improve diagnostic accuracy.

Routine conventional radiography remains the primary diagnostic method to study the twisted ankle, (when a fracture is clinically suspect) and should include lateral and internal oblique views [1,2]. However, some fractures (occult), occurring most frequently in the talus and calcaneus, are not seen on routine plain radiographs [3].

Stress radiography of the ankle joint may be useful for evaluating ligamentous injury after inversion trauma of the ankle. Stress radiographs most often utilized are AP projection, applying varus stress and lateral projection applying vertical stress (drawer sign). Radiological examination of the contralateral ankle joint is useful to differentiate between posttraumatic or congenital relaxation. Normal range of talar tilt varies, ranging from 0-15° [4,5]. In case of instability the range has been reported between 1-24°. So, there is substantial overlap between the normal and pathologic tilt [6].

The subtalar joint has a very complex, multi-faceted surface which makes evaluation with plain radiography and conventional tomography difficult [7].

Subtalar stress views are used to assess the presence of subtalar instability during inversion of the hindfoot [8]. Oblique radiograph (Brodén view) is performed with the x-ray beam rotated 30° in lateromedial and 40° in caudocranial direction, with the subtalar joint inverted by a dedicated stress device [9]. Instability of the subtalar joint is believed to be present when stress radiographs demonstrate loss of parallelity of the posterior articular surfaces of the subtalar joint [4,9,10]. However, there is no general consensus regarding the best method for evaluating subtalar instability [9].

Ankle arthrography is the most commonly performed arthrogram in the foot and ankle. It allows assessment for articular anatomy, loose bodies, ligamentous integrity and capsular abnormalities. Ankle arthrography has been used in diagnosing acute ligamentous injury [11]. Tears of the anterior talofibular ligaments can be detected by leakage of contrast material out of the ankle joint into the spaces around the tibial malleolus [11]. However, arthrography has many limitations in diagnosing ankle ligament injuries [11]. Indications for arthrography became more limited with the developing role of MR imaging [12].

4.2. Ultrasound

Ultrasound is the main alternative to MR imaging in the evaluation of soft-tissue abnormalities. Its main advantage includes wide availability, low cost, direct correlation of sonographic findings with the site of symptoms, dynamic evaluation and feasibility in examining anxious and noncooperative patients [13]. Specific soft-tissue pathology such as ganglia, ligamentous injury and joint effusion are easily detected (Fig. 1) [14]. The main disadvantages of ultrasound are its operator dependence, failure to image bone abnormalities consistently and limited acceptance by referring clinicians as a basis for making surgical decisions [13].

4.3. Bone scintigraphy

Prior to the introduction of MR imaging and CT, nuclear-medicine bone scintigraphy was the next step after conventional radiography in the investigation of foot and ankle pain of unknown cause [15]. By bone scanning anatomic and physiologic information can be obtained. ^{99m}Tc methylene diphosphonate (^{99m}Tc -HDP) is a commonly used bone-scanning agent. The primary option for focal areas of interest is three-phase bone

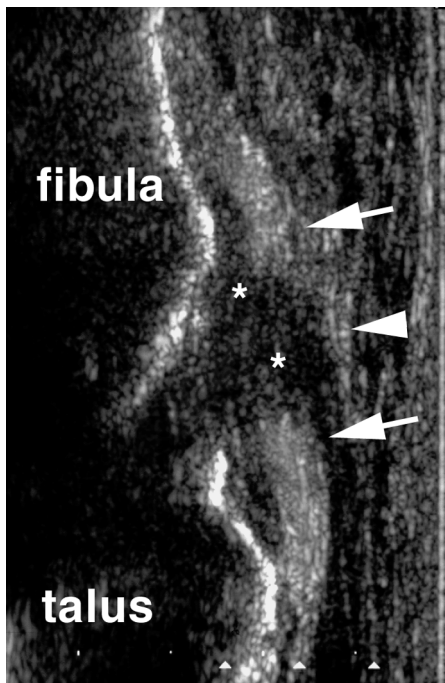


Figure 1.

Complete anterior talofibular ligament (ATFL) tear. Longitudinal ultrasound of the lateral ankle joint with a hypo-echoic gap in the tendon fibers (arrows) consistent with a complete rupture of the anterior talofibular ligament. Effusion (*) distends the joint capsule (arrowhead). Adapted from E. Meijerman.

scanning, with this technique, early vascular phase, blood pool image and delayed images can be obtained (Fig. 2) [15]. However, the spatial resolution of bone scintigraphy is low and cannot distinguish bone bruises from osteochondral fractures [1].

4.4. Computed tomography

With the introduction of CT, the investigation of joints of ankle and hindfoot has been given new opportunities for the investigation of bony anatomic details. The advent of helical CT has markedly increased speed of modern CT systems and has found use in a variety of musculoskeletal applications. In imaging the foot and ankle it is of critical importance that those planes are chosen that are based on an erect anatomic position [16].

Generally, in foot and ankle, 5-mm thick or thinner sections are required. When osseous details are important or reconstructions are planned, very thin contiguous sections (i.e., 1.5-mm thick) or overlapping thin sections (i.e., 3-mm thick, obtained at 2-mm intervals) are useful. Helical CT has made it easier to use multiplanar reconstructions, reduce artifacts and perform dynamic contrast studies [16]. It is regarded as superior to MR imaging in the way it shows (high) contrast between calcific structures and soft tissue. However CT has its limitations for evaluation of soft tissue and bone marrow abnormalities.

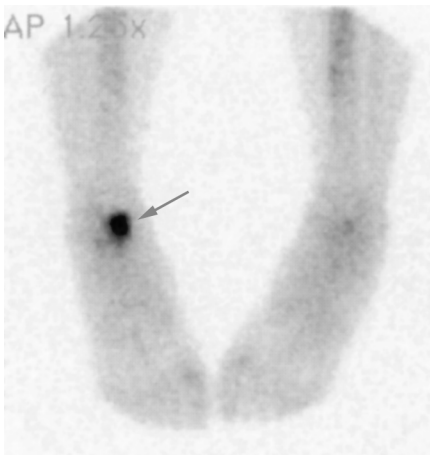


Figure 2.

Early vascular phase of three-phase bone scintigraphy. Increased activity in medial OD lesion of right talar dome (arrow). Left foot is normal.

4.5. MR imaging

The introduction of MR imaging has had a major impact on musculoskeletal imaging. Subtle detection and more precise characterization of soft tissue and bony details coupled with multiplanar imaging capability are ideally suited to evaluate the complex anatomy of foot and ankle [17]. High quality images may be obtained with the use of intermediate or high field strength magnets (0.5-1.5 Tesla). High field strength magnets are currently preferred because of their higher signal-to-noise ratio [18]. With the patient in supine position, the ankle to be examined is placed in neutral position, although partial plantar flexion may be useful when comparing MR images to a CT made in 45° of tibiotalar angulation. With a dedicated extremity surface coil (quadrature or phased-array design), using a 12 to 14 cm field of view (FOV) and a 512 x 256 or 256 x 256 acquisition matrix, thin (3 mm or less) coronal T1 and STIR images are most useful. By placing both legs within the circular extremity coil, comparison of the pathological side with the contralateral ankle and foot can be achieved. Alternatively, when smaller FOVs are needed, extremities can be imaged one at a time by repositioning the surface coil. Kinematic techniques with the ankle in inversion and eversion in the coronal plane, in plantar flexion and dorsiflexion in the sagittal plane, and in internal or external rotation in the coronal or axial plane may also be used. However, these techniques are not routinely employed, and kinematic motion is not physiologic. Restricted range of motion, ligamentous instabilities, and tendon subluxations may necessitate the use of kinematic protocols.

The selection of specific sequences depends on the suspected pathological condition. Most ankle and foot MR imaging studies can be performed using a limited number of pulse sequences, such as two-dimensional multisection spin-echo (SE) techniques. Routine T1-weighted axial, sagittal, and coronal images are obtained with a short repetition time (TR) of 500 to 600 ms and a short echo time (TE) of 15 to 20 ms. Thin (3 mm) sections, either contiguous interleaved or with a 0.5 mm interslice gap, are preferred. With this technique, excellent depiction of the normal or abnormal anatomical structures of the tendons, ligaments, cortical bone, and bone marrow is obtained. T2-weighted (long TR, long TE SE pulse sequences) axial images are obtained with conventional T2-weighted or fat-suppressed T2-weighted fast spin-echo sequences which can detect pathological conditions such as edema, soft-tissue tumors, ligamentous injuries and bone marrow abnormalities [19]. T1- and T2-weighted sequences can be performed at one excitation. T1-weighted images may be supplemented with coronal and sagittal images obtained using either fast STIR or fat-suppressed T2-weighted fast spin-echo sequences.

Gradient-echo pulse sequences with two-dimensional (2D) or three-dimensional (3D) acquisitions can be used to obtain images with contrast in T2*-weighted images in a

relatively brief acquisition time. Effective T2*-weighted contrast can be generated with gradient-echo techniques, using a partial flip angle of less than 90° (20° to 30°). Two-dimensional Fourier-transform multiplanar gradient-echo protocols use a TR of 400 to 600 ms, a TE of 15 to 20 ms, and a flip angle of 20° to 30°. Axial three-dimensional Fourier-transform (3DFT) T2* volume images with 1 to 2 mm slice thickness may also be used to evaluate medial or lateral ligamentous structures. Short T1 inversion recovery (STIR and fast spin-echo STIR) images provide superior contrast in evaluating osteochondral lesions, bone contusions, and tendinitis.

Intravenous administration of a paramagnetic contrast agent, used in association with fat-suppression sequences, has demonstrated usefulness in the evaluation of inflammatory synovial processes, and certain tendon pathologies (partial tear, healing, and infiltrative disorders). Intravenous and intra-articular contrast agents (MR arthrography) has been used on a limited basis in the study of osteochondral lesions and other intra-articular pathology. Articular cartilage is evaluated using a variety of techniques, including fat-suppressed T2-weighted fast spin-echo, fast spin-echo STIR, and MR arthrography. Fat-suppressed T2-weighted fast spin-echo [17]. The introduction of fast MR techniques has allowed better evaluation of the blood flow to the tissues. With gadolinium-enhanced subtraction MR imaging the viability of bone can be depicted. Lack of arterial enhancement of the bone marrow correlated with lack of blood perfusion and thus to ischemia [18,19]. Pre-injection images, followed by a series of images per minute using a TR/TE/of 40/10 and a 90° flip angle (see chapter eight) [20].

References

1. Bonedorf K. Imaging of acute injuries of the articular surfaces (chondral, osteochondral and subchondral fractures). *Skeletal Radiol* 1999;28:545-560.
2. Bencardino J, Rosenberg ZS, Delfaut E. MR imaging in sports injuries of the foot and ankle. *MRI Clin North Am* 1999;7:131-149.
3. Berger PE, Ofstein RA, Jackson DW, et al. MRI demonstration of radiographically occult fractures: what have been missing? *Radiographics* 1989;9:407-436.
4. Clanton TO. Instability of the subtalar joint. *Orthop Clin North Am* 1989;20:583-592.
5. Rubin G, Witten M. The talar-tilt angle and the fibular collateral ligaments. *J Bone Joint Surg* 1960;42(A):311-326.
6. Ahuovuo J, Kaartinen E, Slätis P. Stress radiography in lesions of the lateral ligaments of the ankle. *Acta Radiol* 1988;29:711-714.
7. Heilman AE, Braley WG, Bishop JO. An anatomic study of subtalar instability. *Foot Ankle* 1990;10:224-228.
8. Sijbrandij ES, van Gils APG, Hellemondts van FJ, Louwerens JWK, de Lange EE. Assessing the subtalar joint: the Brodén view revisited. *Foot Ankle Int* 2001;in press.

9. Brodén B. Roentgen examination of the subtalar joint in fractures of the calcaneus. *Acta Radiol* 1949;31:85-91.
10. Laurin CA, Oellet R, St-Jacques R. Talar and subtalar tilt: an experimental investigation. *Can J Surg* 1968;11:270-279.
11. Mesgarzadeh M, Schneck CD, Tehranzadeh J, et al. Magnetic resonance imaging of the ankle ligaments: emphasis on anatomy and injuries to lateral collateral ligaments MRI *Clin North Am* 1994;2:39-58.
12. Traughber PD. Imaging of the foot and ankle. In: Coughlin MJ, Mann RA, eds. *Surgery of the foot and ankle*. 7th ed. St Louis: Mosby, 1999:51-114.
13. Hodler J, Yu JS, Steinert HC, Resnick D. MR imaging versus alternative imaging techniques. *MRI Clin North Am* 1995;4:591-608.
14. Fessell DP, Holsbeeck van MT. Foot and ankle sonography. *Radiol Clin North Am* 1999;37:831-858.
15. Traughber PD, Manaster BJ, Murphy K, et al. Negative bone scans of joints after aspiration or arthrography: experimental studies. *AJR* 1986;146:87-91.
16. Bearcroft PW. The use of spiral computed tomography in musculoskeletal radiology of the lower limb: the calcaneus as an example. *Eur J Radiol* 1998;28:30-38.
17. Beltran J, Rosenberg ZS. Ankle and foot. In: Stark DD, Bradley Jr WG, eds. *Magnetic resonance imaging*. 3 ed. St. Louis: Mosby, 1999:873-929.
18. Cerezal L, Abascal F, Canga A, Bustamanre M, Pinal del F. Usefulness of Gadolinium-enhanced MR imaging in the evaluation of the vascularity of scaphoid nonunions. *AJR* 2000;174:141-149.
19. Munk PL, Lee MJ, Logan M, et al. Scaphoid bone waist fractures, acute and chronic: imaging with different techniques. *AJR* 1997;168:779-786.
20. Byers GE, Berquist TH. MR imaging techniques for soft-tissue lesions. *MRI Clin North Am* 1995;3:563-575.

CHAPTER 5

Stress radiography and stress examination of the talocrural and subtalar joint on helical Computed Tomography

Frank J. van Hellemond¹, Jan-Willem K. Louwerens¹,
Elizabeth S. Sijbrandij², Ad P.G. van Gils²

From the Departments of Orthopaedic Surgery¹ and Radiology²
University Hospital Utrecht and Central Military Hospital Utrecht.

Abstract

The main objective of this study was to compare subtalar inversion stress views using the Brodén view with inversion stress views on helical computed tomography (CT). One of the drawbacks of routine radiography is the imaging of three-dimensional structures in a two-dimensional plane. We investigated whether the use of helical CT would lead to a more objective and clearer measurable method to determine the amount of tilt in the subtalar joint. A group of 15 patients with unilateral chronic instability complaints and clinically suspected subtalar instability was examined. The contralateral asymptomatic foot was used as control.

A variable amount of subtalar tilt (range, 4° to 18°) was demonstrated in all cases on stress radiographs, without finding significant difference between the symptomatic and asymptomatic feet. However, contrary to the findings at the talocrural level, subtalar tilt was found in none of the patients using helical CT. Thus, we now doubt that the tilt seen during stress examination using the Brodén view is the true amount of tilt. It may be that the lateral opening, seen on these radiographs, largely results from imaging two planes that has made a translatory and rotatory movement relative to each other in an oblique direction. It is concluded that the Brodén stress examination might not be useful for screening patients with subtalar instability.

Associated anomalies, not visible on the radiographs, were detected by helical CT. In four cases, narrowing of the articular cartilage and irregular and hypertrophic bone formation at the middle facet joint of the subtalar joints were found. It is likely that these changes cause disturbance of function of this joint and it is suggested that the subjective complaint of instability with "giving way" is not only caused by hypermobility, but can be caused by other disturbances of normal motion.

Introduction

Chronic lateral instability of the ankle/foot may be present in as many as 10% to 30% of people who have sustained an injury of the lateral ligament complex [6,8,21]. It is a clinical condition with frequent inversion injuries/sprains, "giving way" sensations, difficulties in walking on uneven ground, and sometimes pain and swelling. Multiple factors are involved. Abnormal or increased motion in the talocrural joint caused by lateral ligamentous damage is believed to be one of these factors [3,14,28]. Damage to the anterior talofibular ligament results in increased motion in the sagittal plane [25,31]. This ligament, with its more horizontal orientation, plays an important part in transmission of motion between the leg and the foot [12,24]. After this ligament is severed, tibiotalar delay will increase markedly [5,12]. The term "anterolateral/internal rotatory instability" has been used to describe the resulting clinical symptoms [1,7,25]. More severe trauma of the lateral ligament complex may cause injury to both: the anterior talofibular and calcaneofibular ligaments. Damage to both of these ligaments results in an increase of varus tilting of the talus within the ankle mortise [25,27]. The calcaneofibular ligament is rarely injured alone, but with or without a combined lesion of the anterior fibular ligament, rupture of this ligament is reported to result in an increase of motion in the subtalar joint [2,10,16,18,20,26,30,32,33,35]. Increase in talocalcaneal movement is found when a lesion of the calcaneofibular ligament is combined with a lesion of the interosseous talocalcaneal ligament [13]. Laxity or elongation of this interosseous ligament has been reported to be a cause of subtalar joint instability [15,34]. Subtalar instability must be considered as a cause of symptoms in chronic lateral instability, particularly if other causes of instability have been excluded [4].

In a previous study, we found that an increase in talar tilt (in the talocrural joint) between two steps of inversion was present in symptomatic feet only [22]. It was suggested that the increase in tilt between these steps might serve to distinguish between normal and pathologically increased tilt. However, because increased tilt was found only once in the subtalar joint, no conclusions could be drawn regarding the use of this method in diagnosing mechanical instability of the subtalar joint. We also concluded that no consensus existed as to the best method and the criteria to be used for evaluation of abnormal motion in the subtalar joint.

In the present study, a further effort is made to objectify a possible subtalar component in a group of 15 patients with unilateral chronic instability complaints. An identical standardized radiographic assessment of talar and simultaneous subtalar tilt was made, using a 40° Brodén view. This time, the same stress examination was also applied using CT imaging.

Patients and methods

Patients

Fifteen patients (12 men and 3 women) with chronic unilateral foot instability were consecutively recruited from the orthopaedic outpatient departments of the Central Military Hospital and the University Hospital of Utrecht. All patients complained of frequent unilateral inversion injuries and instability (with giving way sensations) of the foot. Typically, sprains already occurred when they walked on an uneven surface. Sometimes, a short period of pain and swelling followed such a sprain, but otherwise the patients were without pain. At physical examination, an increase in inversion tilt seemed to be present, and there was strong suspicion of the presence of subtalar instability on the symptomatic side. The asymptomatic feet of these patients served as a control group. The number, age, height, and weight of the subjects are shown in Table 1.

Methods

A detailed description of the standardized radiographic assessment of talar and simultaneous subtalar tilt and of the measurements used in the present study has been given previously [22]. The hinge device to stress the joints in the present study was identical to the one previously described, except that all metal was replaced by other materials to make the apparatus suitable for helical CT or Magnetic Resonance Imaging (MR imaging) (Fig. 1) [22]. The consequence of the use of this apparatus is that inversion stress is applied to the foot as a whole, not to one specific joint of the tarsus, and that it allows the joints to move in a normal fashion. A specific subtalar view (Brodén view) was used under fluoroscopic control, using a Philips (Shelton, CT) Angiodiagnostics 96 apparatus.

Radiographs were made of the feet in neutral position (step 0), after inversion with moderate force until the point of fair restraint (step 1) and after inverting as far as possible to the point of pain or until no further closure of the device was possible (step 2). This

Table 1. Age, height, and weight of the patient group (12 M, 3 F).

| | mean \pm SD ^a | range |
|-------------|----------------------------|-----------|
| Age (yr) | 25 \pm 5.3 | 18 - 36 |
| Height (cm) | 181 \pm 7.0 | 166 - 192 |
| Weight (kg) | 82 \pm 9.7 | 64 - 99 |

^aS.D., Standard deviation.



Figure 1.
The hinge device used in this study.

position was held for 1 minute, to ensure full muscle relaxation, before the third radiograph was made.

The amount of talar tilt (TT) found after step 1 was defined as TT1 and after step 2 as TT2. The corresponding subtalar tilt angles were defined as STT1 and STT2, respectively. The difference/increase in tilt found between (S)TT1 and (S)TT2 was calculated for each foot and defined as TTd and STTd. TTd and STTd were used as parameters for comparison between symptomatic and asymptomatic feet.

In the stress device, CT of the inverted hindfeet was performed with a high resolution technique on a helical CT scanner (Tomoscan SR 7000; Philips Medical Systems, Best, the Netherlands). Stress was gradually increased to compensate for the effect of ligamentotaxis, and the hinge device was closed to the same number of degrees as previously found after step 2. This position was held during a period of 4 minutes, the time required to perform CT scanning. Contiguous axial slices (thickness, 3 mm) from 2 cm above the talocrural joint to the calcaneocuboid joint were obtained. After acquiring the raw data, separate coronal reconstructions were made of the hindfoot using a bone algorithm. Measurements were made analogous to those on the Brodén view.

Statistics

The data were analyzed using SPSS/PC+, version 6.0. *P* values of 0.05 or less were considered significant. TTd and STTd values of the symptomatic feet were compared with those of the asymptomatic feet using a one-tailed sign test. The same test was used to compare the results obtained with CT imaging.

Results

Results for TT, STT, TTd, STTd, TTct and STTct are summarized in Table 2.

Brodén Stress Examination

Talocrural: An increase in TT was found in seven of the symptomatic feet (range, 2° to 7°) but also in three of the asymptomatic feet. In one case, increased TT was found only in the asymptomatic foot, and in two patients an increase was found in both feet. In 7 of the 15 patients, no increase in TT was seen between step 1 and step 2, either in the symptomatic or in the asymptomatic foot. Regarding the increase in TT (TTd), the difference between symptomatic and asymptomatic feet was found to be statistically significant ($P = 0.04$).

Subtalar: An increase in subtalar tilt was found in the symptomatic feet of three patients and in both feet of one patient. Differences between the symptomatic and asymptomatic feet were not significant.

CT Stress Examination

Talocrural: Tilting of the talus within the ankle mortise was found in the symptomatic feet of five patients (range, 5° to 12°). A TT of 10° was also found in the asymptomatic foot of one of these patients. The difference in TT (TTct) between the symptomatic and asymptomatic feet was statistically significant ($P = 0.03$). The five feet with TT during CT stress examination also demonstrated an increase in TT during the Brodén stress examination. In two symptomatic feet, no TT was found during CT examination, whereas these feet did demonstrate an increase in TT during the Brodén stress examination.

Subtalar: Tilting within the subtalar joint was never found using CT stress examination.

Other Findings

Four patients showed changes in the middle facet of the subtalar joints (Fig. 2). Loss of cartilage space and irregular and hypertrophic bone formation is seen, suggesting the existence of a fibrous coalition. One patient had a large posterior calcaneal cyst in the symptomatic foot. No other disorders or signs of osteochondral lesions were found.

Table 2. Results for TT1 and TT2, TTd, STT1 and STT2, STTd, TTct, and STTct.

| Case | S/A | TT1 | TT2 | TTd | STT1 | STT2 | STTd | TTct | STTct |
|-------|-----|-------|-------|------|-------|-------|------|-------|-------|
| 1 | S | 3 | 3 | 0 | 14 | 14 | 0 | 0 | 0 |
| | A | 1 | 8 | 7 | 12 | 12 | 0 | 0 | 0 |
| 2 | S | 10 | 10 | 0 | 8 | 8 | 0 | 0 | 0 |
| | A | 7 | 7 | 0 | 7 | 7 | 0 | 0 | 0 |
| 3 | S | 10 | 12 | 2 | 8 | 10 | 2 | 6 | 0 |
| | A | 9 | 9 | 0 | 7 | 7 | 0 | 0 | 0 |
| 4 | S | 0 | 0 | 0 | 8 | 8 | 0 | 0 | 0 |
| | A | 1 | 1 | 0 | 6 | 6 | 0 | 0 | 0 |
| 5 | S | 0 | 0 | 0 | 8 | 8 | 0 | 0 | 0 |
| | A | 0 | 0 | 0 | 10 | 10 | 0 | 0 | 0 |
| 6 | S | 10 | 14 | 4 | 8 | 10 | 2 | 0 | 0 |
| | A | 8 | 8 | 0 | 10 | 10 | 0 | 0 | 0 |
| 7 | S | 8 | 12 | 4 | 10 | 10 | 0 | 5 | 0 |
| | A | 4 | 6 | 2 | 6 | 6 | 0 | 0 | 0 |
| 8 | S | 5 | 5 | 0 | 5 | 5 | 0 | 0 | 0 |
| | A | 5 | 5 | 0 | 5 | 5 | 0 | 0 | 0 |
| 9 | S | 4 | 4 | 0 | 7 | 10 | 3 | 0 | 0 |
| | A | 9 | 9 | 0 | 5 | 5 | 0 | 0 | 0 |
| 10 | S | 4 | 8 | 4 | 12 | 12 | 0 | 9 | 0 |
| | A | 3 | 3 | 0 | 12 | 12 | 0 | 0 | 0 |
| 11 | S | 1 | 18 | 7 | 16 | 18 | 2 | 9 | 0 |
| | A | 10 | 16 | 6 | 7 | 10 | 3 | 0 | 0 |
| 12 | S | 7 | 7 | 0 | 10 | 10 | 0 | 0 | 0 |
| | A | 7 | 7 | 0 | 6 | 6 | 0 | 0 | 0 |
| 13 | S | 9 | 12 | 3 | 8 | 8 | 0 | 12 | 0 |
| | A | 11 | 11 | 0 | 4 | 4 | 0 | 10 | 0 |
| 14 | S | 1 | 1 | 0 | 10 | 10 | 0 | 0 | 0 |
| | A | 1 | 1 | 0 | 8 | 8 | 0 | 0 | 0 |
| 15 | S | 8 | 10 | 2 | 6 | 6 | 0 | 0 | 0 |
| | A | 3 | 3 | 0 | 7 | 7 | 0 | 0 | 0 |
| Mean | | 5.63 | 7.07 | 1.43 | 8.33 | 8.73 | 0.40 | 1.700 | |
| S.D. | | 3.72 | 4.93 | 2.22 | 2.81 | 3.03 | 0.93 | 3.620 | |
| Range | | 11.00 | 18.00 | 7.00 | 12.00 | 14.00 | 3.00 | 12.00 | 0 |
| Min. | | 0 | 0 | 0 | 4 | 4 | 0 | 0 | 0 |
| Max. | | 11 | 18 | 7 | 16 | 18 | 3 | 12 | 0 |

S, symptomatic; A, asymptomatic; S.D., standard deviation; Min., minimum; Max., maximum; TT1, talar tilt found after step 1; TT2, talar tilt found after step 2; STT1, subtalar tilt found after step 1; STT2, subtalar tilt found after step 2; TTd, difference in talar tilt; STTd, difference in subtalar tilt; TTct, difference in talar tilt as measured using computed tomography; STTct, difference in subtalar tilt as measured using computed tomography.

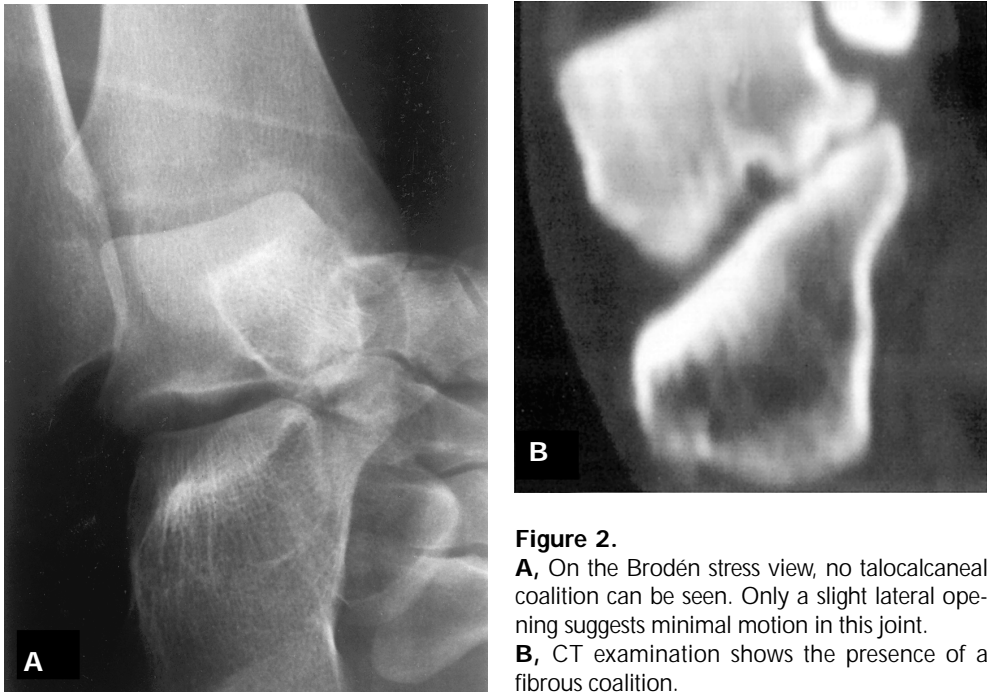


Figure 2.
A, On the Brodén stress view, no talocalcaneal coalition can be seen. Only a slight lateral opening suggests minimal motion in this joint.
B, CT examination shows the presence of a fibrous coalition.

Discussion

Talocrural Joint

The association between chronic lateral instability of the foot and mechanical instability (increased mobility as a result of ligamentous damage) is under debate. Although some authors stress the importance of mechanical stability [3,14], there are others who believe that factors like proprioception, muscle control, and balance control are more important [6,29]. Freeman et al and Tropp [6,29] found no correlation between the patient's subjective complaints, for which the term functional instability was introduced by Freeman et al., and mechanical instability [6]. Obviously, the more importance is attributed to mechanical instability, the more interesting it becomes to be able to differentiate between normal physiological and pathologically increased range of motion of the joints. In a previous study, increase in TT (between step 1 and 2, as also performed in the present study) was only found in symptomatic feet. This was interpreted with the possibility that during the first step the foot is fully inverted and passive structures, such as the ligaments, become increasingly tight until they block further motion. Increasing stress thereafter, as done

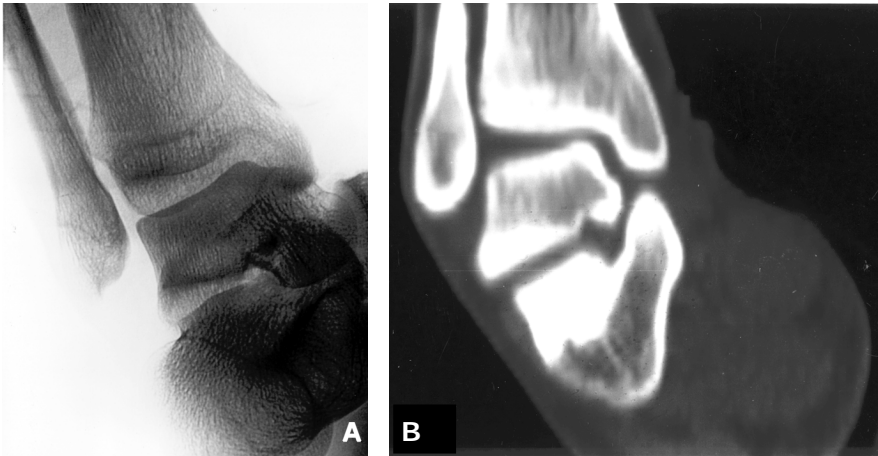


Figure 3.

A, A Brodén stress examination shows both considerable TT and subtalar tilt.

B, CT stress examination confirms the existence of TT; however, no tilt is found at the subtalar level.

during step 2, will only show an increase in tilt in feet with damaged lateral ligamentous structures. It was suggested that this increase might serve as a new parameter in diagnosing mechanical instability of the talocrural joint.

In the present study, a statistically significant difference was found between symptomatic and asymptomatic feet with regard to increase in TT (TTd); however, an increase in tilt was also found in three asymptomatic feet, and in one case a clear TT and increase in TT was found in the asymptomatic foot only (Table 2). The use of increased tilt as a definite parameter has therefore become doubtful. Again, the relation between the radiographic diagnosis of mechanical instability and chronic lateral instability complaints remains questionable. Both mechanical as well as functional instability are involved, and they may be parallel phenomena, as described by Tropp [29]. In our patient group, mechanical instability was not a dominant factor.

To our knowledge, no previous investigation has been published combining stress examination of the foot and CT scanning. One of the drawbacks of routine radiography is the imaging of three-dimensional structures on a two-dimensional plane. When motion takes place in complex geometric structures like the subtalar joint, the articular surfaces lose congruency. It may become a problem to draw the lines that represent the tangents to these surfaces and thus to measure the amount of tilt. This problem does not occur when CT scanning is used.

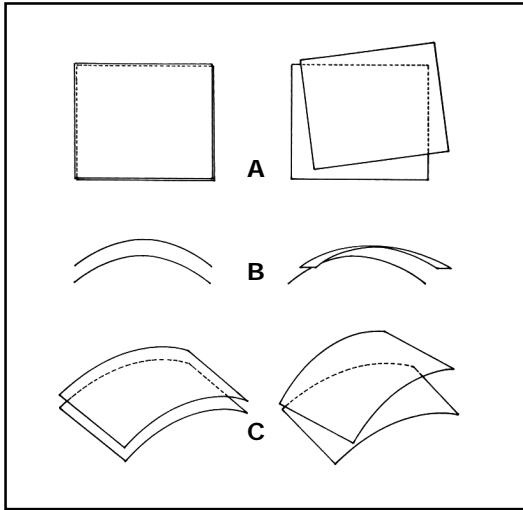


Figure 4.

Two curved parallel surfaces seen on the left side before translation (the surfaces are still fully congruent) and on the right side after translation and rotation relative to each other.

A, seen from above

B, from the side

C, in an oblique direction.

In only six feet, an angulation was found in the talocrural joint during CT stress examination (Table 2). In five cases, this was in the symptomatic foot, and in these feet it was associated with increased tilt with Brodén stress radiography. In the sixth case, it concerned an asymptomatic foot in which a TT of 11° was found, but no TTd. An increase in tilt is not always associated with a tilt during found with CT scanning. Although explanations can be found for differences in the amount of tilt between the two examinations, we cannot explain why not all feet that exhibit an evident TT with stress radiography also show tilting during CT scanning. It cannot be excluded that slight concessions were made regarding the amount of stress applied during CT examination, although subjectively both the examiner and the subjects experienced the amount of stress and closing of the hinge device to be equal. Another explanation for the difference would be that the talocrural joint was cut in a different plane, but this does not explain why in some feet no tilting at all is seen with CT examination, while they show a TT of 10° and sometimes more. In conclusion, there seems to be some relation between chronic lateral instability, increase in TT, and CT angulation of the talocrural joint during stress examination, but the results are inconsistent, and none of these examinations are found to be more specific for the radiographic assessment of mechanical instability.

Subtalar Joint

A wide range of motion (range, 4° to 18°) of the subtalar joint was found during Brodén stress radiography. These results are comparable to those found in previous studies [9,22,26]. An increase in subtalar tilt was found in only four symptomatic feet and in one asymptomatic foot. This increase was never more than 3°, and what influence any slight "errors" in drawing the lines representing the articular surfaces might have is open to discussion. As mentioned earlier, this can be a problem for the subtalar joint, with its complex geometry. It was hoped that CT scanning would bring clarity and make measurements more reproducible. However, not once was an actual opening of the subtalar joint found on the lateral side. One would have expected similar to findings at the talocrural level in at least one of the patients.

Incongruity occurring between the bones of the tarsus during motion has been noted as early as the second half of the 19th century and has been extensively described by Huson [11,12]. Roentgen-stereophotogrammatic studies have demonstrated translation and rotation of the talus and calcaneus in relation to one another during inversion of the injured foot [19]. As a result, the calcaneus inverts in relation to the talus [17,23]. However, a tilting motion between the two bones is not mentioned. Kjaersgaard-Andersen et al. found an increase in adduction in the talocalcaneal joint to a maximum of 5° after cutting the calcaneofibular ligament [18]. Smaller increases were found after cutting the ligaments of the sinus and canalis tarsi only [17]. The results of a study performed by Heilman et al. [10], in which the calcaneofibular and talocalcaneal ligaments were selectively cut, suggest that this increase is a result of tilting, and Clanton [4], in a review article, concludes that it appears that any loss of parallelism is indicative of instability. In fact, practically all clinical radiographic studies on this matter, including the present study, have focused on finding a subtalar tilt to establish mechanical instability.

We now doubt that the tilt seen during the Brodén stress examination (Fig. 3) is the true amount of tilt. It seems that there is no important tilting in the subtalar joint and that it is erroneous to translate the pattern of motion, as applied to the ankle joint, to this joint. If surfaces have a curved geometry, as drawn in figure 4, some amount of tilt will occur when these planes translate and rotate on each other (Fig. 4B), but the angulation that seems to occur (Fig. 4C) is the result of viewing two planes that make such movements relative to each other in an oblique direction. Obviously, there is a direct relation between the amount of motion and the so-called tilt, but we suggest that determining the amount of translation and rotation in a direct manner might prove to be more helpful in objectifying abnormal motion in the subtalar joint. Recently, Kato [15] described a method to measure anterior displacement of the calcaneus in relation to the talus. This translation is only one

of the components. Harper [9] suggested that the assessment of the rotational component of hindfoot inversion might help to document subtalar instability. Possibly, a combination of both above mentioned components occurs, resulting in anterolateral rotatory instability of the subtalar joint. Further research must be performed to confirm these suggestions.

Finally, CT examination of the hindfoot itself might prove to be helpful in diagnosing problem cases with chronic lateral instability. Unexpectedly, a fibrous talocalcaneal coalition was found in four patients (Fig. 2). In these patients, the subjective complaints seem to be caused by disturbance of the coupling between the foot and the leg (possibly abnormal motion at the talocrural level) as a result of decreased motion in the tarsus rather than hypermobility.

References

1. Anderson KJ, Lecocq JF, Lecocq EA. Recurrent anterior subluxation of the ankle joint: a report of two cases and an experimental study. *J Bone Joint Surg* 1952;34(A):853-860.
2. Brantigan JW, Pedegana LR, Lippert FG. Instability of the subtalar joint: diagnosis by stress tomography in three cases. *J Bone Joint Surg* 1977;59(A):321-324.
3. Broström L. Sprained ankles VI: surgical treatment of "chronic" ligament ruptures. *Acta Chir Scand* 1966;132:551-565.
4. Clanton TO. Instability of the subtalar joint. *Orthop Clin North Am* 1989;20(4):583-592.
5. Fiévez AWF, Spoor CW. A kinematical analysis of the ankle joint in relation to lateral ligamentous and capsular injuries. In *Op de Voet Gevolgd*. Course book of the Boerhaave Committee for Postgraduate Courses of the Leiden University, 1987:101-112.
6. Freeman MAR, Dean MRE, Hanham IWF. The etiology and prevention of functional instability of the foot. *J Bone Joint Surg* 1965;47:678-685.
7. Glasgow M, Jackson A, Jamieson AM. Instability of the ankle after injury of the lateral ligaments. *J Bone Joint Surg* 1980;62(B):196-200.
8. Hansen H, Damholt V, Termansen NB. Clinical and social status following injury to the lateral ligaments of the ankle joint. *Acta Orthop Scand* 1979;50:699-704.
9. Harper MC. Stress radiographs in the diagnosis of lateral instability of the ankle and hindfoot. *Foot Ankle* 1992;13:435-438.
10. Heilman AE, Braly WG, Bishop JO, Noble PC, Tullos HS. An anatomic study of subtalar instability. *Foot Ankle* 1990;10:224-228.
11. Huson A. Een ontleedkundig, functioneel onderzoek van de voetwortel. Thesis. University of Leiden, Leiden, the Netherlands, 1961.
12. Huson A. Functional anatomy of the foot. In Jahss M.H, ed. *Disorders of the foot and ankle*, 2nd ed. Philadelphia: W.B. Saunders, 1991:409-432.
13. Ishii T, Miyagawa S, Fukubayashi T, Hayashi K. Subtalar stress radiography using forced dorsiflexion and supination. *J Bone Joint Surg* 1996;78(B):56-60.
14. Karlsson J. Chronic lateral instability of the ankle joint: a clinical, radiological and experimental study. Thesis. University of Göteborg, Göteborg, Sweden, 1989.
15. Kato T. The diagnosis and treatment of instability of the subtalar joint. *J Bone Joint Surg* 1995;77(B):400-406.

16. Kjaersgaard-Andersen P, Wethelund JO, Heimig P, Nielsen S. Effect of the calcaneofibular ligament on hindfoot rotation in amputation specimens. *Acta Orthop Scand* 1987;58:135-138.
17. Kjaersgaard-Andersen P, Wethelund JO, Heimig P, Sballe K. The stabilizing effect of the ligamentous structures in the sinus and canalis tarsi on movements in the hindfoot: an experimental study. *Am J Sports Med* 1988;16(5):512-517.
18. Kjaersgaard-Andersen P, Wethelund JO, Nielsen S. Lateral talocalcaneal instability following section of the calcaneofibular ligament: a kinesiological study. *Foot Ankle* 1987;7:355-361.
19. Langelaan van EJ. A kinematical analysis of the tarsal joints. *Acta Orthop Scand* 1983;54(Suppl):204.
20. Laurin CA, Oellet R, St. Jacques R. Talar and subtalar tilt: an experimental investigation. *Can J Surg* 1968;11:270-279.
21. Linde F, Hvass I, Sijrgensen U, Madsen F. Early mobilizing treatment in lateral ankle sprains: course and risk factors for chronic painful or function-limiting ankle. *Scand J Rehab Med* 1986;18:17-21.
22. Louwerens JWK, Ginai AZ, Linge van B, Snijders CJ. Stress radiography of the talocrural and subtalar joints. *Foot Ankle Int* 1995;16(3):148-155.
23. Lundberg A. Patterns of motion of the ankle/foot complex. Thesis. University of Stockholm, Karolinska Institute, Stockholm, Sweden, 1988.
24. Prins JG. Diagnosis and treatment of injury to the lateral ligament of the ankle. *Acta Chir Scand* 1978;(Suppl):486.
25. Rasmussen O. Stability of the ankle joint: analysis of the function and traumatology of the ankle ligaments. *Acta Orthop Scand* 1985;56(Suppl):211.
26. Rubin G, Witten M. The subtalar joint and the symptom of turning over on the ankle: a new method of evaluation utilizing tomography. *Am J Orthop* 1962;4:16-19.
27. Rubin G, Witten M. The talar tilt angle and the fibular collateral ligaments. *J Bone Joint Surg* 1960;42(A):311-326.
28. Staples OS. Ruptures of the fibular collateral ligaments of the ankle: result study of immediate surgical treatment. *J Bone Joint Surg* 1975;57(A):101-107.
29. Tropp H. Functional instability of the ankle joint. Thesis. University of Linköping, Linköping, Sweden, 1985.
30. Vidal J, Fassio B, Buscayret C, Escare P, Allieu Y. Instabilité externe de la cheville: importance de l'articulation sous-astragalienne: nouvelle technique de réparation. *Rev Chir Orthop* 1974;60:635-642.
31. Vogel de PL. Enige functioneel-anatomische aspecten van het bovenste spronggewricht. Thesis. University of Leiden, Leiden, the Netherlands, 1970.
32. Zell BK, Shereff MJ, Greenspan A, Liebowitz S. Combined ankle and subtalar instability. *Bull Hosp Joint Dis Orthop Inst* 1986;46(1):37-46.
33. Zollinger H, Kubik S, Langlotz M, Waidis M, Manestar M. Instabilität des unteren Sprunggelenkes: anatomische Grundlagen und röntgenologische Diagnostik. In: Hackenbroch H, Refior HJ, Jager M, Plitz W, eds. *Funktionelle Anatomie und Pathomechanik des Sprunggelenkes*. Stuttgart: Thieme-Verlag, 1984:131-134.
34. Zwipp H, Kretek C. Diagnostik und Therapie der akuten und chronischen Bandinstabilität des unteren Sprunggelenkes. *Orthopäde* 1986;15(6):472-478.
35. Zwipp H, Tscherne H. Die radiologische Diagnostik der Rotationsinstabilität im hinteren unteren Sprunggelenk. *Unfallheilkunde* 1982;85:494-498.

CHAPTER 6

Assessing the subtalar joint: The Brodén view revisited

Elizabeth S. Sijbrandij¹, Ad P.G. van Gils¹, Frank J. van Hellemond²,
Jan-Willem K. Louwerens², Eddy E. de Lange³

From the Departments of Radiology¹ and Orthopaedic Surgery²
University Hospital Utrecht and Central Military Hospital Utrecht.

From the Department of Radiology³
University of Virginia Health Sciences Center, Charlottesville, USA.

Abstract

We prospectively evaluated subtalar inversion stress views (Brodén view) with inversion stress views on helical CT in a group of 10 patients with unilateral instability. The contralateral, asymptomatic ankle was used as control. All patients were examined with inversion stress views on plain stress radiography and helical CT. Subtalar tilt was demonstrated in all cases on conventional stress radiography. Helical CT didn't show tilting in any of the patients except in the subluxated posteromedial part of the subtalar joint. Our data do not support prior reports that the Brodén view is useful for screening patients with subtalar instability.

Introduction

Lateral instability of the ankle joint is one of the most common sequelae of an inversion injury to the ankle [1,10,13,15]. Patients with ankle instability usually complain of a sensation of the joint giving way with or without pain and swelling, and they frequently have a history of recurrent sprains [12,15]. For implementing of proper treatment, it is important to determine the degree of instability. A severely affected joint requires more aggressive therapy such as surgery, while a conservative approach is usually sufficient in mild cases [3,5].

It is believed that the talocrural joint is the major cause of instability of the hindfoot after inversion injury [13,18]. Traditionally, inversion stress views of the joint have been used as a non-invasive method for evaluating the degree of instability, thereby indirectly evaluating the integrity of the ligaments [22,24]. With this method, tilting of the talus is measured in a standard manner by defining on radiographs the angle between the talar dome and tibia plafond [7]. The normal range of talar tilt varies, ranging from 0-15 degrees [5,22]. In case of instability the range has been reported between 1-24 degrees. Thus, there is substantial overlap between the normal and pathologic tilt [1].

The role of the subtalar joint as a cause of hindfoot instability is less well understood [5,7,28]. A number of tests have been developed to evaluate this joint, such as oblique radiographs, arthrography and dedicated radiographs obtained under stress [4]. These stress views, of which the Brodén view is the most widely used, have been introduced to assess the presence of subtalar instability during inversion of the ankle [9,18,29]. However, there is no general consensus regarding the best method for evaluating subtalar instability [4].

The subtalar joint has a very complex, multi-faceted surface which makes evaluation with plain radiography and conventional tomography difficult [9]. The oblique radiograph such as the Brodén view is performed with the x-ray beam rotated 30 degrees in lateromedial and 40 degrees in caudocranial direction and with the subtalar joint inverted using a dedicated stress device [4]. With these angles, only the posterior part of the joint is visualized and thus only the "subluxated" part of the joint rather than the paralleling parts are seen. Instability of the subtalar joint is believed to be present when the stress radiographs demonstrate loss of parallelity of the posterior articular surfaces of the subtalar joint [4,5,14]. Other studies have indicated that tilting may be normal, with the subtalar tilt varying between 6-15 degrees in healthy, asymptomatic individuals [7,10,15]. In patients with instable joints, subtalar tilts between 7-22 degrees have been reported [7]. Since the movements of the hindfoot are complex during stressing, it is possible that the widening of the subtalar joint may be suggested by the rotatory changes of the bones and that there is no true angulation [5,10].

With helical CT, high resolution images of the ankle can be obtained, visualizing the many curved bony surfaces of the subtalar joint in greater detail. In addition, multiplanar reconstruction of images allows evaluation of the joint in a multidirectional way, potentially providing better and easier evaluation of the hindfoot than is possible with conventional radiography. It is expected that with this modality also incongruence of surfaces of the joint after injury may be better demonstrated, particularly when the CT examination is performed while inversion stress is applied. The purpose of our study was to determine whether instability of the subtalar joint as demonstrated by the Brodén view can be reproduced under equal circumstances with helical CT.

Materials and methods

The study group of this prospective study consisted of 10 consecutive patients, who had unilateral subtalar joint instability on physical examination. All patients complained of frequently recurring inversion injuries of the ankle occurring between two times a week to five times a year over a period of several years. This chronic subtalar instability consisting of: "giving way" sensation and frequently there was pain and some swelling of the ankle that usually persisted for several days after the injury. There were 8 men and 2 women with ages ranging from 18 to 36 years (mean age, 25 years). Physical examination, performed by an orthopaedic surgeon, demonstrated an increase in inversion tilt and there was strong clinical suspicion of the presence of subtalar instability.

Radiographic examination of both feet was performed in all patients, and in each the results of the healthy asymptomatic foot served as the standard of reference [4]. In each patient, Brodén views were obtained with the foot stressed and the x-ray beam angled as described above [4,7,15,23].

A dedicated stress device was used similar to the one described by Rubin and Witten allowing both feet to be tested simultaneously with equal stress [22]. For this study the hinge device we used was predominantly made of wood to avoid metallic artifacts at CT scanning. The feet were strapped to the device and placed in a neutral position [13]. Stress was performed by inverting the feet as much as possible without creating significant pain. Both feet were examined simultaneously under identical conditions.

CT was performed with a helical technique (Tomoscan SR 7000, Philips Medical Systems, Best, the Netherlands). Contiguous axial slices (thickness 3 mm) of the hindfeet were obtained covering the area from 2 cm above the talocrural joint to below the Chopart joint. Multiplanar reconstructions (MPRs) were made in coronal, (parallel to the talotibial joint), and sagittal orientations (perpendicular to the posterior facet of the subtalar joint). A dedicated workstation (Easy Vision workstation Release 2.1, Philips Medical Systems Best, the Netherlands) was used for the MPRs.

On the radiographs tilting of the talus was measured in the standard manner, using handheld calipers by defining the angle between the talar dome and tibia plafond after inversion of the foot [7]. Subtalar tilt was defined as the angle between the articular surface of the talus and calcaneus [15,23]. The CT images were reconstructed in coronal orientation and measurements were made on these images at three levels, the anterior, middle and posterior part of the posterior subtalar joint using a dedicated workstation. The tilt angles of the talar and subtalar joints on the CT images of both ankles were compared with the angles obtained from the Brodén views in each case using a paired *t*-test with a level of significance $p < 0.05$. Of these patients, the symptomatic feet were compared with the asymptomatic feet, using the asymptomatic feet as a control (paired *t*-test).

Results

Talocrural joint

Brodén view: The talocrural tilt of the symptomatic ankles ranged between 0-18 degrees (mean, 9.7 degrees) and of the asymptomatic between 0-16 degrees (mean, 7.2 degrees).

CT: The talocrural tilt of the symptomatic ankles ranged between 0-12 degrees (mean, 4.1 degrees) and of the asymptomatic between 0-10 degrees (mean, 1 degree) (Table 1A).

Subtalar joint

Brodén view: The subtalar tilt of the symptomatic ankles ranged between 6-18 degrees (mean, 10.8 degrees) and of the asymptomatic between 4-12 degrees (mean, 7.9 degrees).

CT: Using CT, no tilt was found in the symptomatic and asymptomatic ankles (Table 1B), except in the most posterolateral part where the tilt ranged for the symptomatic ankles between 8-13 degrees (mean 10.2 degrees) and for the asymptomatic ankles between 6-12 degree (mean, 8.4 degrees) (Table 1C).

In all reconstructed orientations both feet showed an equal shift of the bones of the hindfoot in the symptomatic and asymptomatic ankle, and all subtalar joints showed some loss of congruity. The coronal reconstructions of the posterior subtalar joints of the symptomatic and asymptomatic ankles showed a similar, mild degree of incongruence of the articular surfaces between the talus and calcaneus. For both the symptomatic and asymptomatic ankles only a tilt was found in the most posterolateral aspect of the joint between the opposing articular surfaces, both on the CT and Brodén view. No significant difference was found between the posteromedial tilt of the symptomatic and asymptomatic ankle.

Table 1A-C. Talotibial, mid subtalar, and posteromedial subtalar joints.

| | CT | Brodén |
|---------------------------------|------|--------|
| a. talotibial joint | | |
| symptomatic | 4.1 | 9.7 |
| asymptomatic | 1.0 | 7.2 |
| b. mid subtalar joint | | |
| symptomatic | 0 | 10.8 |
| asymptomatic | 0 | 8.2 |
| c. posteromedial subtalar joint | | |
| symptomatic | 10.2 | 10.8 |
| asymptomatic | 8.4 | 8.2 |

Discussion

Subtalar instability is defined as chronic functional instability with increased values of subtalar tilt and talocalcaneal displacement as measured with standardized stress radiographs [12]. The diagnosis of subtalar instability remains difficult, both clinically and radiographically [16]. Clinically it may not be easy to differentiate subtalar motion from soft tissue laxity and/or talotibial motion at clinical examination [21]. Radiographically special inversion stress views have been introduced, of which the Brodén view is the most widely used [5,14] for identifying subtalar instability [4,9,17,29]. Instability of the subtalar joint is generally considered when the Brodén radiograph demonstrates loss of parallelity of the articular surfaces of the talus and calcaneus [5,14] (Fig. 1).

Helical CT together with multiplanar data reconstruction provides the possibility to evaluate the joint in a multi-directional manner. We found in our patients on helical CT, with both symptomatic and asymptomatic ankles, that there was an unexpected, high degree of adduction and rotation in the subtalar joints with no significant differences between groups.

Using the reconstructed coronal CT images, we found that the subtalar joint surfaces were almost completely parallel during inversion in both symptomatic and asymptomatic patients (Fig. 2), non-parallelity was only seen in the most posteromedial part of the joint due to translation and rotation (Fig. 3), mimicking tilting. In our study no significant differences in tilting between symptomatic and asymptomatic patients were found.

The calcaneal facet of the posterior subtalar joint can be divided into a posteromedial and anterolateral aspect of the joint. The posteromedial portion shows an almost horizontal orientation and makes an angle of approximately 40 degrees craniocaudally with the anterolateral portion [6]. When the ankle inverts, the spherical and cylindrical surfaces of the subtalar joint rotate and translate without losing much contact between the surfaces [18] (Fig. 4). In the normal, neutral position of the ankle, the talus and calcaneus are not perfectly juxtaposed and the joint surfaces are not exactly the same in size [2]. Thus, there is a mild degree of incongruency between the two bones. With inversion of the hindfoot, a shift occurs between talus and calcaneus causing even more loss of congruency between the bones [15,20] (Fig. 5). As a result, the contact area between the articular surfaces of the two bones diminishes [27].

The Brodén view is performed with the x-ray beam rotated 30 degrees in lateromedial and 40 degrees in caudocranial direction and with the subtalar joint inverted using a dedicated stress device [4]. With these angles, only the posterior part of the joint is visualized and thus only the non-parallelity parts of the joint rather than the paralleling parts are seen.

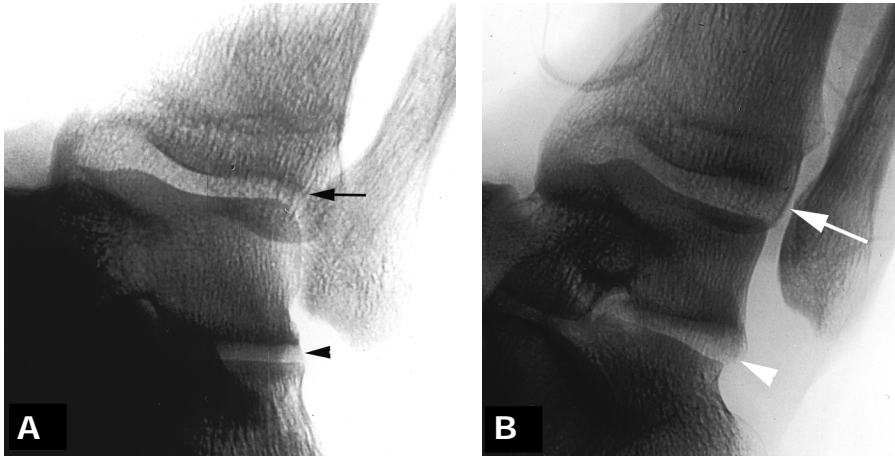


Figure 1. Brodén view.

A, Brodén stress view demonstrates no talar tilt (arrow) nor any subtalar tilt (arrowhead). The talar tilt, is measured with a line along the domes of the tibia and a line across the talar eminences. The subtalar tilt is measured along the articular surfaces of the talus and the calcaneus.

B, Brodén stress view demonstrates tilting in the talotibial joint (arrow) as well as loss of parallelity of the articular surfaces of the talus and calcaneus (arrowhead).



Figure 2.

Coronal CT reconstruction in the posterior part of the subtalar joint, the subtalar joint surfaces are almost completely parallel during inversion (arrow). A tilt of the articular surfaces in the talotibial joint is seen (arrowhead).

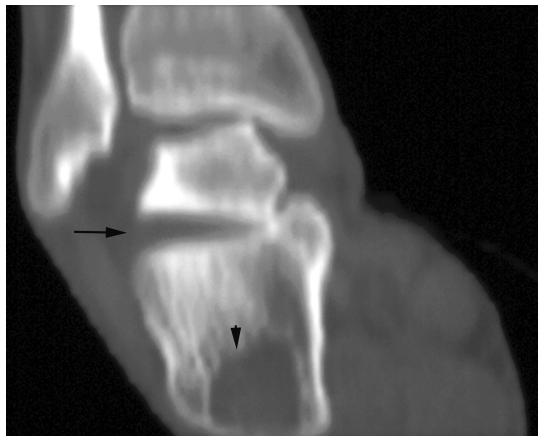


Figure 3.

Coronal CT reconstruction in the most posteromedial part of the subtalar joint, only in this part incongruence was seen (arrow). Bone cyst in calcaneus (arrowhead).



Figure 4. Inversion stress view of coronal CT reconstruction in the posterior subtalar joint. The joint surfaces of the talus and calcaneus show a mild degree of incongruity between the two bones (arrow), notice the talotibial tilt with a vacuum phenomenon (arrowhead).

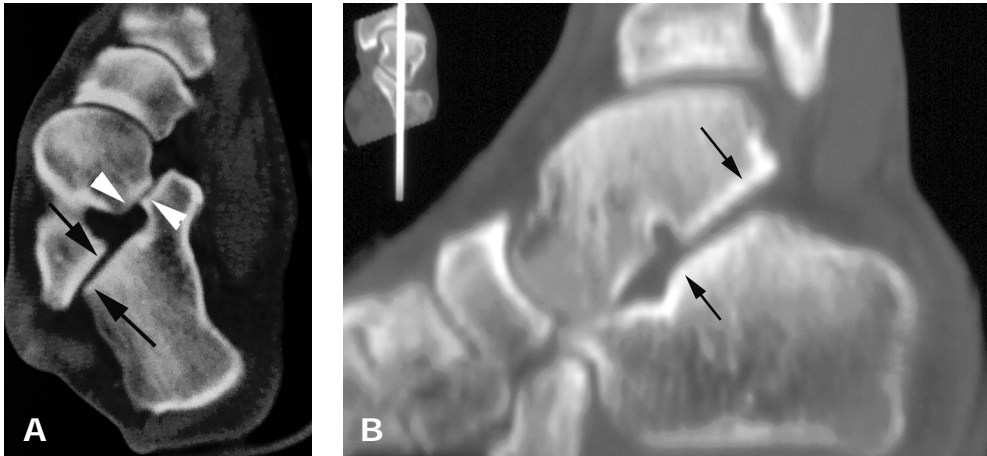


Figure 5. A, Axial CT section during inversion stress. Subluxation in the posterior (arrows) and middle subtalar joint (arrowheads). **B,** Sagittal CT reconstruction of the subluxation in the talus and calcaneus (arrows).

Considering this fact that on the Brodén view only the posterior component of the subtalar joint is visualized, a false impression of tilt in the normal subtalar joint may be given because only the “subluxated” part of the joint is seen. Furthermore the utility of the Brodén view in assessing patients with clinical subtalar instability is limited, as a wide range of overlap between the unstable and stable subtalar joint is seen [15].

An additional clinical cause, given the “false” impression of tilting in the subtalar



Figure 6.
Coronal CT reconstruction of the subtalar joint with talotibial tilt.
Notice the subluxation in the middle subtalar joint (arrows) and the large medial shift of the soft tissue of the hindfoot (arrowheads).

joints, may be the factor that a clinical diagnosis of subtalar instability cannot be isolated from soft tissue motion and talocrural motion (Fig. 6) and therefore overestimating tilting of the subtalar joint [21].

Helical CT scanning is not hampered by all these drawbacks, and therefore may be of more use in evaluating the subtalar joint.

Conclusion

The findings of our study indicate that the Brodén view is of limited value when examining the ankle in patients with the clinical diagnosis of subtalar instability. During inversion of the ankle, complex rotational and translational changes occur in the hindfoot. The standard Brodén view of the subtalar joint only visualizes the most posterior aspect of the joint, tilting may be suggested by the presence of rotation and translation in this posteromedial joint. Comparison with the asymptomatic ankle showed that similar changes were present in the normal ankles.

References

1. Ahuovuo J, Kaartinen E, Slätis P. Stress radiography in lesions of the lateral ligaments of the ankle. *Acta Radiol* 1988;29:711-714.
2. Anathakrisnan D, Ching R, Tencer A, Hansen ST, Sangeorzan BJ. Subluxation of the talocalcaneal joint in adults who have symptomatic flatfoot. *J Bone Joint Surg* 1999;81(A):1147-1154.
3. Brantigan JW, Pedegena LR, Lippert FG. Instability of the subtalar joint. Diagnosis by stress tomography in three cases. *J Bone Joint Surg* 1977;59(A):321-324.
4. Brodén B. Roentgen examination of the subtalar joint in fractures of the calcaneus. *Acta Radiol* 1949;31:85-91.
5. Clanton TO. Instability of the subtalar joint. *Orthop Clin North Am* 1989;20(4):583-592.
6. Ebraheim NA, Mekhail AO, Yeasting RA. Components of the posterior calcaneal facet: anatomic and radiologic evaluation. *Foot Ankle Int* 1996;17:751-757.
7. Harper MC. Stress radiographs in the diagnosis of lateral instability of the ankle and hindfoot. *Foot Ankle* 1992;13(8):435-438.
8. Heger L, Wulff K. Computed Tomography of the calcaneus: normal anatomy. *AJR* 1985;145:123-129.
9. Heilman AE, Braley WG, Bishop JO. An anatomic study of subtalar instability. *Foot Ankle* 1990;10(4):224-228.
10. Hellemondts van FJ, Louwerens JWK, Sijbrandij ES, Gils van APG. Stress radiography and stress examination of the talocrural and subtalar joint on helical computed tomography. *Foot Ankle Int* 1997;18:482-488.
11. Huson A. Een ontleedkundig, functioneel onderzoek van de voetwortel. Thesis, University of Leiden, Leiden, the Netherlands. 1961.
12. Karlsson J, Eriksson BI, Renström PA. Subtalar ankle instability. *Sports Med* 1997;24:337-346.
13. Kjærsgaard-Andersen P, Wethelund JO, Helmig P, Sballo K. The stabilizing effect of the ligamentous structures in the sinus and canalis tarsi on movements in the hindfoot: an experimental study. *Am J Sports Med* 1988;16:512-517.
14. Laurin CA, Oellet R, St-Jacques R. Talar and subtalar tilt: an experimental investigation. *Can J Surg* 1968;11:270-279.
15. Louwerens JWK, Ginai AZ, Linge van B, Snijders CJ. Stress radiography of the talocrural and subtalar joints. *Foot Ankle* 1995;16:148-155.
16. Mabi C, Boncoeur-Martel MP, Chaudruc JM, et al. Anatomic and MRI study of the subtalar ligamentous support. *Sur Rad Anat* 1997;19:111-117.
17. Magid D, Michelson JD, Ney DR, Fishman EK. Adult ankle fracture: comparison of plain film and interactive two and three dimensional CT scans. *AJR* 1990;154:1017-1023.
18. Mandell GA, Harcke HT, Hugh J, Kumar SJ, Maas KW. Detection of talocalcaneal coalitions by magnification bone scintigraphy. *J Nucl Med* 1990;31(11):797-801.
19. Masciocchi C, Maffey MV. Subtalar instability in athletes. In: Masciocchi C, ed. *Radiologic imaging of sports injuries*. Berlin: Springer, 1998:151-163.
20. Parlasca R, Shoji H, D'Ambrosia. Effects of ligamentous injury on ankle and subtalar joints: a kinematic study. *Clin Orthop* 1978;140:266-272.
21. Pearce TJ, Buckley RE. Subtalar joint movement: clinical and computed tomography scan correlation. *Foot Ankle Int* 1999;20:428-432.
22. Rubin G, Witten M. The talar-tilt angle and the fibular collateral ligaments. *J Bone Joint Surg* 1960;42(A):311-326.
23. Sarrafian SK. Biomechanics of the subtalar joint complex. *Clin Orthop* 1993;290:17-26.
24. Sauser DD, Nelson RC, Lavine MH, Wu C. Acute injuries of the lateral ligaments of the ankle. Comparison of stress radiography and arthrography. *Radiology* 1983;148:653-657.

25. Siegler S, Chen J, Schneck CD. The three-dimensional kinematics and flexibility characteristics of the human ankle and subtalar joints Part I: kinematics. *J Biomech Eng* 1988;110:364-373.
26. Ugai K, Morimoto K. Magnetic resonance imaging of pigmented villonodular synovitis in subtalar joint. Report of a case. *Clin Orthop* 1992;(283):281-284.
27. Wagner UA, Sangeorzan BJ, Harrington RM, Tencer AF. Contact characteristics of the subtalar joint: load distribution between the anterior and posterior facets. *J Orthop Res* 1992;10:535-543.
28. Zell BK, Shereff MJ, Greenspan A, Liebowitz S. Combined ankle and subtalar instability. *Bull Hosp Joint Dis Orthop Inst* 1986;46:37-46.
29. Zwipp H, Tscherne H. Die radiologische Diagnostik der Rotationsinstabilität im hinteren unteren Sprunggelenk. *Unfallheilkunde* 1982;85:494-498.

CHAPTER 7

Posttraumatic subchondral bone contusions and fractures of the talotibial joint: Occurrence of "kissing" lesions

Elizabeth S. Sijbrandij¹, Ad P.G. van Gils¹, Jan Willem K. Louwerens²,
Eduard E. de Lange³

From the Departments of Radiology¹ and Orthopaedic Surgery²
University Hospital Utrecht and Central Military Hospital, Utrecht.

From the Department of Radiology³
University of Virginia Health Sciences Center, Charlottesville, USA.

American Journal of Roentgenology 2000;175:1707-1710.

Abstract

Objective. To determine the presence and location of subchondral bone contusions, fractures and kissing lesions of the talotibial joint after sprain of the ankle visualized by MR imaging.

Materials and methods. We retrospectively reviewed the images of all consecutive patients who underwent MR imaging of the ankle after acute or recurrent sprain occurring between January and December 1997. The number and location of subchondral contusions or fractures visualized by MR imaging were recorded and a comparison was made with the radiographs obtained in each case.

Results. Of the 146 ankles, 42 osteochondral lesions were identified by MR in 26 (18%) ankles involving 23 patients. Twenty-three lesions were localized in the dome of the talus and 19 in the tibia plafond. In 16 (11%) of the 146 ankles, the lesions were present in the opposing bones of the joint ("kissing" lesions). Only six of the 12 talar fractures and none of the tibial fractures involving the 26 ankles were visualized by conventional radiography.

Conclusion. Subchondral lesions in talus and tibia are relatively common after ankle trauma occurring in 18% of our series. Kissing lesions were present in more than half of these.

Introduction

A ligament sprain is one of the most common sports-related injuries of the ankle [1]. When the pain persists, the possibility of an osteochondral contusion or fracture of the dome of the talus should be considered [1]. Studies have shown that patients with disability after an ankle sprain show an osteochondral fracture of the talus more often than expected [2,3]. Repeated trauma can lead to more severe osteochondral injury which, in turn, may result in progressive disability [4]. The osteochondral lesions, particularly when minor, are generally not visualized by conventional radiography [1,2,5].

The most widely accepted classification of osteochondral talar injury introduced by Berndt and Harty and based on research on cadavers, is as follows:

- Stage 1 - localized area of subchondral trabecular compression
- Stage 2 - incomplete separation of transchondral fragment
- Stage 3 - fragment is completely separated but not displaced
- Stage 4 - fragment is displaced or inverted in its fracture bed [5].

The first two stages are difficult to visualize by conventional radiography, and the lesions may go undetected when radiographs are obtained for evaluation. MR imaging has been shown to demonstrate the lesions with high sensitivity allowing early detection and treatment of the abnormalities [1].

It has been noted that in patients with traumatic osteochondral contusions of the dome of the talus similar lesions can be seen occasionally on the opposite site of joint, the tibio-fibular plafond. Lundeen (1990), using arthroscopy, was one of the first to postulate that the tibial lesions were the result of the talus impinging on the cartilage of the tibia plafond at the time of injury [6]. Similar findings, referred to as "kissing" contusions, have also been described in the knee [7]. Bone bruises are not uncommon after severe ankle sprain. To our knowledge, there have been no detailed studies on bone bruises associated with osteochondral fractures in the ankle. Canosa was the first to describe the CT appearances of the kissing lesions in the ankle in a patient who had an osteochondral fracture of the talus and a "mirror" image fracture of the adjacent tibia plafond [8].

We have noted in our patient group undergoing MR examination of the ankle after injury a relative high incidence of subchondral bone contusions, fractures and kissing lesions involving the talus and tibio-fibular plafond. The purpose of our study was to determine the presence and location of subchondral bone contusions, fractures and kissing lesions of the talo-tibial joint after sprain of the ankle visualized by MR imaging.

Materials and Methods

We retrospectively reviewed 146 MR images of all consecutive patients who had undergone MR imaging of the ankle at our institution for sustained acute or recurrent injury to the ankle between January 1997 to December 1997. Abnormalities of the subchondral bones were found in 26 ankles, involving 23 patients. Twenty of these were males and three were females with ages ranging between 12 and 51 years (mean, 30 years). Seventeen of the 23 patients were military recruits. All patients could relate the symptoms to acute or recurrent sprains of the ankle. Time between injury and imaging varied from one to 43 weeks (mean, 14 weeks). In all cases there were persisting symptoms after an episode of trauma such as stiffness, swelling and pain aggravated by weight bearing or activity [2,3]. The indication for performing a MR imaging examination was the clinical suspicion of osteochondral injury established by an experienced orthopaedic foot surgeon.

MR imaging was performed at 0.5 Tesla (Philips, Best, the Netherlands) with the ankle placed in a dedicated receive-only extremity coil. Conventional T1-weighted SE (TR/TE,

600/23), and T2-weighted SE (2000/100) images were obtained in sagittal and coronal orientation in all patients. Short tau inversion recovery (STIR) images (3600/20; inversion time, 150) were obtained in coronal orientation. Image section thickness ranged between 3 and 5 mm with an interslice gap between 0 and 1.5 mm. Matrix size was 256 x 256, and the field-of-view was 16 cm. All patients also underwent radiographic examination of the ankle in anteroposterior, lateral and mortise view projections.

The MR images were reviewed with special attention for bony abnormalities suggestive of osteochondral contusions or fractures. Associated ligamentous injuries were not evaluated in this study. Two radiologists reviewed the images in consensus and the diagnosis of a contusion was based on the criteria described by Kaplan and Magee: the presence of a subchondral, well-defined, semi-circular area of decreased signal intensity on T1-weighted images and increased signal intensity on T2-weighted and STIR images [7,9]. An osteochondral fracture was considered to be present when disruption of the subchondral bone plate was identified on T2-weighted images extending through the cortical surface. After review of each MR imaging study, the reviewers analyzed the ankle radiographs of each case with knowledge of the MR imaging findings. In addition, all MR examinations and radiographs of the ankle obtained during the two years following the initial injury were also reviewed.

Results

Of the 146 consecutive MR examinations of the ankles performed for persistent symptoms following sprain, 42 abnormalities of the subchondral bones were found in 26 (18%) ankles, involving 23 patients. The 42 subchondral lesions were present in 17 right and nine left ankles, with 23 of the lesions in the talus and 19 in the tibia. In 13 of the 42 lesions, the MR imaging findings were consistent with fractures and the remaining 29 were contusions. Twelve of the fractures were located in the talus and one in the tibia. Seven of the 23 talar and three of the 19 tibia plafond lesions were present on only one side of the joint. We found no significant difference in time between the injury and imaging in patients with and without bone contusions or fractures. In 16 ankles, the subchondral lesions involved the two opposing bones of the talo-tibial joint (kissing contusions). In six of those, the subchondral lesions were diametrically opposed to each other and involved the weightbearing area (Fig. 1 and 2). In the remaining 10, the lesions were not directly opposed (Figs. 3 and 4). All, except one of the 16 kissing lesions involving the tibia were contusions. Only 7 contusions were seen in the talus, while a majority (9) of the talar



lesions were osteochondral fractures. Only six of the 12 talar fractures and none of the tibial fractures involving the 26 ankles were visualized by conventional radiography.

Of the 23 patients, arthroscopy with drilling through the subchondral bone was performed in four patients with a subchondral fracture of the talus, within two months of the injury. In 16, conservative treatment was given and in three the treatment was unknown.

Twenty of the 23 patients had follow up imaging evaluation. MR imaging performed in two patients with kissing contusion showed persistence of the tibial lesion in one after one month follow-up and complete resolution in another one after 10 months. MR imaging performed in two patients both with kissing lesions (an osteochondral fracture of the talus and a contusion of the tibia), showed complete healing in one patient 11 months after the

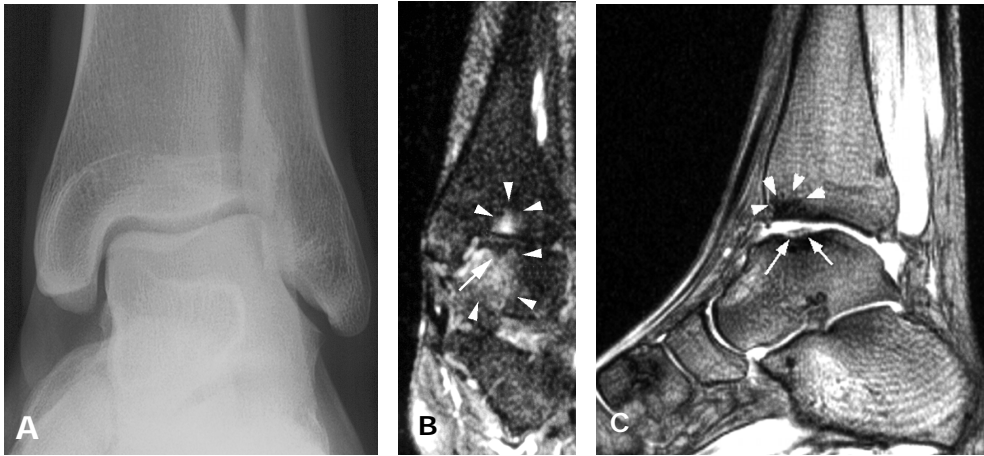


Figure 2. 22-year-old male six weeks after distorsion of left ankle.

A, Anteroposterior radiograph demonstrates no abnormalities.

B, Coronal short tau inversion recovery (STIR, TR/TE/TI 3600/20/150) shows bone contusion in opposing areas of medial tibia plafond (arrowheads) and osteochondral fracture in medial talar dome (arrow).

C, Sagittal T1-weighted spin-echo (TR/TE 600/23) MR image shows osteochondral fracture in medial talar dome (arrows) and bone contusion in tibia plafond (arrowheads).

initial injury, and in the other patient, minimal residual edema in the talus after 17 months. CT arthrography obtained in one patient with a solitary talus fracture showed that the fracture was still visible after 7 months. Radiography in 15 patients with 12 kissing and three solitary lesions showed osteochondral fractures of the talus in three and no evidence of subchondral injury in the others between one month and two years after the initial injury.

Discussion

MR imaging has been shown to be a highly sensitive modality for evaluating the subchondral tissues after injury [4,9]. A variety of changes can occur after trauma ranging from bone bruises or contusion to frank osteochondral fractures. The bone bruises are thought to represent trabecular microfractures associated with hemorrhage, edema and hyperemia [7]. On MR images, they present as relatively ill-defined semi-circular areas of abnormal signal intensity in the subcortical bone that do not extend through the cortex [7]. When a fracture is also present, there is disruption of the cortical bone visualized as a low signal



Figure 3. 42-year-old man with persistent pain after recurrent sprains of right ankle.

A, Anteroposterior radiograph of ankle shows osteochondral defect in lateral aspect of talus (arrow).

B, Coronal short tau inversion recovery (STIR, TR/TE/T1 3600/20/150) with osteochondral lesion in lateral talus (arrow) and osteochondral lesions in medial tibia plafond (arrowhead). Lesions are not diametrically opposed probably as result of rotation during injury.

C, Coronal T1-weighted SE (TR/TE 600/23) MR image shows osteochondral fracture in lateral talus (arrow) and osteochondral contusion in medial tibia plafond (arrowhead).

intensity line by T2-weighted imaging extending through the cortical surface. The subchondral abnormalities are believed to be caused by trauma that causes impaction of the bones. In the ankle, there may be additional rotational forces contributing to the mechanism of injury [10]. It has been reported that bone bruises occurred in 7% of the ankles following first-time sprain [11]. The higher incidence of bone bruises following recurrent sprains suggests that re-injuries may play an important role in their occurrence [11]. Bone contusions in the ankle are often associated with ligamentous injury [12]. But on the other hand they may occur in the absence of major ligament disruptions [11]. Knee bone contusions are known to resolve in 1-4 months after injury. We found some cases of edema in the ankle persisting for a longer period of time. This may suggest that the time necessary for healing in the ankle is longer. On the other hand ankle instability

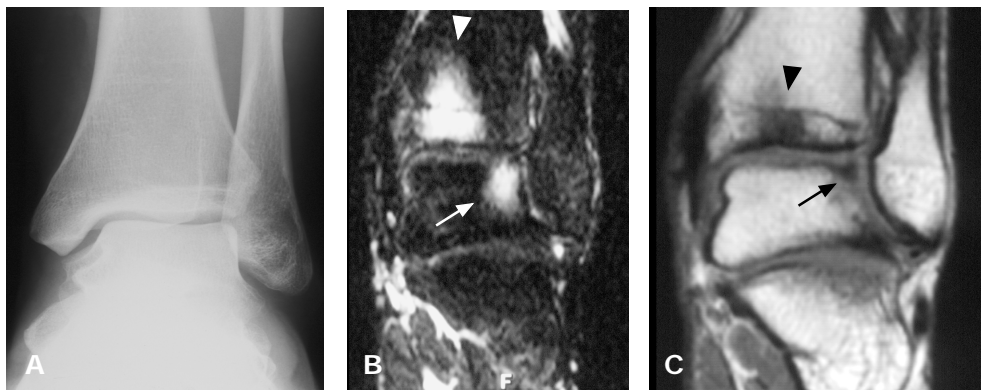


Figure 4. 25-year-old male 7 weeks after severe sprain of left ankle. **A**, Anteroposterior radiograph of left ankle shows no abnormalities. **B**, Coronal short tau inversion recovery (STIR, TR/TE/TI 3600/20/150) shows bone contusions in opposing areas of medial tibia plafond (arrowhead) and lateral talar dome (arrow). Contusions are recognized by demonstration of areas of increased signal intensity. **C**, Coronal T1-weighted spin-echo (TR/TE 600/23) MR image shows osteochondral contusions in lateral talar dome (arrow) and tibia plafond (arrowhead). Contusions are not diametrically opposed probably as result of rotation.

due to ligamentous injury and recurrent sprains may also be responsible for the persisting bone marrow edema in the ankle. The healing period of the osteochondral injury in the ankle therefore still remains unknown [11,13].

We found 42 osteochondral lesions in our series of 146 patients. Of those, there were 36 bone contusions. The frequency of the findings is well within the range (6.5%-39%) reported in the literature [13,14]. However, the number of patients with kissing lesions (11%) was much higher than that reported by others. For instance, Labovitz and Schweitzer found kissing lesions in only 5 (5%) of 109 subjects [13]. It is unclear why the number of kissing lesions was relatively high in our series. However, a large proportion (17 of 23) of the patients with subchondral injury consisted of personnel of the military forces, subjects in whom it is known that osteochondral lesions are more likely to occur [5,14]. We found in the patients with kissing lesions that all osteochondral fractures were located in the talus while the contusions were predominantly seen in the tibial plafond. There are several possible explanations for the higher occurrence of the subchondral fractures in the talus than the tibio-fibular plafond. First, osteochondral lesions are more commonly observed at the convex surface of a joint, while the concave surface is generally spared. The convex surface is believed to transmit the forces (convergence of force) toward a central focus, whereas a concave surface dissipates the forces. As a result, the concave joint surface,

such as that of the talus is likely to be more severely damaged by trauma than the tibial plafond [10]. Second, the cartilage of the tibia is stiffer than that of the talus due to differences in composition [15]. In six of the 16 kissing lesions, the abnormalities were directly opposite of each other making it likely that the lesions of the tibio-fibular plafond were the result of direct impaction of the talar bone onto the opposing tibial bone. In the remaining 10 the lesions were not diametrically opposed probably because rotation occurred during the injury [7].

A shortcoming of our study is that there was limited follow-up with MR imaging. In the one case where CT was obtained no changes were noted of the osteochondral fractures after seven months. No osteochondral lesions were seen in any of 15 patients who had radiographic follow-up. However, the latter technique is insensitive in detecting these lesions. Thus, the changes over time of bone contusions in the ankle remain uncertain. Nevertheless, the clinical significance of bone contusions in the ankle has not been established and it has been suggested that these contusions do not need treatment [9]. Osteochondral fractures, on the other hand, do need to be treated with reduced weight bearing for an extended period of time [11]. A further shortcoming of our study is the retrospective study design. Because of the large number of military recruits, our study is subject to selection bias. This bias makes it difficult to extrapolate these findings to a general orthopaedic practice.

In conclusion, we found a relatively high number (11%) of subchondral injury involving the subchondral bone of both the talus and tibia. Of these kissing lesions, bone contusions were most commonly seen in the tibia plafond and osteochondral fractures in the talar dome. The kissing lesions are most likely caused by impaction of the talus onto the tibia with or without torsion.

References

1. Anderson IF, Crichton KJ, Grattan-Smith T, Cooper RA, Brazier D. Osteochondral contusions of the dome of the talus. *J Bone Joint Surg* 1989;71(A):1143-1152.
2. Ferkel RD. Articular surface defects, loose bodies, and osteophytes. In: Ferkel RD, ed. *Arthroscopic Surgery: The foot & ankle*. 1st ed. Philadelphia: Lippincott - Raven, 1996:145-184.
3. Ly PN, Fallat M. Transchondral contusions of the talus: a review of 64 surgical cases. *J Foot Surg* 1993;32:352-374.
4. Schweitzer ME. Magnetic resonance imaging of the foot and ankle. *Magn Reson Q* 1993;9:214-234.
5. Berndt AL, Harty M. Transchondral contusion (osteochondritis dissecans) of the talus. *J Bone and Joint Surg* 1959;41(A):988-1020.
6. Lundeen RO. Ankle arthroscopy in the adolescent patient. *J Foot Surg*. 1990;29:510-515.

7. Kaplan PA, Craig WW, Kilcoyne RF, Brown DE, Tusek D, Dussault RG. Occult fracture patterns of the knee associated with anterior cruciate ligament tears: assessment with MR imaging. *Radiology* 1992;183:835-838.
8. Canosa J. Mirror image osteochondral defects of the talus and distal tibia. *Int Orthop* 1994;18:395-396.
9. Magee TH, Hinson GW. Usefulness of MR imaging in the detection of talar dome injuries. *AJR* 1998;170:1227-1230.
10. Camasta CA, Pitts TE, Corey SV. Bilateral osteochondritis dissecans of the first metatarsophalangeal joint. *J Am Podiatr Med Assoc* 1994;84:297-310.
11. Pinar H, Akseki D, Kovanlikaya I, Kovanlikaya I, Arac S, Bozkurt M. Bone bruises detected by magnetic resonance imaging following lateral ankle sprains. *Knee Surg Sports Traumatol Arthroscopy* 1997;5:113-117.
12. Nishimura G, Yamato M, Togawa M. Trabecular trauma of the talus and medial malleolus concurrent with lateral collateral ligamentous injuries of the ankle: evaluation with MR imaging. *Skeletal Radiol* 1996;25:49-54.
13. Labovitz JM, Schweitzer ME. Occult osseous injuries after ankle sprains: incidence, location, pattern, and age. *Foot Ankle* 1998;19:661-667.
14. Flick AB, Gould N. Osteochondritis dissecans of the talus (transchondral fractures of the talus): review of the literature and new surgical approach for medial dome lesions. *Foot Ankle* 1985;5:165-185.
15. Athanasiou KA, Niederauer NG, Schenck RC. Biomechanical topography of human ankle cartilage. *Ann Biomed Eng* 1995;23:697-704.

CHAPTER 8

Osteochondritis dissecans of
the talar dome:
Evaluation of bone viability
with dynamic gadolinium-enhanced
MR imaging in comparison with
dynamic bone scintigraphy.

Elizabeth S. Sijbrandij¹, Ad P.G. van Gils¹, Jan Willem K. Louwerens²,
Eduard E. de Lange³

From the Departments of Radiology¹ and Orthopaedic Surgery²
University Hospital Utrecht and Central Military Hospital, Utrecht.

From the Department of Radiology³
University of Virginia Health Sciences Center, Charlottesville, USA.

Submitted for publication

Abstract

Objective. To determine the viability of osteochondritis dissecans (OD) in the talar dome with dynamic (dyn) contrast-enhanced MR imaging using dynamic (dyn) scintigraphy as the standard of reference.

Materials and methods. Dyn MR images and bone scintigraphy scans of 9 consecutive patients, evaluated between January 1998 to December 2000, were reviewed. MR imaging was performed using a fast gradient echo technique with acquisition of a single slice section positioned over the area of OD. Three-phase bone scintigraphy with administration of 600 MBq ^{99}Tc HDP and dyn image acquisition for 3 minutes and after 3 hours post injection was performed. Signal intensity (SI) and radioactivity curves were compared between the two techniques.

Results. Eight of the nine cases showed good correlation between the findings of dyn MR and dyn scintigraphy. In seven of the eight patients there was contrast enhancement and radioactivity uptake in the central area of the OD lesion consistent with good vascularization of the lesion. No enhancement or activity was seen in one patient. In the other case dyn MR imaging showed no central enhancement of the OD lesion, while three-phase bone scintigraphy depicted uptake in the OD lesions.

Conclusion. The findings suggest that dyn MR imaging in comparison with dyn scintigraphy better determines the viability of OD lesions. It is our belief that due to the relative poor spatial resolution of scintigraphy central necrosis is not visualised. An additional advantage of dyn MR imaging is that the procedure is easily performed following conventional MR imaging without exposing the patient to ionizing radiation.

Introduction

Osteochondritis dissecans (OD) of the talar dome is a relatively common complication occurring in 6% of patients who have sustained an inversion injury [1]. There are no known specific clinical signs or symptoms indicating the presence of OD; however, persistent pain, despite treatment, is suggestive of this entity [2]. It has been demonstrated that repeated trauma may lead to progression of OD which, in turn, may result in progressive disability [3,4,5]. Although the exact cause of OD is unknown, it is thought that in mild cases microfractures, hemorrhage and edema occur [4,5]. When this subsides, the disease is reversible. However, in more severe instances, the subchondral fractures together with the vascular insufficiency, can eventually lead to avascular necrosis of the

bone fragment [4,6]. If healing does not occur, the fragment becomes necrotic and encased along its articular surface by hyaline cartilage and its trabecular surface by fibrocartilage, which is impenetrable to capillary ingrowth [7,8]. Healing of the OD requires ingrowth of capillaries into a stable fragment. Lesions with viable bone are likely to heal spontaneously with conservative treatment, while with necrosis the bone may collapse, leading to degenerative changes in the ankle joint [4,9].

Current treatment of OD is aimed at prevention of a necrotic section in order to maintain the integrity of the joint. Such treatment includes drilling (with fixation) of the subchondral bone in an attempt to facilitate revascularization of the compromised subchondral tissues, or excision of the unstable fragment [10]. Currently, in order to determine the status of the subchondral bone, diagnostic arthroscopy is performed whereby the articular cartilage is inspected. The OD lesion is considered to be stable when the overlying cartilage is firm on palpation [10]. When the cartilage is unstable and gives way, this suggests the presence of a loose fragment which in turn, would be indicative of necrosis of the bone fragment [6]. However, arthroscopic palpation is relatively insensitive in diagnosing necrosis of the underlying bone, and drilling of the OD is usually done empirically even when the findings of palpation are normal [10].

OD, particularly at an early stage, is difficult to visualize by conventional radiography [11,12]. Static bone scintigraphy with technetium ^{99m}Tc HDP is more sensitive at detecting the disease; however, the specificity in determining the presence of OD is low [11,13]. In addition, it provides no information in assessing the viability of the lesion [14,15]. Dyn bone scintigraphy studies have shown to be accurate in assessing disease activity since it gives quantitative information of blood flow and this method is most commonly used to determine bone viability [9,14-17].

Conventional MR imaging has been shown to be a sensitive diagnostic tool for detecting OD of the talar dome [18]. In addition, with this technique the various stages of this disease can be determined [2,4,18]. However, despite extensive investigation evaluating the signal intensity (SI) appearances of the affected bone using conventional MR imaging, it has not been possible to determine the viability of the bone fragment in the OD lesion [19]. Studies have shown that dyn gadolinium-DTPA (Gd-DTPA) -enhanced MR imaging is more sensitive than unenhanced or non-dyn enhanced MR imaging in detecting osteonecrosis in the femoral head, knee and navicular bone [13,14,20,21]. Ceval et al., who investigated the navicular bone, found that lack of enhancement of bone marrow in the early phase of the study indicated lack of blood perfusion and the findings corresponded to variable degrees of ischemia [13]. The purpose of our study was to determine the ability of dyn contrast-enhanced MR imaging in assessing the vascularization of OD of the talar dome using the findings of dyn ^{99m}Tc bone scintigraphy as the standard of reference.

Materials and methods

Dyn contrast-enhanced MR imaging of the ankle was performed in all patients who had OD of the talar dome between January 1998 and December 2000. The diagnosis of OD was based on the commonly used MR criteria using non-dyn imaging [2,5,12]. All patients had persistent pain and a history of acute or recurrent inversion injury of the ankle occurring between 4 weeks and 1.5 years before MR imaging. There were 9 patients (9 ankles), seven males and two females with ages ranging from 13 to 41 years (mean age, 25 years). Bone scintigraphy of the affected ankles was performed in all patients, and intervals between dyn scintigraphy and dyn MR imaging ranged between 2 days and 5 weeks. Radiography of the ankles was also obtained in all cases.

MR imaging was performed at 0.5 Tesla (Philips, Best, the Netherlands) with the ankle placed in an extremity coil. Conventional sagittal and/or coronal T1- and T2-weighted images were obtained prior to dyn imaging, using the following parameters: T1-weighted spin-echo (SE) with repetition time/echo time (TR/TE) 600 ms/23 ms, T2-weighted SE (TR/TE 2000 ms/100 ms) and short tau inversion recovery (STIR) 3600 ms/20 ms; inversion time = 150 ms. The precontrast T1- and T2-weighted images were used to determine the position of the image plane that included the most representative part of the lesion. Dyn imaging was performed using a fast T1-weighted, magnetization-prepared, gradient-echo (MP-GRE) sequence with the following parameters: TR/TE/flip angle 15 ms/6.8 ms/ 30°, 741 msec preparatory pulse delay time (centric phase encoding), one signal acquired per data line, 128 or 256 x 256 matrix size, 160-450 mm field of view. The images were obtained as a single slice section and the image plane was chosen such that an artery, either the anterior or posterior tibial artery, was included to determine the time of arrival of the contrast bolus [22]. The temporal resolution was one image/3 seconds. Images were acquired at initiation of an intravenous bolus injection [2-3 cc/sec manual injection of 15 cc Gd-DTPA (Magnevist, Schering, Berlin, dose 0.1 mmol/ml] in the right antecubital vein followed by a saline flush, and imaging was continued until 5 min after beginning of the dyn examination.

Once obtained, the contrast-enhanced dyn images were subtracted from the first MP-GRE image of the dyn series that was obtained before arrival of the contrast material bolus. Regions of interest (ROI) were drawn in the central portion of the OD lesion and one in the normal bone marrow for comparison. Time intensity curves (TICs) of the two areas were then generated covering the first 5 minutes after injection of the contrast agent. Two observers in consensus did selection of the ROIs. Using each TIC the slope

and the time to maximum enhancement were determined. Using the TICs it was determined whether the central area demonstrated enhancement.

As surgery consisting of drilling of the lesions was performed in 5 of the 9 patients, the results of these findings was not used as the standard of reference since histologic examination were not performed [13]. We therefore used the results of three-phase bone scintigraphy as the standard of reference. Dyn scintigraphy was performed by injecting 600 MBq of ^{99m}Tc HDP [17]. The patient was placed under a large field-of-view camera with a 15% window, 140 keV setting and high-resolution collimator [17]. Blood flow and blood pool data were obtained from AP and lateral views of the hindfoot in the first 3 minutes.

Dyn scintigraphic activity was classified as symmetric, increased or decreased as compared with the unaffected side [9,15-17]. Increased activity was considered indicative of increased local metabolic activity and regional blood flow to the bone. This increased scan activity was interpreted as a positive predictive sign for viability [15-17]. Curves with minimal or decreased extraction of the farmacon were indicative of delayed or absence healing [15]. Using the dyn phase of the three-phase bone scan, a ROI was drawn in the most central area and around the lesion. TICs of the two areas of both feet were then generated covering the first 3 minutes after ^{99m}Tc HDP injection. Static bone scintigraphy was obtained 3 hours after injection of the nuclear farmacon.

Results

Analysis of the MR images

The results of enhancement of OD lesions by dyn MR and dyn scintigraphy are shown in table 1. In 8 of the 9 cases the flow curves showed a good correlation between the findings of dyn MR and dyn scintigraphy. In 7 of the 8 patients the increased enhancement or increased uptake in the central OD lesion was equal (Fig. 1). There was no enhancement or uptake, with both techniques, in one patient. In only one of the 9 cases the findings between the two techniques did not correlate. The dyn scintigraphy demonstrated increased radioactivity of the OD lesion while dyn MR detected a central area of diminished enhancement (Fig. 2).

The *static* bone scans showed activity in all of the patients.

Table 1. Demonstration of enhancement of the central bone area at 2 minutes after injection.

| Patient no. | MR imaging | Scintigraphy |
|-------------|------------|--------------|
| 1 | yes | yes |
| 2 | yes | yes |
| 3 | yes | yes |
| 4 | yes | yes |
| 5 | no | yes |
| 6 | yes | yes |
| 7 | yes | yes |
| 8 | yes | yes |
| 9 | no | no |

Figure 1. 37-year-old man with kissing contusion after inversion injury.

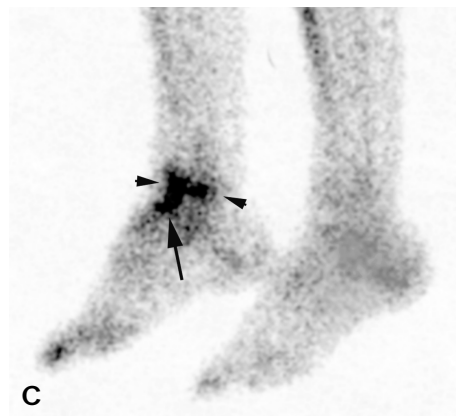
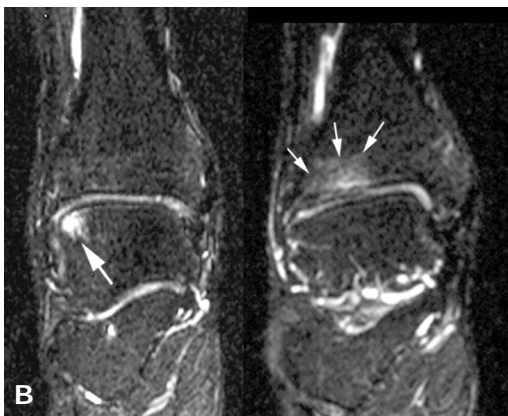
A, Anteroposterior radiograph of the right ankle.

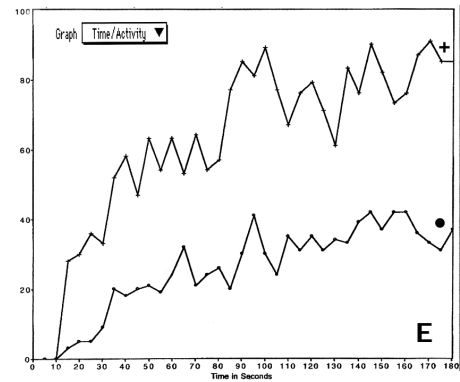
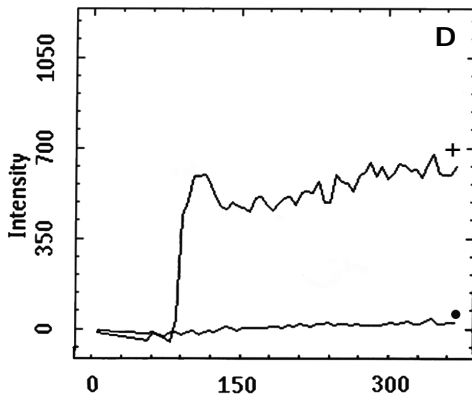
B, STIR images of the right ankle, showing increased SI in the OD lesions of the lateral talar dome (arrow) and the lateral tibia plafond (small arrows) ("kissing lesion").

C, Dyn bone scintigraphy with increased flow at lateral side of the talar dome (arrow) and tibia plafond (arrow-heads).

D, TICs of dyn MR images with increased enhancement in the talar OD lesion indicating increased vascularisation. The ROI was sampled in the centre of the OD lesion (+) and the talus marrow (-).

E, TICs of dyn bone scintigraphy with increased activity indicating increased vascularisation of OD lesion. The ROI was sampled in the centre of the OD lesion (+). Left ankle for comparison (-).





Discussion

The treatment goal in OD lesions after trauma is to promote healing and prevent localized osteonecrosis or detachment of the fragment [16,17]. Since there is increased risk of ischemia of the OD lesion, it is important that early treatment is given to prevent deformity of the subchondral bone and overlying cartilage with resulting osteoarthritis [9,23]. Several authors have emphasized the importance of determining the viability of tissues of OD lesions when forming a treatment plan [16,17]. Only dyn bone scintigraphy has been reported to accurately identify preoperatively those patients whose lesions are unlikely to heal [15-17].

The talus is a unique bone in the foot. There are no direct tendon or muscle attachments to it. It is covered by cartilage for more than 60%, because of this blood supply to the talus is limited, as there are only a few areas for entry of arteries into the bone. The talar dome is supplied by small end-arteries extending from these vessels, so blood supply to the dome is vulnerable and can easily be compromised after trauma [24]. As a result, when injured, there is an increased risk for developing osteonecrotic areas in the talar dome [6,25].

Static bone scintigraphy depicts the focal distribution of the bone-seeking agent and is not a direct assessment of the dynamic processes of the disease [16]. In our series all of the static images showed a hot spot.

Dyn bone scintigraphy with technetium ^{99m}Tc HDP has been shown to be a reliable method diagnosing OD of the talar dome. The ability of this technique to visualize bone perfusion provides a highly sensitive and specific means of early recognition of ischemia

Figure 2. 25-year-old man with persistent ankle pain after ankle sprain.

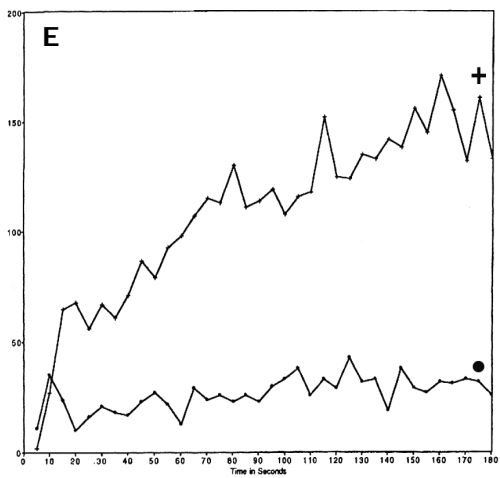
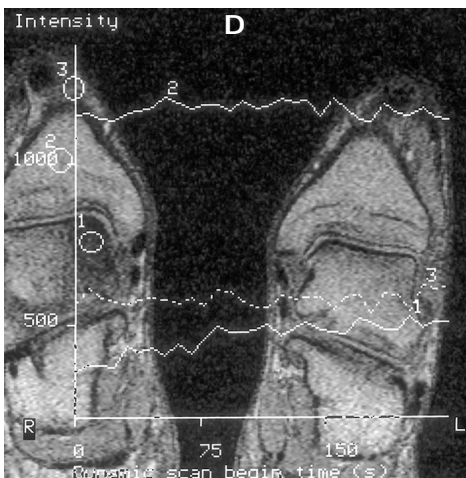
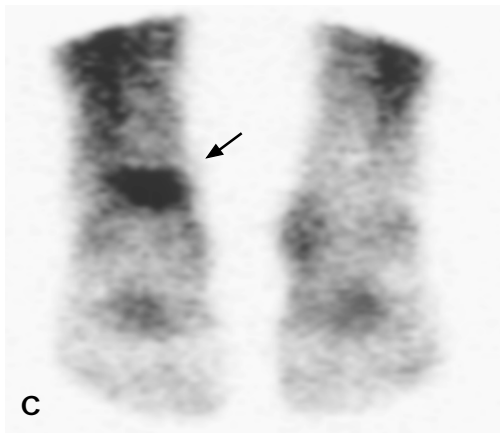
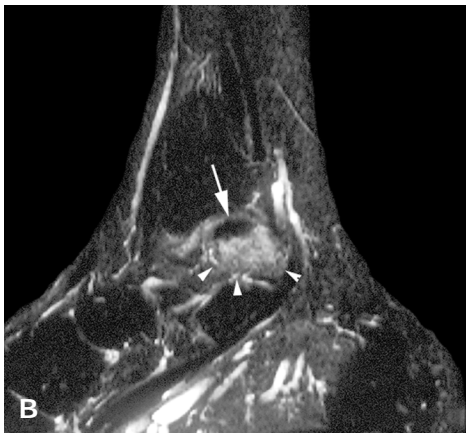
A, Anteroposterior radiograph of the right ankle, with lucency in the medial talar dome (arrow).

B, Sagittal STIR image showing an OD lesion with decreased SI (arrow) and increased SI in the surrounding talar marrow (arrowheads).

C, Dyn bone scintigraphy with increased flow at right talar OD lesion (arrow).

D, TICs of dyn MR image indicating decreased vascularisation in OD lesion. The ROI was sampled in the centre of the OD lesion (1), artery (2) and tibia (3).

E, TICs of dyn bone scintigraphy with increased flow indicating increased vascularisation of the OD lesion. ROI was sampled in the centre of the OD lesion (+). Left ankle for comparison (-).



[11,14]. Using the flow phase of the test, an assessment can be obtained of the vascularity of the lesion [15,16,24,27]. Studies have also shown that the degree of osseous uptake reflects accurately the metabolic status of the bone which seems to be related to the potential for healing of the fragment [15,16,24].

Using MR imaging, the bone marrow normally enhances following intravenous injection of Gd-DTPA. In normal bone tissue early, rapid enhancement occurs in the first two minutes after injection, followed by a slow decrease during the next 2 to 5 min [13]. In conventional T1-weighted post-contrast-enhanced images, obtained in the late vascular phase (between 4 -9 min after injection), the contrast agent is already diffusely distributed in the interstitium of bone marrow and maximal marrow enhancement is already passed [14,28]. Therefore, in order to optimally depict viability of the bone or ischemia, it is important that images are obtained in the early vascular phase [14].

Recent introduction of fast, contrast-enhanced MR imaging techniques have permitted studies of the arterial blood flow of the tissues. These have shown that lack of arterial enhancement of the bone marrow is correlated with lack of blood perfusion and thus to ischemia [13,29].

In our study we found decreased enhancement of the central area of the OD lesion in two of the 9 patients who had sustained injury to the ankle. However, this was confirmed by dyn bone scintigraphy in only one. In the other one, no central area of decreased uptake was visualized by bone scintigraphy. A potential explanation for this discrepancy could be that the superior spatial and contrast resolution of MR allowed better visualization of the small region of decreased blood flow and thus ischemia in the OD lesion. Although dyn bone scintigraphy is frequently used as the "gold standard" for determining ischemia in case of an OD lesion, the findings of our study suggest that this modality may not be accurate enough for detecting small areas of necrosis due to the inferior image resolution in comparison with dyn MR imaging. However, a disadvantage of dyn MR imaging is that with this technique only one (sometimes three) slice sections are obtained for evaluation and as a result, sampling errors may occur when the OD lesion is partially included in the image [22,28].

Although we believe that MR imaging is very sensitive in detecting vascularisation of an OD lesion, our study is limited by the fact that only a small group of patients was evaluated and that follow-up was available in only a fraction of them. Another problem is that with dyn MR imaging it is difficult to differentiate between reactive synovitis, regenerating osteochondral tissue and fibrosis [29]. However, the same is true for bone scintigraphy. Furthermore, a limitation of our study was that no histologic material was available to proof the necrotic character of the non-enhancing area in the OD lesion.

However, when surgery is performed, biopsies are not routinely obtained. In addition, it is well recognized that the findings from random biopsies cannot be used to determine the histologic status of the entire specimen because focal areas of normal appearing bone may exist adjacent to regions of necrosis making it impossible to accurately determine whether ischemia is present [13].

In conclusion, in this series of patients with OD of the talar dome we found ischemia in two cases using dyn MR imaging while this was found in only one case with dyn scintigraphy. In all likelihood the area of necrosis was not visualized with scintigraphy due to its relatively poor spatial resolution in comparison to MR imaging. Therefore, dyn MR imaging appears to be the preferred method for evaluating the viability of the OD lesions. Additional advantage of dyn MR imaging is that the procedure is easily performed following conventional MR imaging without any exposure of the patient to ionizing radiation.

References

1. Bosien WR, Staples OS, Russell SW. Residual disability following ankle sprains. *J Bone Joint Surg* 1955;37(A):1237-1243.
2. Anderson IA, Crichton MB, Grattan-Smith T, Cooper RA, Brazier D. Osteochondral fractures of the dome of the talus. *J Bone Joint Surg* 1989;71(A):1143-1152.
3. Schweitzer ME. Magnetic resonance imaging of the foot and ankle. *Magn Reson Q* 1993;9:214-234.
4. Deutsch AL. Osteochondral injuries of the talar dome. In: Deutsch AL, Mink JH, Kerr R, eds. *MRI of the foot and ankle*. Philadelphia: Lippincott-Raven, 1992:111-134.
5. Stoller DW. The ankle and foot. In: Stoller DW, ed. *Magnetic resonance imaging in orthopaedics and sports medicine*. Philadelphia: Lippincott-Raven, 1997:373-509.
6. Loomer R, Fisher C, Lloyd-Smith R, Sisler J, Cooney T. Osteochondral lesions of the talus. *Am J Sports Medicine* 1993;21:13-19.
7. Berndt AL, Harty M. Transchondral contusion (osteochondritis dissecans) of the talus. *J Bone Joint Surg* 1959;41(A):988-1020.
8. Yulish BS, Mulopulos GP, Goodfellow DB, et al. MR imaging of osteochondral lesions of talus. *J Comp Assist Tomogr* 1987;11:296-301.
9. Urman M, Ammann W, Sisler J, et al. The role of bone scintigraphy in the evaluation of talar dome fractures. *J Nucl Med* 1991;32:2241-2244.
10. Kumai T, Takakura Y, Higashiyama I, Tamai S. Arthroscopic drilling for the treatment of osteochondral lesions of the talus. *J Bone Joint Surg* 1999;81(A):1229-1235.
11. Kabbani YM, Mayer D. Magnetic resonance imaging of osteochondral lesions of the talar dome. *J Am Podiatr Med Assoc* 1994;84:192-195.
12. Nelson DW, DiPoala J, Colville M, et al. Osteochondritis dissecans of the talus and knee: prospective comparison of MR and arthroscopic classifications. *J Comput Assist Tomogr* 1990;14:804-808.
13. Cerezal L, Abascal F, Canga A, Bustamanre M, del Pinal F. Usefulness of Gadolinium-enhanced MR imaging in the evaluation of the vascularity of scaphoid nonunions. *AJR* 2000;174:141-149.
14. Sebag G, Ducou Le Pointe H, Klein I, et al. Dynamic gadolinium-enhanced subtraction MR

- imaging -a simple technique for the early diagnosis of Legg-Calvé-Perthes disease: preliminary results. *Pediatr Radiol* 1997; 27:216-220.
15. McCullough RW, Gandsman EJ, Litchman HE, Schatz SL. Dynamic bone scintigraphy in osteochondritis dissecans. *Int Orthop* 1988;12:317-322.
 16. Litchman HM, McCullough RW, Gandsman EJ, Schatz SL. Computerized blood flow analysis for decision making in the treatment of osteochondritis. *J Pediatr Orthop* 1988;8:208-212.
 17. Patetta GA, Bednarz PA, Stanitski CL, et al. The prognostic value of quantitative bone scan in knee osteochondritis dissecans a preliminary experience. *Am J Sports Med* 1998;26:7-14.
 18. Magee TH, Hinson GW. Usefulness of MR imaging in the detection of talar dome injuries. *AJR* 1998;170:1227-1230.
 19. Berg van de B, Malghem J, Labaisse MA, Noel H, Maldague B. Avascular necrosis of the hip: comparison of contrast-enhanced and nonenhanced MR imaging with histologic correlation. *Radiology* 1992;182:445-450.
 20. Cova M, Young SK, Tsukamoto H, Jones LC, et al. Bone marrow perfusion evaluated with gadolinium-enhanced dynamic fast MR imaging in a dog model. *Radiology* 1991;179:535-539.
 21. Pathria MN, Issacs P. Magnetic resonance imaging of bone marrow. *Curr Opin Radiol* 1992;4:21-31.
 22. Verstraete KL, Dierick A, De Deene Y, Uyttendaele D, et al. First-pass images of musculoskeletal lesions: a new and useful diagnostic application of dynamic contrast-enhanced MRI. *Mag Reson Imag* 1994;12:687-702.
 23. Newburg AH. Osteochondral fractures of the dome of the talus. *Br J Radiol* 1979;52:105-109.
 24. Schenck RC, Goodnight JM. Current concepts review osteochondritis dissecans. *J Bone Joint Surg* 1996;78(A):439-456.
 25. Mesqarzadeh M, Sapega A, Bonakdarpour A, et al. Osteochondritis dissecans: analysis of mechanical stability with radiography, scintigraphy and MR imaging. *Radiology* 1987;165:775-780.
 26. Bluemke DA, Petri M, Zerhouni EA. Femoral head perfusion and composition: MR imaging and spectroscopic evaluation of patients with systemic lupus erythematosus and at risk for avascular necrosis. *Radiology* 1995;197:433-438.
 27. Munk PL, Lee MJ, Logan M, Connell DG, et al. Scaphoid bone waist fractures, acute and chronic: imaging with different techniques. *AJR* 1997;168:779-786.
 28. Woude van der HJ, Verstraete KL, Hogendoorn PCW, et al. Musculoskeletal tumors: does fast dynamic contrast-enhanced subtraction MR imaging contribute to the characterization? *Radiology* 1998; 208:821-828.
 29. Stuckey SL, Kalf V, Hoy G. Bone scan findings in Kienbock's disease. A case report with atypical findings and literature review. *Clin Nucl Med* 1997;22:481-483.

CHAPTER 9

Bone marrow hyperintensities with tarsal coalition: MR imaging findings

Elizabeth S. Sijbrandij¹, Ad P.G. van Gils¹, Eduard E. de Lange²

From the Department of Radiology¹
University Hospital Utrecht and Central Military Hospital, Utrecht.
From the Department of Radiology²
University of Virginia Health Sciences Center, Charlottesville, USA.

Submitted for publication

Abstract

Objective. To report the occurrence and pattern of ill-defined subchondral hyperintensities on MR (MR) imaging in patients with talocalcaneal coalition (TCC).

Method and material. MR imaging of both feet was performed in 10 consecutive patients with 14 TCCs. There were 8 males and 2 females with ages ranging from 9-52 years (mean 25 years). Twelve of the 14 TCCs were symptomatic. MR imaging sequences included T1- and T2-weighted as well as short tau inversion time inversion-recovery (STIR) images. The images were evaluated for the presence, extent and location of ill-defined subchondral hyperintensities on MR in the hindfoot.

Results. Ill-defined subchondral hyperintensities on MR imaging were present in 12 (86%) of the 14 hindfeet with TCCs. Two of these were without symptoms. No abnormalities were seen in two symptomatic hindfeet.

Discussion and conclusion. In our series hyperintensities located in the subchondral bone adjacent to the coalition were relatively common in TCC. The presence of this specific pattern in the subchondral bone adjacent to the coalition may be indicative of tarsal coalition.

Introduction

A tarsal coalition refers to abnormal fusion of two or more independent bones of the hindfoot [1]. The most common coalitions are those between the talus and calcaneus, and between calcaneus and the navicular bone. Of these, the talocalcaneal coalition (TCC), as a weightbearing joint, is clinically the most important because it frequently causes symptoms, such as pain and giving way (instability), starting when the coalition ossifies and the foot becomes rigid [1]. In most instances, the symptoms begin at puberty sometimes following a traumatic event or repetitive injury [1-4].

With conventional radiography secondary signs of the hindfoot such as degenerative changes, talar beaking and narrowing of the posterior subtalar joint may suggest a coalition, resulting from longstanding abnormal subtalar movement. These changes, indicating hindfoot abnormality, have also been demonstrated with radionuclide studies using bone-seeking radiopharmaceuticals, although the findings have been rather non-specific [3].

It may be difficult to demonstrate the TCC by conventional x-ray radiography because visualization of the middle facet of the posterior subtalar joint is frequently hampered by

superposition of the tarsal bones and by the oblique orientation of the coalition. Demonstration may also be difficult when the coalition is non-osseous, consisting of fibrocartilagenous tissue, or when there is incomplete skeletal maturation [5].

CT has been demonstrated to be useful in depicting the site of the talocalcaneal fusion, but has limitations in visualizing fibrous coalitions [2,4,6].

MR imaging is a noninvasive procedure, which has been shown to depict the bony structures in great detail, including those of the hindfoot [6]. It has also been demonstrated that coalitions are better depicted with MR imaging than with CT, particularly the fibrous types [2,6]. An additional advantage of MR imaging is that the bone marrow is well-visualized [2]. Studies have shown that reactive changes such as arthritis or edema from stress, involving the marrow, are readily depicted with MR imaging [7].

Treatment usually consists of conservative measures. Resection of the coalition is advocated when conservative therapy fails and symptoms persist [8]. Preferably, surgery is performed early when the lesion still consists of cartilaginous tissue or immature bone. Early treatment allows improved remodeling of the adjacent foot bones and more effective improvement of the subtalar mobility, thereby preventing the development of (further) osteoarthritis [9].

The purpose of our study was to determine prevalence and extent of a hyperintensity pattern in the hindfoot in patients with TCC as demonstrated by MR imaging.

Materials and methods

We retrospectively reviewed the MR images of all consecutive patients who had undergone MR imaging of the hindfoot at our institution for pain and instability, between January 1996 and December 1998. In all patients symptoms persisted for at least three months. Often the patients could relate the onset of the symptoms to a (minor) trauma. The clinical symptoms consisted of pain in the hindfoot aggravated by exercise, limited or absent subtalar motion, flatfoot and peroneal spasm [4,7]. MR images were reviewed by two reviewers in consensus for the presence of hyperintensities on T2-weighted and short tau inversion time inversion-recovery (STIR) images, around the middle facet of the subtalar joint. The reviews were done without knowledge of the clinical findings and the results of the radiographs. Only when there was an area of abnormal marrow signal intensity (SI) located in the adjacent subcortical regions of talus and calcaneus, consisting of increased SI on T2-weighted and STIR images, it was considered as an abnormal bone marrow pattern.

The MR images were reviewed with special attention to bony abnormalities suggestive of a TCC. A coalition was considered to be 'osseous' when there was continuity of bone marrow across the mid-subtalar joint. The coalition was considered 'non-osseous' when there was subtle, irregular narrowing or an abnormal slope of the middle facet joint, with the SI of cartilage or joint fluid depicted between the suspected bones, or an area of intermediate to low SI bridging the adjacent bones within an aberrant articulation [2]. The presence of abnormal subchondral bone marrow pattern in the symptomatic feet was compared with the presence of subchondral bone marrow pattern in the asymptomatic feet using an unpaired *t*-test with a level of significance $P < 0.05$.

MR imaging was performed using a 0.5 Tesla system (Philips, Best, the Netherlands) with both hindfeet placed in a dedicated receive-only extremity coil. In each patient, the feet were imaged together. Conventional T1-weighted SE (repetition time (TR)/echo time (TE) 600 ms/23 ms) and T2-weighted SE (TR/TE 2000 ms/100 ms) images were obtained in axial and coronal orientation. STIR (3600 ms/20 ms; inversion time (TI) = 150 ms) images were obtained in coronal and/or sagittal planes. Slice thickness varied between 3 and 5 mm; the interslice gap varied between 0 and 1.5 mm. The matrix size was 256 x 256 and the field-of-view was 16 cm.

CT was performed in 7 patients, with a high-resolution technique on a helical CT scanner (Tomoscan SR 7000, Philips Medical Systems, Best, the Netherlands). Angled coronal contiguous slices (thickness 3 mm) above the talocrural joint to the calcaneocuboid joint, using a bone algorithm, were obtained. The CT criterium for osseous TCCs was a complete osseous bar between the mid-subtalar joint. Non-osseous TCCs were described as articular narrowing and cystic cortical irregularity, subchondral sclerosis, or abnormal slope of the joint.

All patients had a conventional x-ray examination of the hindfoot in anteroposterior, lateral and oblique projections.

After each MR review the reviewers analyzed the hindfoot radiographs or CT examination, if available, of each case with knowledge of the MR imaging findings.

Results

A TCC was present in 14 hindfeet of 10 patients. Of the 343 consecutive MR examinations of the hindfoot performed for persisting symptoms of pain or stiffness in the foot, ill-defined hyperintensities on both sides of the talocalcaneal joint were found in 12 feet, involving 10 patients (table 1). The duration of the symptoms in this group of 10 patients

Table 1. Talocalcaneal coalition.

| | Hyperintensities* | Normal |
|--------------|-------------------|--------|
| Symptomatic | 10 | 2 |
| Asymptomatic | 2 | 0 |

* On T2-weighted and short inversion time inversion recovery (STIR) images, around middle facet of subtalar joint.

ranged between 3 and 26 months (mean, 16 months) before MR imaging was performed. There were 8 males and 2 females with ages ranging between 9 and 52 years (mean 25 years). TCCs were present in 12 symptomatic feet and two additional TCCs were found in two asymptomatic feet.

In 5 patients the coalition was confirmed by surgery. In another 7 patients CT confirmation was made. In two coalitions only MR examination was performed.

Non-osseous union was suggested by x-ray radiography in 7 of the 14 coalitions by subtle irregularity and narrowing or abnormal slope of the middle facet joint, narrowing of the posterior subtalar joint, talar beaking or overgrowth or undergrowth of the sustentaculum tali and medial process of the talus. Incomplete skeletal maturation existed in 2 patients, but the coalition was suggested in one patient by secondary signs of the hindfoot: irregularity and narrowing of the middle facet joint.

Only one of the coalitions was osseous, and all other ones were non-osseous. Six TCCs were present in the right and eight in the left foot. In 9 of the 14 hindfeet there was focal increased SI involving the bone marrow of both the talus and calcaneus directly adjacent to the coalition (Fig. 1 and 2). None of the 329 asymptomatic feet showed the typical ill-defined bone marrow pattern. In the two children the specific "heterogeneous bone marrow signal" involved the talus and calcaneus adjacent to the coalition (one bilateral and one unilateral coalition), together with foci of high SI also noted to be present in the remainder of talus and calcaneus on the symptomatic and contralateral, asymptomatic side (Fig. 3). No hyperintensities were found in two of the 14 hindfeet, with one of those involving an osseous TCC. There was a significant difference in the symptomatic and asymptomatic group ($P < 0.05$), as regards to the presence of typical bone marrow pattern.

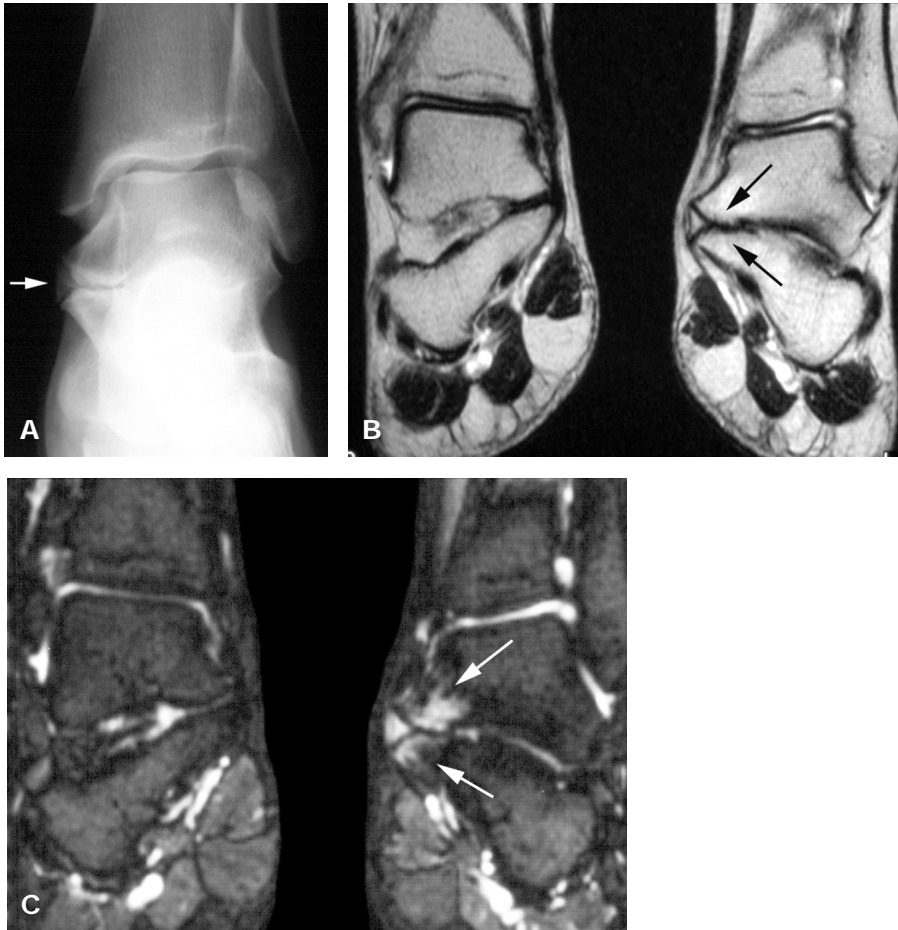


Figure 1.

A, Anteroposterior radiograph of the hindfoot of a 20-year-old man with unilateral pain and instability, showing coalition (arrow) of the middle facet of the subtalar joint.

B, Coronal T2-weighted SE (TR/TE 2000 ms/100 ms) MR image of the left hindfoot showing fibrous coalition (arrows) with an enlarged sustentaculum and medial process of the talus and abnormal slope of the middle facet joint. The contralateral middle facet joint is normal.

C, Coronal short tau inversion recovery (STIR, repetition time/echo time/ inversion time 3600 ms/20 ms/ 150 ms) demonstrates ill-defined hyperintensities (arrows) in the subchondral bones adjacent to the coalition.

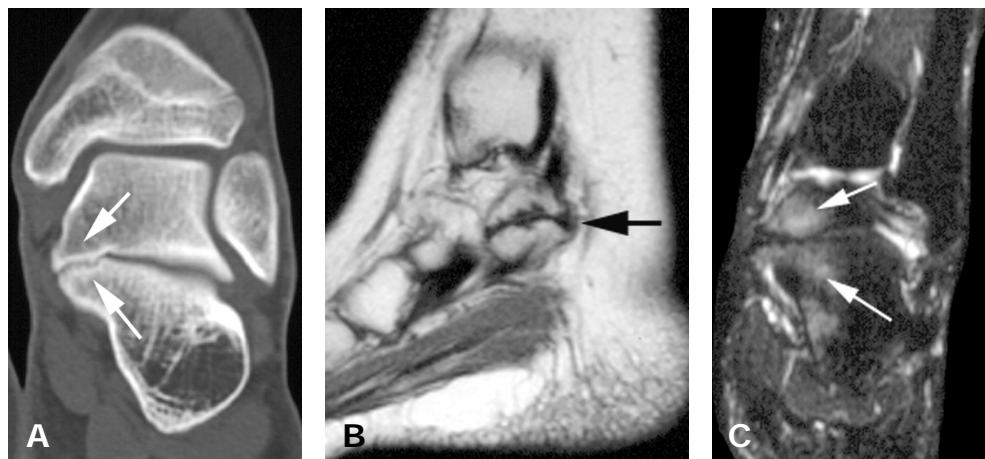


Figure 2.

A, Coronal CT scan of a 28-year-old man with unilateral painful hindfoot, showing a fibrous coalition as evidenced by an irregular narrow middle facet joint (arrows).

B, Sagittal T1-weighted SE (TR/TE 600 ms/23 ms) MR image shows fibrous coalition with an abnormally narrowed and irregular middle facet joint (arrow).

C, Coronal short tau inversion recovery (STIR, repetition time/echo time/ inversion time 3600 ms/ 20 ms/150 ms) demonstrated the presence of ill-defined hyperintensities adjacent to the middle facet of the subtalar joint (arrows).

Discussion

Tarsal coalitions are believed to be congenital in origin and caused by failure to segment the tarsal bones resulting in absence of normal joint formation. The most common types are those between the talus and calcaneus and between calcaneus and navicular bone; however other bones of the foot can also be involved [9]. Tarsal coalitions are often bilateral (50%). Simultaneous evaluation of the opposite foot is therefore recommended [4]. Men are more commonly affected than women [2]. Early diagnosis is important because the coalition may lead to joint problems and disability of the foot, particularly when activities are performed that are stressful for the foot.

The first symptoms usually appear between the ages of 12 and 16, when the coalition ossifies, causing increased rigidity of the foot [1,7]. However, limitation of the subtalar motion may sometimes be difficult to diagnose in the presence of a coalition. Pain is usually not the result of the fusion itself, but is caused by disturbances in the inversion/eversion motion of the hindfoot [3,9,10]. In adult patients it may be caused by arthritis rather than muscle spasm [8].

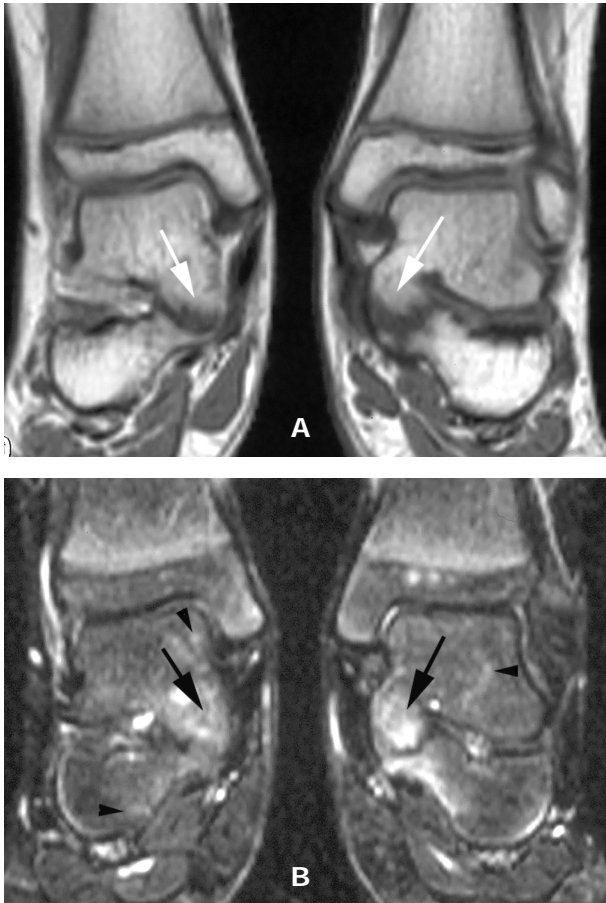


Figure 3.

A, Coronal T1-weighted SE (TR/TE 600 ms/23 ms) MR image of a 10-year-old boy with bilateral painful hindfeet, showing a bilateral fibrous coalition (arrows).

B, Coronal short tau inversion recovery (STIR, repetition time/echo time/ inversion time 3600 ms/20 ms/150 ms) shows hyperintensities involving the subchondral bones around the coalition (arrows). Bone marrow heterogeneously (high signal foci) in the talus and calcaneus (arrowheads).

We found 14 (4%) TCCs in 343 patients, this is well within the range 1-6 % reported in the literature [1]. In twelve patients (86%) the hyperintensity pattern was present in the subchondral bone marrow adjacent to the coalition. This bone marrow pattern was absent in two of the symptomatic coalitions (one of them involving an osseous coalition), while there was hyperintensity around the subtalar joint in two of the asymptomatic patients with TCCs.

It remains unclear what the exact cause of the hyperintensity pattern is in patients with TCC. It is possible that, due to the rigidity of the joint involved by the lesion, the gliding motion of the joint is hampered, causing abnormal stress on the articular surfaces and the subchondral bone of the joints adjacent to the fusion. As a result, "stress may exceed

bone strength" resulting in microfractures of the subchondral trabecular bone, causing edema. It has also been postulated that the augmented concentration of radionuclides in scintigraphy is most likely the result of abnormal forces on the bone adjacent to the subtalar coalition and not at the side of the fusion itself where there is no motion or bone turnover [3]. Predominance of the hyperintensity in the tarsal bones appears to correlate with the distribution of stress fractures [2]. Reactive changes as focal marrow fibrosis, fibrovascular granulation tissue replacing fatty marrow, or early avascular necrosis at the subchondral location secondary to degenerative articular disease, must also be considered, especially in the adult patient [13].

In the two children of our series with symptomatic coalitions, hyperintensities were seen adjacent to the coalitions, together with foci of high SI involving the entire talus and calcaneus of both feet. A similar pattern has been described in a series of children without coalition [12]. A symmetric, heterogeneous edema pattern was found in 57% of those children (N=35) aging between 6 and 15 years, who had no evidence of coalitions or other pathologic findings, leading to the conclusion that these patterns of edema in the hindfoot represented a normal finding in the growing skeleton [12].

To our knowledge, the presence of a hyperintensity pattern in patients with coalition has not been described in earlier series involving patients who underwent MR imaging. One case report noticed "bone marrow edema" in the calcaneus, talus and cuneiform in a 41 year old woman with a TCC [8]. However, in most reports dedicated MR pulse sequences such as STIR were not used to provide good image contrast between fat and water [5]. The use of such sequences has been shown to be important in demonstrating bone marrow hyperintensities [7].

Our study does have several limitations. First, it involved only a small number of patients. However, coalitions of the hindfoot are relatively uncommon. Second, surgical proof of the coalition was only obtained in five patients who underwent exploration or arthroscopy of the foot. However, the presence of a coalition was also confirmed in all of the patients based on the findings of CT and radiography. Third, the finding of bone marrow ill-defined high-signal-intensity zones on STIR or T2-weighted images is nonspecific and other diagnoses also need to be considered [13]. These include stress response, transient osteoporosis or reactive changes secondary to degenerative articular disease.

In conclusion, on MR imaging T2-weighted and short tau inversion-recovery (STIR) images we found a high occurrence of (ill-defined) hyperintensities (86%) in patients with a coalition of the hindfoot. In most cases, the findings were focal and involved the subchondral bones adjacent to the TCC. In our opinion the presence of this typical bone marrow

pattern in the middle facet joint between talus and the calcaneus is suggestive for tarsal coalition. So when ill-defined hyperintensities are found in the talus and calcaneus adjacent to the middle facet in a patient undergoing MR imaging of the foot, the presence of a coalition needs to be considered.

References

1. Mosier KM, Asher M. Tarsal coalition and peroneal flat foot. *J Bone Joint Surg* 1984;66(A):976-984.
2. Wechsler RJ, Schweitzer ME, Deely DM, Horn BD, Pizzutillo PD. Tarsal coalition: depiction and characterization with CT and MR imaging. *Radiology* 1994;193:447-452.
3. Goldman AB, Pavlov H, Schneider R. Radionuclide bone scanning in subtalar coalitions: differential considerations. *AJR* 1982;138:427-432.
4. Pineda C, Resnick D, Greenway G. Diagnosis of tarsal coalition with computed tomography. *Clin Orthop* 1986;208:282-288.
5. Lee MS, Harcke HT, Kumar SJ, Bassett GS. Subtalar joint coalition in children: new observations. *Radiology* 1989;172:635-639.
6. Masciocchi C, D'Archivio C, Barile A, et al. Talocalcaneal coalition: computed tomography and magnetic resonance imaging diagnosis. *Eur J Rad* 1992;15:22-25.
7. Lazzarini KM, Troiano RN, Smith RC. Can running cause the appearance of marrow edema on MR images of the foot and ankle. *Radiology* 1997;202:540-542.
8. Mandell GA, Harcke HT, Hugh J, Kumar SJ, Maas KW. Detection of talocalcaneal coalitions by magnification bone scintigraphy. *J Nucl Med* 1990;31:1797-1801.
9. Herzenberg JE, Goldner JL, Martinez S, Silverman P. Computerized tomography of talocalcaneal tarsal coalition: a clinical and anatomic study. *Foot Ankle Int* 1986;6:273-288.
10. Resnick D. Radiology of the talocalcaneal articulations. *Radiology* 1974;111:581-586.
11. Knapp HP, Tavakoli M, Levitz SJ, Sobel E. Tarsal coalition in an adult with cavovarus feet. *J Am Podiatr Med Assoc* 1998;88:295-300.
12. Pal CR, Tasker AD, Ostlere SJ, Watson MS. Heterogeneous signal in bone marrow on MRI of children's feet: a normal finding? *Skeletal Radiol* 1999;28:274-278.
13. Zanetti M, Bruder E, Romero J, Hodler J. Bone marrow edema pattern in osteoarthritic knees: correlation between MR imaging and histologic findings. *Radiology* 2000;215:835-840.

CHAPTER 10

Overuse and sports-related injuries of the ankle and hindfoot: MR imaging findings

Elizabeth S. Sijbrandij¹, Ad P.G. van Gils¹, Eduard E. de Lange²

From the departments of Radiology¹
University Hospital Utrecht and Central Military Hospital, Utrecht
From the department of Radiology²
University of Virginia Health Sciences Center, Charlottesville USA

Submitted for publication

Abstract

Professional and recreational sporting activities have increased substantially in recent years and have led to a rise in the number of sports-related and overuse injuries. Magnetic Resonance (MR) imaging has become an important tool for evaluating the lower leg, providing the necessary information for patient management and rehabilitation following this injury [1]. The purpose of this essay is to give an overview of the MR findings of common overuse injuries and sports-related injuries to the bones and soft-tissue structures of the hindfoot and ankle.

Introduction

Professional and recreational sporting activities have increased substantially in recent years and have led to a rise in the number of sports-related injuries. The foot and ankle are often affected, particularly by exercise activities such as running and aerobics. Magnetic Resonance (MR) imaging has become an important tool for evaluating the lower leg providing the necessary information for patient management and rehabilitation following sports-related injury [1]. Although most studies have focussed on the changes occurring after trauma, the effect of continued, repetitive stress has had less attention. The purpose of this essay is to give an overview of the MR imaging findings of common stress syndromes of the foot and ankle.

Osseous injuries

Bone bruises

Bone bruises together with ligament injuries are common after recurrent ankle sprains. These subchondral contusions, particularly when they are minor, are usually not detected by conventional radiography [2]. The clinical manifestation of these lesions is often nonspecific. Repeated trauma can lead to more severe osteochondral injury which in turn may result in osteochondral fractures with progressive disability [3]. Bone bruises usually arise when impactional and rotational forces occur during an inversion injury, causing trabecular microfractures, hemorrhage, edema and hyperemia [4,5]. Using MR imaging, the hemorrhage and edema are visualized as ill-defined semi-circular areas of abnormal signal intensity in the subcortical bone especially short tau inversion recovery (STIR) images have been shown to be helpful (Fig.1). With MR imaging the abnormalities are demonstrated with high sensitivity, allowing early detection and treatment of the findings.

Figure 1. Runner, 18-year-old, with a bone contusion after inversion injury. Coronal short tau inversion recovery (STIR) demonstrates a bone contusion in the lateral aspect of the talar dome, with an area of high-signal intensity presenting hemorrhage and edema (white arrow). The overlying cortex is intact (small white arrows).



Osteochondritis dissecans

Osteochondritis dissecans occurs with (repetitive) inversion injury to the ankle. In particular, the talus is prone to these changes because of its blood supply and the convex surface of the joint. Military recruits are especially prone to this kind of injury. With conventional radiographs the osteochondral fracture is difficult to diagnose or may not be recognized [2,5]. Using MR imaging, the fractured segment can be visualised and the condition of the articular cartilage can be assessed with high accuracy [2,5]. In particular, it can be assessed whether the fragment is still situated in its fracture bed or whether loosening has occurred (Fig. 2). Diagnosis of the severity of osteochondritis dissecans is important as treatment is based on the status of the osteochondral fragment [5].

Stress response and stress fractures

The bones are in a constant process of resorption and formation as a response to daily activities. With repetitive stress this remodeling of the bone is distorted, leading to an increase of bone resorption and less bone formation. This in turn is followed by focal trabecular microfractures with associated edema and hemorrhage, (stress response, Fig. 3) which may further progress into a stress fracture (Fig. 4) [5]. Considering the foot and ankle, runners and jumpers are by far the most affected group with changes of stress to the bones. In these individuals, the tibia, fibula and calcaneus are most commonly involved [1]. MR imaging has been demonstrated to be a highly sensitive technique for detecting changes of stress at an early stage.

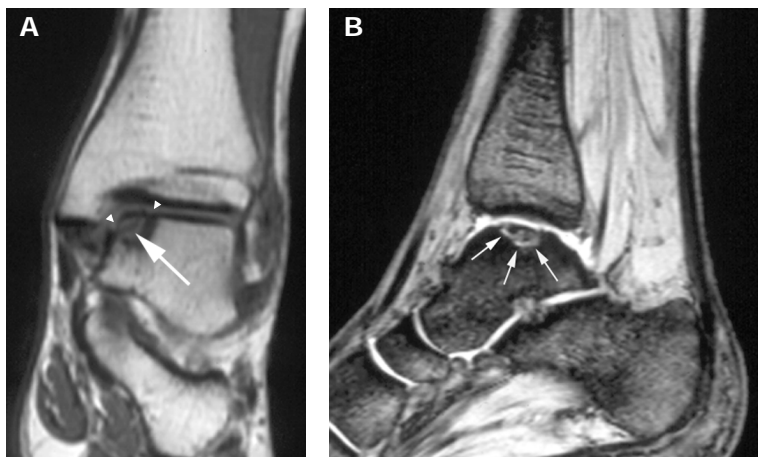


Figure 2. Male jumper with two years pain in the medial side of the ankle. **A**, Coronal T1-weighted SE demonstrates an osteochondral fragment in the medial aspect of the talar dome (white arrow). The talar cortex is fractured (arrowheads). **B**, Sagittal GRE MR image demonstrates an area of high-signal intensity around the osteochondral fragment typical of loosening (arrows).

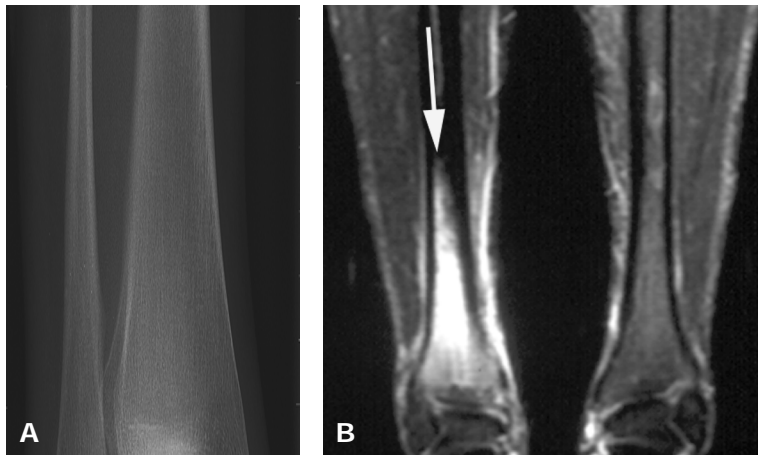


Figure 3. Stress response in the distal tibia in a 42-year-old male runner. **A**, Anteroposterior radiograph demonstrates no abnormalities. **B**, Coronal STIR T2-weighted MR image demonstrates diffuse high signal intensity (arrow) in the intramedullary space of the right tibia, representing bone marrow edema. The cortex shows no abnormalities.

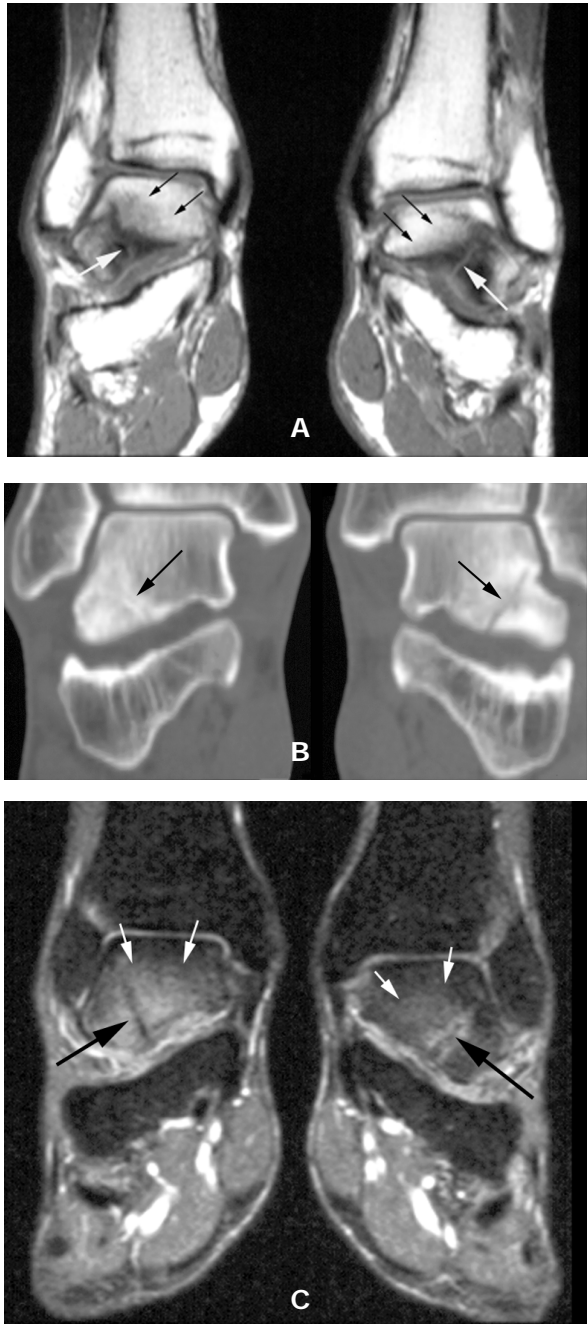


Figure 4. Tri-athlete with stress fractures of both tali.

A, Coronal T1-weighted spin-echo MR image shows moderately decreased signal intensity (black arrows) of the tali with a line (white arrows) representing stress fractures.

B, Coronal CT of both hindfeet showing stress fractures (arrows).

C, Coronal STIR T2-weighted MR image obtained at the same level as figure B demonstrates edema (white arrows) in the talus and the low signal intensity fracture lines (black arrows) extending to the cortex.

Impingement syndromes

Anterior impingement syndrome

Osteophyte formation in the ankle joint is most often seen at the anterior lip of the tibia secondary to athletic injuries [6]. Repetitive bouncing of the anterior aspect of the tibia onto the neck of the talus, resulting in anterior impingement syndrome with joint swelling, limited motion and pain. Entrapment of synovial tissue between the talus and tibia leads to osteophytes which maintain the inflammation and irritation of the synovia [5].

Anterolateral impingement syndrome

After (repetitive) ankle sprain, intra-articular hematoma and/or capsular tear of the anterior talofibular ligament and synovitis causes hyperplasia of synovial tissue in the anterolateral gutter. This increases further hyperplasia and subsequent fibrosis of synovial tissue in the anterolateral gutter, causing the anterolateral impingement syndrome [5,6]. Typically with this syndrome, a soft tissue mass can be found with MR imaging, representing hyperplastic synovia and fibrotic tissue (Fig. 5).

Posterior impingement syndrome

In case of posterior impingement syndrome, the talus and posterior capsule of the ankle joint and attached synovium become entrapped between the posterior aspect of the tibia and posterior facet of the calcaneus during plantar flexion of the foot. This results in bone and/or soft tissue lesions. The synovia hypertrophies due to the repetitive entrapment and becomes inflamed. Ballet dancers repetitively plantar hyperflex the foot are most commonly affected by this entity [7]. However, posterior impingement can also be the result of repetitive trauma due to impingement, occurring in runners. On occasion, the syndrome may be caused by a prominent os trigonum. With MR imaging, the hypertrophied synovial tissue is identified as a soft tissue mass in the posterior aspect of the joint (Fig. 6 and 7).

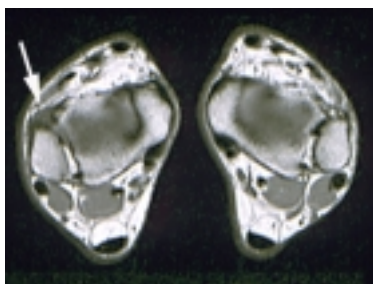


Figure 5. Female runner (21-year-old) with anterior impingement syndrome of the right ankle resulting from repetitive inversion injuries.

Axial proton density weighted fast spin-echo MR image demonstrates increased soft tissue mass (arrow) in the right anterolateral gutter representing thickening of the anterior tibiofibular ligament, synovial hyperplasia and fluid. The left ankle is normal.

Tenosynovitis, Tendinosis and tendon rupture

Achilles tendon

Achilles tendon injury is very common in running athletes. Typically, the entity occurs when there is a sudden increase in training frequency or intensity [5]. With overuse, the peritendinous structures of the Achilles tendon and the bursa between the tendon and calcaneus become inflamed, a condition termed peritendinitis (posterior located called paratenonitis) and bursitis. Achilles tendinosis represents intratendinous degeneration of the tendon itself with focal areas of mucoid degeneration and intrasubstance hemorrhage (Fig. 8 and 9). This degeneration leads to weakness of the tendon, thereby increasing the risk of a rupture. When the tendinosis is located near the insertion of the Achilles tendon together with a prominent posterior superior tuberosity of the calcaneus and bony impingement on the retrocalcaneal bursa, the entity is called the Haglund syndrome (Fig. 10) [5] .

Tibialis anterior, tibialis posterior, and peroneal tendons

Tenosynovitis of the tibialis anterior, tibialis posterior and/or peroneal tendon resulting from overuse is frequently seen in runners. Repetitive microtrauma of the tendon in these individuals causes an increase of the synovial fluid which in turn causes distention of the

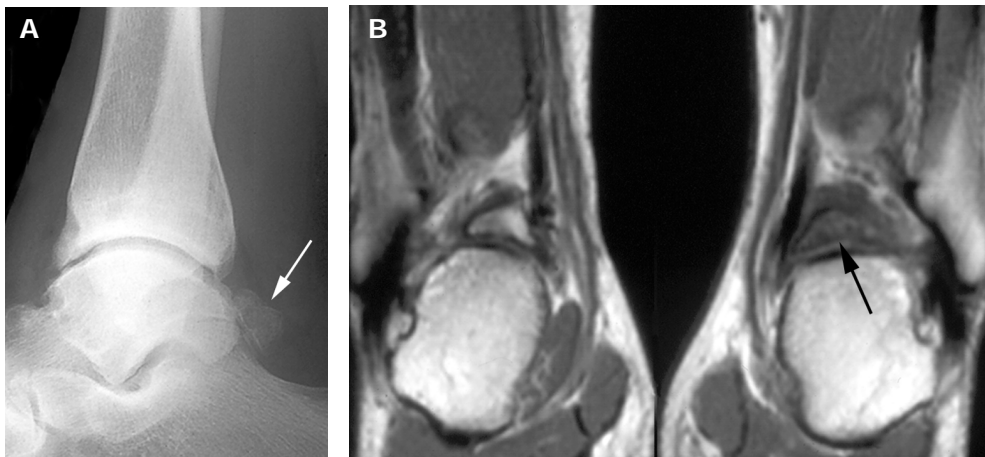


Figure 6. Os trigonum in a 44-year-old ballet dancer.

A, Lateral radiograph of the ankle demonstrates a prominent os trigonum (arrow) at the posterior aspect of the talus.

B, Coronal T1 -weighted spin-echo MR image with edema in the left os trigonum (arrow). Right os trigonum is normal.



Figure 7. Posterior impingement syndrome in 24-year-old runner. Sagittal T2-weighted GRE MR image shows soft tissue mass (arrow) representing hypertrophied synovia caused by repetitive entrapment of the talus and soft tissue between the tibia and calcaneus during hyperflexion of the foot.

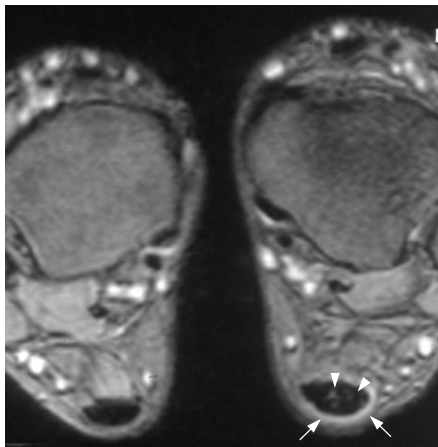


Figure 8. Peritendinitis in male marathon runner. Axial T2-weighted spin-echo MR image at the level of the talus shows fluid (arrows) around the posterior aspect of the Achilles tendon. The tendon is also slightly thickened with subtle intratendinous signal intensity (arrowheads)

tendinous sheath (Fig. 11). With further progress chronic tendinitis occurs with thickening of the tendon and eventually, the tendon can rupture. Posterior tibialis tendinitis at the insertion of the tendon is often associated with an accessory navicular bone (Fig. 12). A peroneal splits syndrome is present when there are repetitive subluxations of the peroneus brevis tendon over the lateral ridge of the fibula, leading to longitudinal rupture of the tendon (Fig. 13) [8].

Plantar Fasciitis

The plantar fascia is a thick aponeurosis in the foot that arises from the medial calcaneal tuberosity and inserts onto the base of each proximal phalanx. Inflammation of the fascia near its attachment is frequently seen in distance runners caused by repetitive trauma. Due to microtears, inflammation and fibrous repair degeneration and focal thickening of the plantar fascia surrounded by edema occurs [9]. In chronic plantar fasciitis the entire fascia is thickened. As the plantar fascia is not attached to the heel spur often found on x-ray films, the presence of such a spur is not reliable for making the diagnosis of plantar fasciitis (Fig. 14) [9].



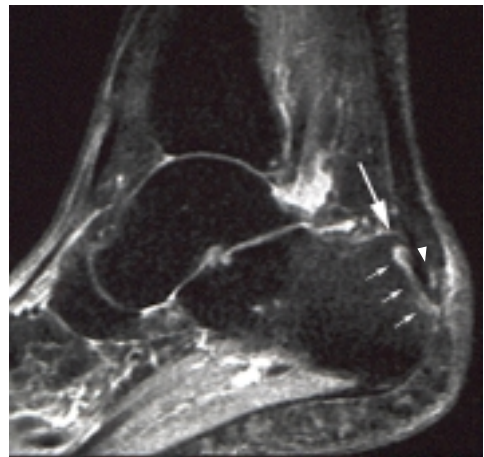
Figure 9. Long distance runner, 29-year-old, with inflammation of the Achilles tendon and retrocalcaneal bursitis.

A, Sagittal T2-weighted GRE MR image demonstrates fluid in the distended bursa between the Achilles tendon and calcaneus (arrow). There is also moderately increased signal intensity in the distal Achilles tendon (arrowhead).

B, Axial T2-weighted GRE MR image showing the enlarged, fluid filled retrocalcaneal bursa (arrow) and increased signal intensity in the Achilles tendon (arrowhead).

Figure 10. Haglund syndrome in a 23-year-old female runner.

Sagittal fast spin-echo inversion recovery MR image shows focal edema in the calcaneus (small arrows), and around the Achilles tendon near its insertion. An associated Haglund's deformity with bony prominence of the postero-superior calcaneal tuberosity is seen (white arrow). Intratendinous high signal intensity (arrowhead).



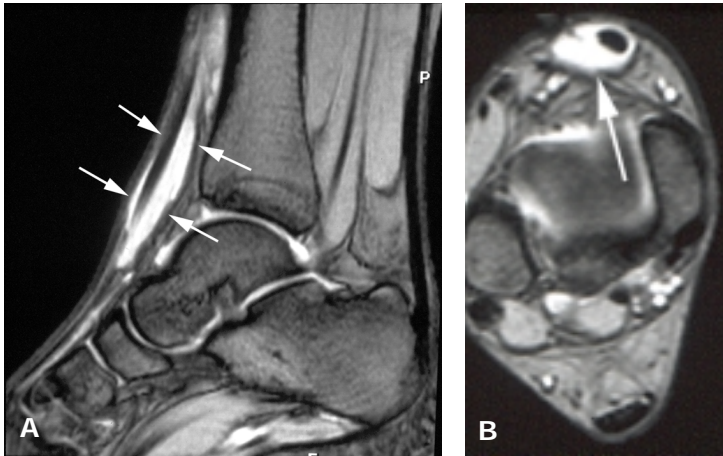


Figure 11. Acute tenosynovitis of the tibialis anterior tendon in a 38-year-old sportsman.
A, Sagittal T2-weighted gradient echo MR image demonstrates normal caliber of tibialis anterior tendon surrounded by fluid in the tendon sheath (arrows).
B, Axial T2-weighted fast spin-echo GRE MR image of the ankle shows the fluid (arrow) in the distended tendon sheath.

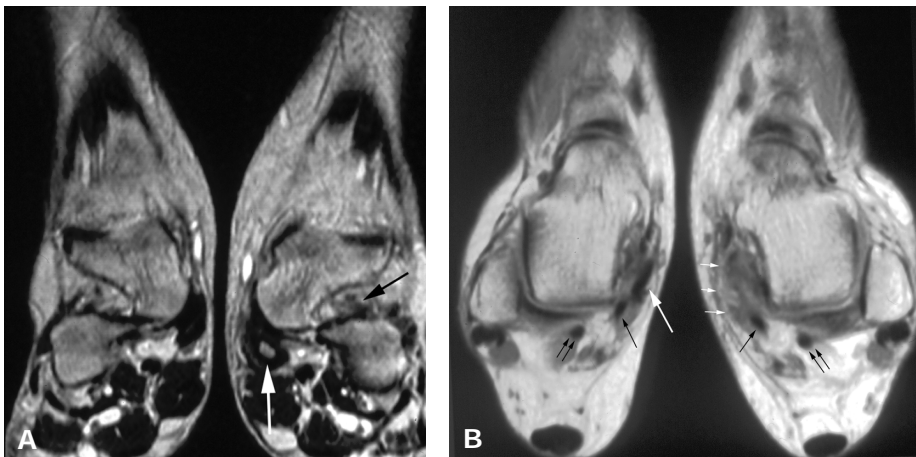
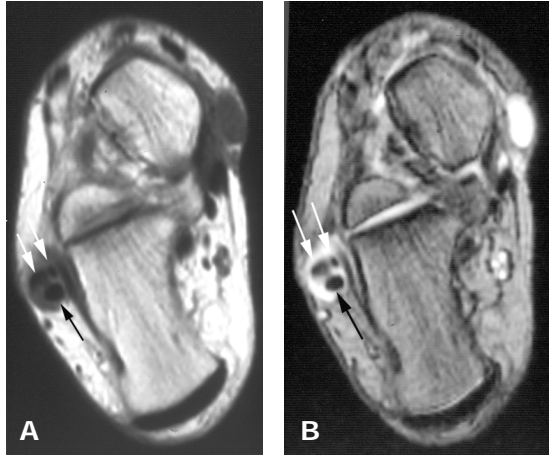


Figure 12. 40-year-old runner with rupture of the posterior tibialis tendon associated with accessory navicular bone.
A, Coronal T1-weighted GRE MR image at the level of the sinus tarsi (black arrow) showing accessory navicular bone on the medial side (white arrow).
B, Axial proton density weighted fast spin-echo MR image at the level of the talus demonstrates rupture of the left posterior tibialis tendon at the insertion of the accessory navicular bone. There is edema (small white arrows) in the adjacent soft tissue. Normal right posterior tibialis tendon (white arrow), flexor hallucis longus tendons (black arrows), and flexor digitorum longus tendons (double black arrows).

Figure 13. Male runner, 41-year-old, with peroneal splits syndrome.

A, Axial T1-weighted spin-echo MR image of the left ankle at the level of the posterior subtalar joint. There is enlargement of the peroneal tendon sheath due to fluid with two peroneal brevis tendons (white arrows) and one peroneus longus tendon (black arrow).

B, Axial T2-weighted GRE MR image, at the same level better demonstrates the fluid in the enlarged tendon sheath. Also noted is splitting of the peroneal brevis tendon seen anteriorly in the tendon sheath: the tendon is seen as two separate structures (white arrows). The peroneus longus tendon seen posteriorly is normal (black arrow).



Sinus tarsi syndrome

The tarsal sinus is an anatomic space between the inferior aspect of the talus and the superior aspect of the calcaneus, just anterior to the posterior subtalar joint [10]. It consists of ligaments, vessels and nerves, surrounded by connective and fatty tissue. Inversion injury either as a result of single or repetitive trauma of the ankle can lead to stretching and tearing of the ligamentous structures of the sinus tarsi, causing inflammation of the structures and subtalar instability [11]. Routine radiographs are negative as are stress views [1]. The edema and fibrosis of inflamed tarsal sinus fat are readily visualized with MR imaging (Fig. 15) [1,10,11].

Tarsal tunnel syndrome (jogger's foot)

Tarsal tunnel syndrome occurs when the posterior tibial nerve becomes entrapped as it passes through the tarsal tunnel. A tumor, ganglion-cyst or large accessory soleus muscle can compress the entrance or the tarsal tunnel itself (Fig. 16). Blood supply of the soleus muscle is marginal and therefore exercise may induce ischemia and edema in this muscle. Typically, after sports training when the medial neurovascular bundle is compressed, the patient notices a burning pain in the heel and a reduced sensation in the sole of the foot [12].

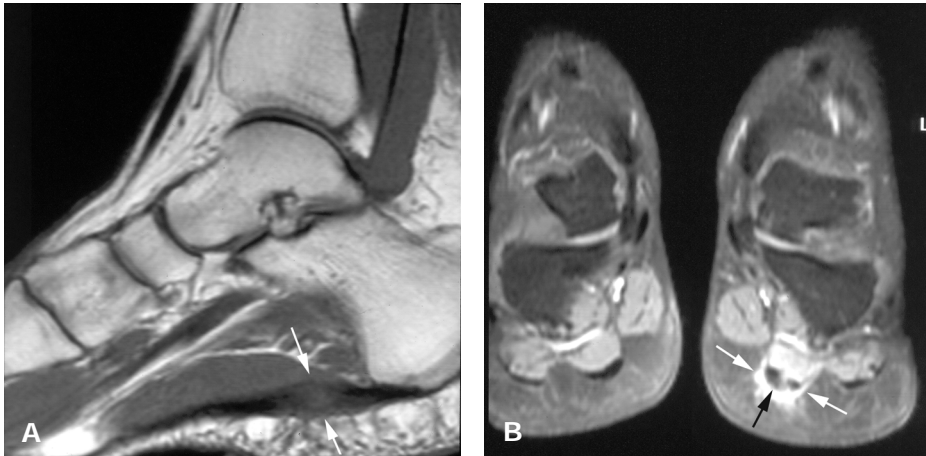


Figure 14. Plantar fasciitis in a 18-year-old jumper.
A, Sagittal T1-weighted spin-echo image of the left foot shows marked thickening and signal heterogeneity (arrows) of the plantar fascia near its attachment to the medial calcaneal tuberosity.
B, Coronal T2-weighted fast inversion recovery MR image demonstrates thickened fascia (black arrow) surrounded by edema (white arrows). The right ankle is normal.

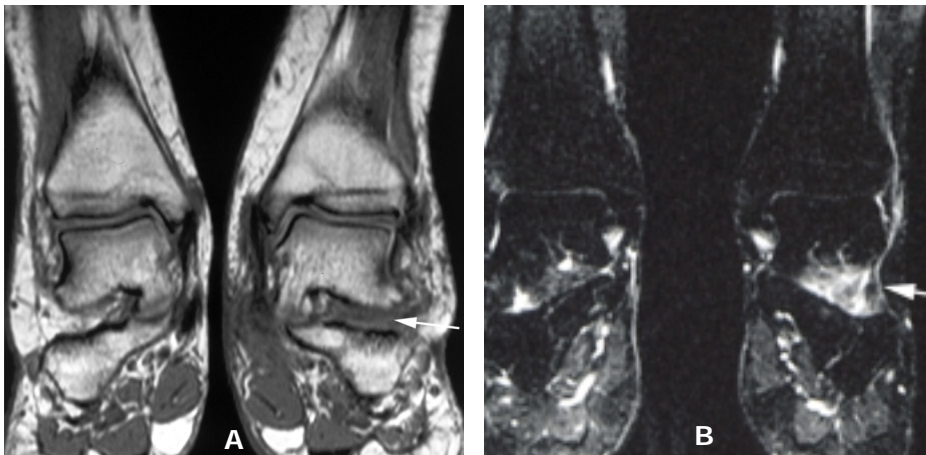


Figure 15. Sinus tarsi syndrome in a 22-year-old female runner after recurrent inversion injuries.
A, T1-weighted coronal spin-echo MR image shows diffuse infiltration (arrow) of the left tarsal sinus obliterating the fat and interosseous talo-calcaneal ligament. The right side is normal.
B, Coronal STIR T2-weighted MR image at the level of the sinus tarsi demonstrates increased signal intensity (arrow) on the left, representing chronic synovitis and inflammation.

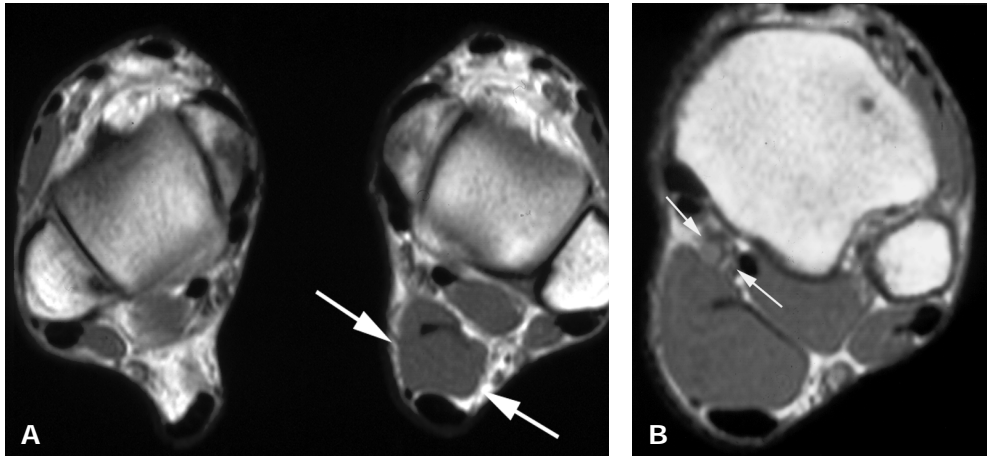


Figure 16. Tarsal tunnel syndrome in a 36-year-old runner with symptoms caused by hypertrophy of an accessory soleus muscle.

A, Axial T1-weighted spin-echo MR image at the level of the talus demonstrates accessory soleus muscle (between white arrows). The right ankle is normal.

B, Axial T1-weighted spin-echo MR image at a higher level shows accessory soleus muscle causing compression of the medial neurovascular bundle after exercise (between white arrows).

References

1. Clanton TO. Athletic injuries to the soft tissue of the foot and ankle. In: Coughlin MJ, Mann RA, eds. *Surgery of the foot and ankle* St Louis: Mosby, 1999:1090-1209.
2. Deutsch AL. Osteochondral injuries of the talar dome. In: Deutsch AL, Mink JH, Kerr R, eds. *MRI of the foot and ankle*. Philadelphia: Lippincott-Raven, 1992:75-109.
3. Schweitzer ME. Magnetic resonance imaging of the foot and ankle. *Magn Reson Q* 1993;9:214-234.
4. Kaplan PA, Craig WW, Kilcoyne RF, Brown DE, Tusek D, Dussault RG. Occult fracture patterns of the knee associated with anterior cruciate ligament tears: assessment with MR imaging. *Radiology* 1992;183:835-838.
5. Bencardino J, Rosenberg ZS, Delfaut E. MR imaging in sports injuries of the foot and ankle. *MRI Clin North Am* 1999;7:131-149.
6. Farooki S, Yao L, Seeger LL. Anterolateral impingement of the ankle: effectiveness of MR imaging. *Radiology* 1998;207:357-360.
7. Khan K, Brown J, Way S, et al. Overuse injuries in classical ballet. *Sports Med* 1995;19:341-357.
8. Schweitzer ME, Eid ME, Deely D et al. Using MR imaging to differentiate peroneal splits from other peroneal disorders. *AJR* 1997;168:129-133.
9. Kier R. Magnetic resonance imaging of plantar fasciitis and other causes of heel pain. *MRI Clin North Am* 1994;2:97-107.
10. Beltran J. Sinus tarsi syndrome. *MRI Clin North Am* 1994;2:59-65.
11. Klein MA, Spreitzer AM. MR imaging of the tarsal sinus and canal: normal anatomy, pathologic findings, and features of the sinus tarsi syndrome. *Radiology* 1993;186:233-240.
12. Kerr R. Spectrum of disorders. In: Deutsch AL, Mink JH, Kerr R, eds. *MRI of the foot and ankle*. Philadelphia: Lippincott-Raven, 1992:345-365.

———— CHAPTER 11 ————

Summary and conclusions

General discussion and recommendations

General discussion

Ankle sprains are extremely common. The recurrence rate of this heterogeneous disorder is high. Approximately 40% of the patients suffer from residual symptoms. The radiologist who is asked to provide the clinician with anatomical and pathological information of the foot and ankle has to consider different diagnostic imaging modalities: conventional radiography, stress views, ultrasound, helical CT and MR imaging. At present no single method clearly stands out as superior for foot and ankle problems. With the introduction of CT and MRI, cross-sectional images have allowed new opportunities for the examination of ankle and hindfoot. Helical CT is the first choice for imaging bony structures such as fractures or loose fragments and has the advantage of a wider availability and a shorter acquisition time compared with MR imaging. With MR imaging early identification of osteochondral, ligamentous or bone marrow lesions after inversion sprains of the ankle is possible now. The relative lack of familiarity with this anatomic region and stringent technical demands are responsible for the initial slower acceptance of the use of MR imaging. For the radiologist, this new modality requires knowledge of normal anatomy, essential for the performance and interpretation of an MR imaging examination, as well as know-how of the technical details regarding MR imaging of foot and ankle together with the clinical significance of the results of these examinations. The clinician on the other hand needs some familiarity with the technical possibilities and indications of the MR imaging together with more detailed and specific questions regarding foot and ankle pathology. Despite MR imaging's well-known capacity for depicting pathology in ankle and foot, its indications may be limited to the evaluation of highly competitive athletes or those patients with a history of *chronic* ankle instability as the availability is still/yet restricted. The decreasing costs of MR imaging should be no longer a factor in decision-making in medicine today. However, an appropriate work-up with a thorough history and physical examination, as well as adequate radiological evaluation has to be made. Otherwise without a functional diagnosis, ankle and hindfoot pain and/or instability can lead to prolongation and worsening of symptoms.

The role of radiology in the sprained ankle syndrome

Sprained Ankle Syndrome (SAS) is a chronic syndrome for which there is no single cure to date. Primarily the treatment for ankle sprains should be conservative as the natural course of SAS is often quite benign. The process should always begin with conservative treatment. If the results are not satisfactory, a clinical evaluation of the patient and a

radiological work-up need to be done in order to decide whether the patient is eligible for prolonged conservative treatment or (eventually) more invasive treatment such as arthroscopy or operation. The principle of reserving invasive therapy as the last possible method of action is important. Especially when competitive or recreational athletes develop pain, the natural tendency is to ascribe those symptoms to a sports-related injury. Delayed diagnosis of unrelated pathology can occur because of this clinical bias. It must not be forgotten that patients with pain (whether or not athletes) deserve an unbiased evaluation in order to exclude more ominous disease. Clinical signs may aid in the diagnosis of extent of the injury, but are not diagnostic for specific injuries. With the new possibilities of imaging a lot of serious injuries and other than sports-related abnormalities are seen in the ankle and foot. Merely treating interesting MR or CT images has to be avoided. Therefore CT and/or MRI investigation is recommended on all patients after ankle sprain if a painful condition persists after conservative treatment. Only when a complete diagnosis is made, more appropriate treatment can be instituted.

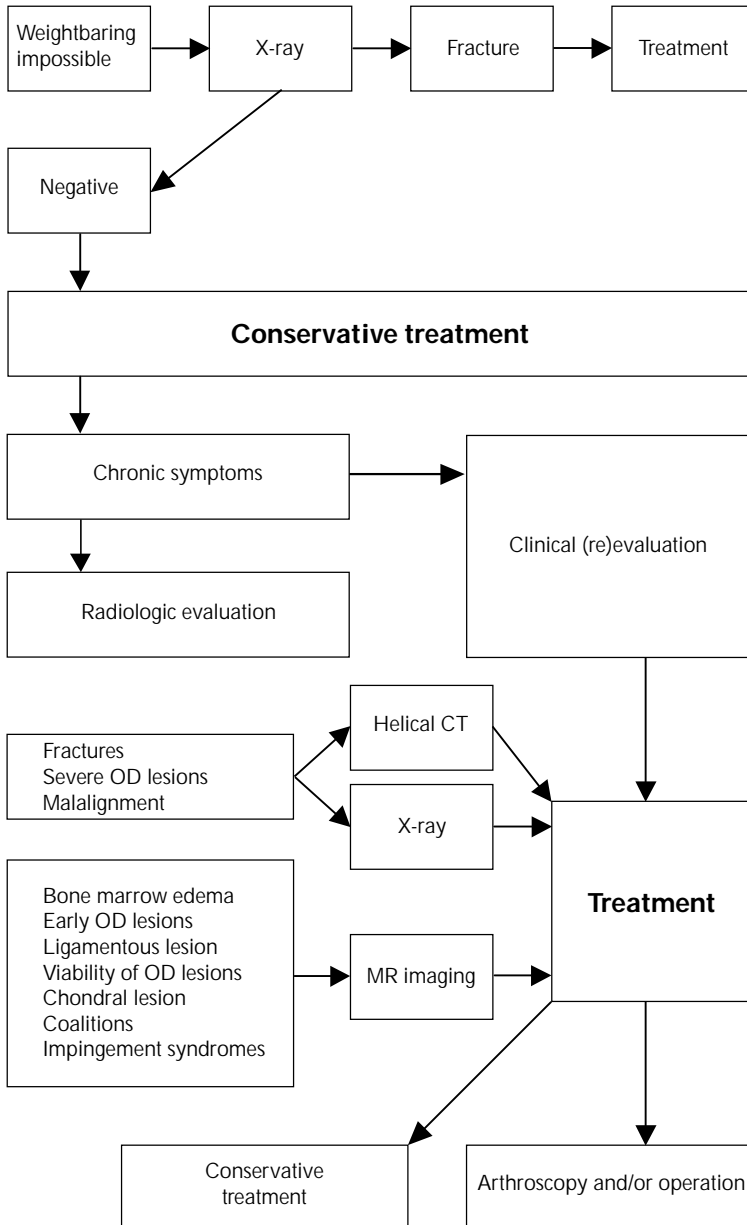
In this thesis it is shown that helical CT and MRI provide a third dimension by providing better anatomical details and even physiological data. As a lot of "new underlying abnormalities" with MR imaging and CT, both modalities are extremely helpful to examining acute and chronic ankle and hindfoot problems.

In conclusion, **helical CT** can play a role in specific bone pathology such as fractures and malalignment of foot and ankle. For diagnostic imaging of OD lesions stage three and four and loose bodies in the ankle joint helical CT is an excellent technique.

1. Subtalar instability is defined as chronic functional instability with increased values of subtalar tilt and talocalcaneal displacement. Subtalar tilt was demonstrated in all cases on conventional stress radiographs. With helical CT we found loss of congruency between talus and calcaneus and soft tissue motion in the hindfoot during inversion stress. However helical CT didn't show tilting in any of the patients except in the subluxated posteromedial part of the subtalar joint. So our data do not support prior reports that the Brodén view is useful as screening modality for instability of the subtalar joint.

MR imaging is indicated in situations in which initial plain films appear normal but the patient continues to experience pain or instability. Bone marrow pathology can be very accurately evaluated. Fatigue-type stress fractures resulting from repetitive overloading of normal bone marrow and cortex can be seen early, due to the accompanying bone marrow edema.

Recommendations for radiological evaluation of patients with sprained ankle syndrome



2. In the past, disability after an ankle sprain was mainly focussed on ligamentous injury. Early OD lesions described by Berndt and Harty could not be diagnosed with clinical examination, conventional radiography or CT. With MR imaging we found a relatively high number of this subchondral microfractures in the talar dome. Related with the spraining was the high number of patients with early OD lesions in the tibiofibular plafond (kissing lesions). The resolving time of these "new" lesions is unclear, as prospective studies are not yet available.
3. With MR imaging a hyperintensity patterns in the subchondral bone marrow was seen in 86% of the talocalcaneal coalitions. This abnormal bone marrow pattern related to stress (microfractures) or reactive changes secondary to degenerative articular diseases are easily depicted with MR imaging.
4. With dynamic contrast-enhanced MR the enhancement pattern of bone tissue and bone fragments can be assessed. So a statement about the viability of bone tissue can be made without invasive procedures.
5. Soft tissue impingement syndromes (anterolateral, anterior or posterior) as well as sinus tarsi syndrome are late sequelae in ankle sprains and not easily diagnosed by clinical examination. MR imaging can be used for accurate evaluation of these syndromes.

Summary and conclusions

Chapter one describes purpose and outline of this thesis.

In **Chapter two** an introduction is given of some clinical and functional aspects of ankle sprains. The ankle joint and the anterior and posterior subtalar joint are described. The embryological development of the hindfoot is represented. Talar and subtalar joint are outlined in relation to shape and movements of the articular surfaces. The ligamentous complex of the ankle and hindfoot is discussed. Four layers of the articular cartilage can be distinguished and the role of the osteochondral plate in relation to trauma is reviewed.

Chapter three mainly deals with the classification system of the osteochondral lesions, introduced by Berndt and Harty. A modified classification system of Berndt and Harty is given, based on computed tomography. Radiolucent (fibrous) defects, visible in 77%, are staged as type V. Not infrequently traumatic lesions can be seen on the opposite side of the joint, the tibia plafond. Healing of the OD depends on the viability of the injured

bone. The talar dome is feeded by a small end-arteries that have no collaterals, which increases the incidence of delayed or non-union and avascular necrosis in osteochondral defects. Lesions with viable bone are likely to heal spontaneously, whereas necrotic bone may collapse, leading to destruction of the joint. Treatment includes percutaneous drilling of the subchondral bone in an attempt to facilitate revascularization of the compromised tissues or excision of the unstable fragment.

In **Chapter four** an introduction is given of radiological modalities used after ankle sprain. Conventional radiography, tomography, stress radiography, and arthrography of the ankle and subtalar joint are discussed. Although these techniques have been used for years, they lack sufficient anatomic detail. Arthrography is no longer applied in acute sprains for evaluation of the ligaments. Ultrasound of the soft tissue structures of the foot is more commonly used. Bone scintigraphy is a common indication for foot and ankle pain of unknown cause. The introduction of spiral CT and MR imaging has had a major impact on musculoskeletal diagnostics. Subtle detection and more precise characterization of soft tissue and bony details are possible now. As the anatomy of ankle and hindfoot is quite complex with overlapping structures, the multiplanar imaging capability of MRI and helical CT are ideally suited. Protocols for helical CT and MR imaging are discussed.

In **Chapter five** the main objective of the study is to compare subtalar inversion stress views using the Brodén view with inversion stress views on helical CT. One of the drawbacks of conventional radiography is the imaging of three-dimensional structures in a two-dimensional plane. We investigated whether the use of helical CT would lead to a more objective and clear measurable method determining the amount of tilt in the subtalar joint. A variable amount of subtalar tilt (range 4° to 18°) was demonstrated in all cases on stress radiographs, without finding significant difference between the symptomatic and asymptomatic foot. However, contrary to the findings at the talocrural level, subtalar tilt was found in none of the patients using helical CT. It is concluded that the Brodén stress examination might not be useful for screening patients with subtalar instability.

In **Chapter six** we study prospectively subtalar inversion stress views with inversion stress views on helical CT in a group of 10 patients with unilateral instability of the subtalar joint. All patients were examined with inversion stress views on plain stress radiographs and helical CT. Subtalar tilt was demonstrated in all cases on conventional stress radiographs. Helical CT didn't show tilting in any of the patients except in the subluxated posteromedial part of the subtalar joint. Our data do not support prior reports that the Brodén view is useful for screening patients with subtalar instability.

In **Chapter seven** we review the MR imaging appearance of kissing contusions in the ankle joint after sprain. MR imaging was performed in 146 patients with the clinical diagnosis of acute or recurrent ankle sprain. The number and location of subchondral contusions or fractures revealed on MR imaging were recorded, and a comparison was made with the conventional radiographs obtained for each patient. Subchondral lesions in the talus and tibia plafond were relatively common after ankle trauma as they occurred in 18% of patients in our series. Kissing contusions were present in more than half of the lesions in these patients.

In **Chapter eight** we evaluate the application of fast MRI techniques after intravenous paramagnetic contrast material to assess vascularity and perfusion of the subchondral bone of the talus. The viability of osteochondritis dissecans lesions of the talar dome with dynamic gadolinium-enhanced MR imaging was compared with dynamic bone scintigraphy. In nine patients with OD lesions we found ischemia in two cases using dynamic MR imaging, while this was found in only one case with scintigraphy. In all likelihood the area of necrosis was not visualized with scintigraphy due to its relatively poor spatial resolution in comparison to MR imaging. Therefore, dynamic MR appears to be the preferred method for evaluating the viability of the OD lesion. An additional advantage of MR imaging is that the procedure is easily performed following conventional MR imaging and the patient is not exposed to ionizing radiation.

In **Chapter nine** we analyze MR images of 14 talocalcaneal coalitions. A coalition of the talocalcaneal joint is clinically important because it frequently causes symptoms such as pain and giving way "instability", starting when the coalition ossifies after a traumatic event or repetitive injury. In our series hyperintensity patterns on T2-weighted images, located in the subchondral bone adjacent to the coalition, were relatively common in the talocalcaneal coalition (present in 86% of the coalitions). Due to the rigidity of the joint, abnormal stress on the articular surfaces and the subchondral bone can result in microfractures, edema or reactive changes with marrow fibrosis, fibrovascular granulation tissue or early avascular necrosis, secondary to degenerative articular disease. The presence of a hyperintensity pattern in the subchondral bone adjacent to the coalition may be indicative of tarsal coalition.

In **Chapter ten** we present an overview of the MR imaging findings of common overuse injuries to the bones and soft-tissue structures such as ligaments, tendons and muscles of the foot and ankle. Sporting activities like running and aerobics have substantially increased in the recent years and have led to a rise in the number of sports-related injuries in the foot and ankle. MR imaging has become an important tool for evaluating the lower leg in order to provide the necessary information for patient management and rehabilitation.

Discussie en aanbevelingen

Acute klachten na een inversietrauma van de enkel, het "door de enkel gaan", is een frequent gebeuren. In 40% van de gevallen blijven restklachten aanwezig. Voor het adviseren van de behandelaar heeft de radioloog de keuzemogelijkheid uit verschillende diagnostische modaliteiten: conventioneel röntgenonderzoek, stress onderzoek, echografie, spiraal CT en MRI. Vandaag de dag is geen enkele methode duidelijk superieur boven de andere wat betreft enkel- en voetproblemen. De introductie van spiraal CT en kernspintomografie of "Magnetic Resonance Imaging" (MRI) met hun doorsnedentechnieken, hebben grote invloed gehad op de diagnostiek van de voet en enkel. Spiraal CT is vooral geïndiceerd bij benige afwijkingen zoals fracturen en/of losse fragmenten en heeft (in Nederland) het voordeel van een grotere beschikbaarheid in vergelijking met de MRI.

Met MRI is het zeer goed mogelijk een indruk te krijgen van de gevolgen van het inversietrauma voor het bandapparaat, het beenmerg en het subchondrale bot van de enkel. De oorzaak van de late introductie van kernspintomografie van voet en enkel is gelegen in de relatieve onbekendheid van afbeeldingen van voet- en enkelgewrichten met MRI en de uitgebreide technische knowhow nodig om MRI van de voet en enkel te interpreteren. Voor de radioloog betekent dit dat een gedetailleerde kennis van het normale beeld, essentieel voor het beoordelen en interpreteren van pathologie in dit gebied. Tevens dient hij goed op de hoogte te zijn van de klinische betekenis van een en ander. Voor de verwijzend arts is een zekere kennis nodig van de technische mogelijkheden van kernspintomografie tezamen met een meer gedetailleerde en meer specifieke vraagstelling omtrent de pathologie van voet en enkel. Ondanks de goede detail-waarneembaarheid van MRI is door de matige beschikbaarheid van de apparatuur het onderzoek vaak beperkt tot topatleten of patiënten met chronische enkelklachten. De kosten van het MR onderzoek zijn tegenwoordig geen belangrijke afweging meer. Echter gedegen klinisch en lichamelijk onderzoek gecombineerd met adequaat radiologisch work-up moet eerst plaatsvinden. Zonder deze doeltreffende informatie kan enkel- en voetpijn of instabiliteit leiden tot progressie en kan de aandoening chronisch worden.

De rol van radiologisch onderzoek bij enkelverzwikking

Enkelverzwikking is een klacht waarvoor vandaag de dag geen eenduidige therapie bestaat. In de eerste plaats berust de behandeling op conservatieve therapie omdat het natuurlijk verloop van een enkelverzwikking meestal onschuldig is, en bestaat de behandeling uit een expectatief of conservatief beleid. Bij persisteren van de klachten moeten

zowel een klinische als een radiologische work-up worden verricht. Dit is van belang voor de beslissing of meer invasief ingrijpen in de vorm van arthroscopie of operatief ingrijpen is geïndiceerd. In principe zal deze laatste beslissing met de grootst mogelijke reserve genomen moeten worden.

Wanneer hobbyisten of professionele sporters pijnklachten houden zal dit al gauw toegeschreven worden aan overbelasting. Hierdoor kan andere onderliggende pathologie gemaskeerd worden. Bij elke patiënt met pijn en/of instabiliteitklachten zal dit in overweging genomen moeten worden zonder een en ander direct aan een sportletsel te wijten. Daarbij mag niet vergeten worden dat de klinische symptomen niet voor alle letsels even typisch zijn. Met de nieuwe MRI en spiraal CT-mogelijkheden worden letsels, al dan niet aan de sport gerelateerd, gemakkelijker en beter gevisualiseerd. Hierbij dient opgemerkt te worden dat te allen tijde voorkomen moet worden dat er alleen mooie plaatjes worden behandeld. Concluderend, aanbevolen wordt om bij alle patiënten die klachten houden na conservatieve behandeling van enkelverzwikking, aanvullend CT en/of MR onderzoek te verrichten. Alleen met een juiste en complete diagnose kan adequate therapie worden ingezet.

Spiraal CT wordt geadviseerd bij specifieke botproblematiek zoals fracturen en standaardafwijkingen. Het enkelgewricht is een horizontaal georiënteerde structuur, die moeilijk met een conventionele CT drie-dimensionaal te onderzoeken is. Stress onderzoek van de voeten kan makkelijk worden uitgevoerd met spiraal CT, waarbij drie-dimensionale afbeeldingen worden verkregen voor adequate evaluatie het bovenste en onderste spronggewricht, zoals behandeld in dit proefschrift. Voor het beoordelen van type III en IV OD laesies (en losse fragmenten) in het enkelgewricht is spiraal CT een goede techniek.

MRI is vooral geïndiceerd in situaties waarbij het conventionele röntgenonderzoek geen afwijkingen laten zien, maar de patient toch pijnklachten en instabiliteit ervaart. Beenmerg- pathologie is goed te evalueren. Vermoeidheidsfracturen als gevolg van overbelasting kunnen in een vroeg stadium worden opgespoord als gevolg van het zich ontwikkelende beenmergoedeem. OD laesies (stadium I en II) als gevolg van subchondrale fracturen zijn goed in kaart te brengen. De exacte betekenis van deze afwijkingen is nog niet uitgekristalliseerd aangezien nog geen grote prospectieve studies zijn verricht. Weke delen inklemming (impingement) (anterolateraal, anterior en posterior), sinus tarsi syndroom, welke in een later stadium na de enkelverzwikking kunnen optreden kunnen allen middels MRI zichtbaar gemaakt worden.

Met dynamisch MRI onderzoek waarbij contrast i.v. wordt ingebracht kan een indruk worden verkregen over de doorbloeding van botweefsel en daardoor over de vitaliteit.

Samenvatting en conclusies

In **Hoofdstuk één** wordt het doel van dit proefschrift omschreven en in het kort de inhoud ervan.

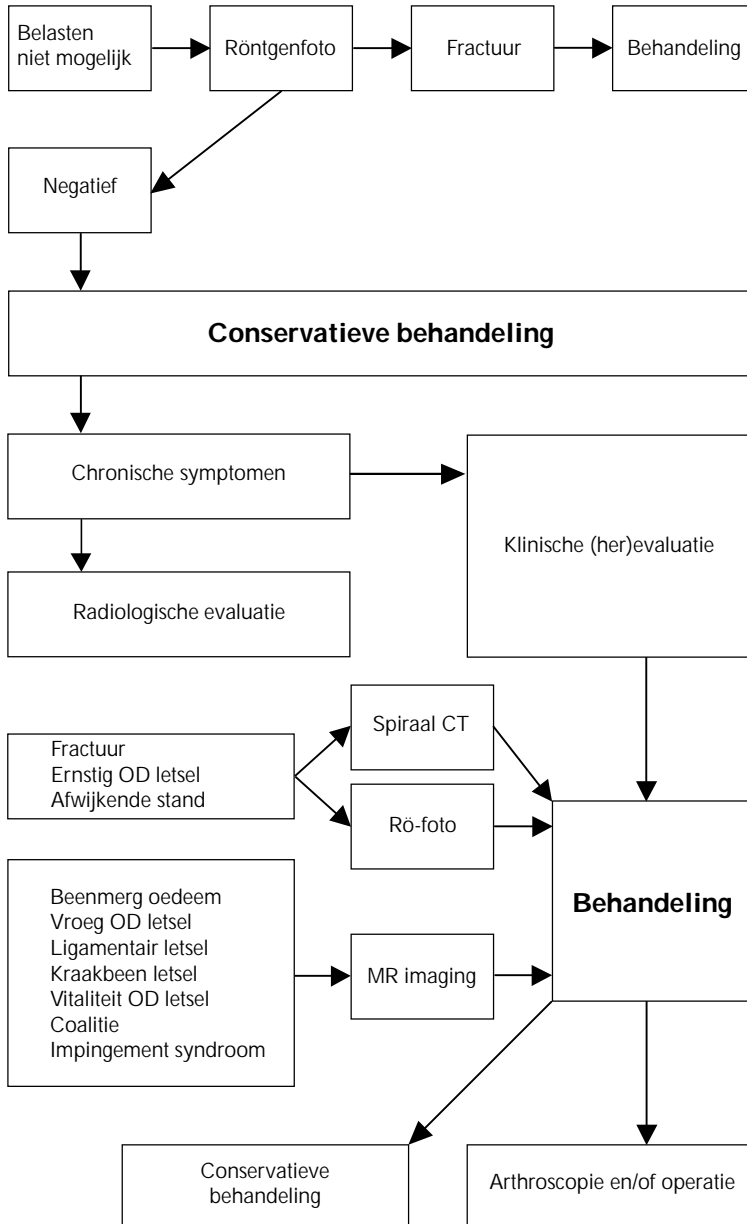
Hoofdstuk twee geeft een overzicht van de klinische symptomen, die optreden na enkelverzwikking. De embryonale ontwikkeling van de enkel en de relevante anatomie worden besproken. Het bovenste spronggewricht is opgebouwd uit een 'talusrol' met hier omheen een vork (de 'enkelvork' gevormd door tibiaplafond en fibula). Het onderste spronggewricht bestaat uit twee gewrichten: het voorste en achterste subtalaire gewricht. De functie van de laterale enkelbanden wordt besproken.

In **Hoofdstuk drie** worden verschillende indelingen van het osteochondrale letsel in het bovenste spronggewricht na verzwikking gepresenteerd. Over het algemeen worden vier stadia herkend, variërend van schade, beperkt tot het kraakbeen, fractureren van bot en kraakbeen tot necrose van bot. Deze necrotische botstukjes kunnen losliggen in het enkelgewricht en geven dan samen met defecten in het gewrichtsoppervlak soms arthrose. De talus is voor ca. 60% bekleed met kraakbeen. Hierdoor zijn er weinig entreeplaatsen voor bloedvaten. Na fracturering kan de bloedvoorziening tekort schieten waardoor het bot sterft. De therapie bestaat uit het opboren en behandelen van het osteochondraal defect of het verwijderen van dode losliggende stukjes uit het enkelgewricht.

In **Hoofdstuk vier** worden de gangbare radiologische onderzoeksmethoden besproken, beginnend met de conventionele enkelfoto voor het uitsluiten van fractures. Vervolgens kan stress-onderzoek van het bovenste en onderste gewricht worden uitgevoerd voor het testen van het bandapparaat. Arthrografie (inspuiten van het gewricht met contrastvloeistof) of echografie, onderzoek met ultrageluid, voor het beoordelen van bandlaesies, worden niet veel meer toegepast. Bij osteochondraal defecten kan een botscan worden vervaardigd ter bepaling van verhoogde activiteit ter plaatse van de laesie. CT en MRI-technieken worden vervolgens uitvoerig besproken.

Hoofdstuk vijf geeft de resultaten van een studie over de CT doorsnede van het onderste en bovenste spronggewricht gedurende inversiestress. Bij 15 proefpersonen met een afwijkende instabiele enkel werd getracht verschillen in kantelingshoek te vinden, waarbij de gezonde enkel ter vergelijking werd gebruikt. Met spiraal CT kon bij geen van de voeten een kanteling in het subtalaire gewricht worden verkregen, alleen het posterolaterale gedeelte van het subtalaire gewricht liet een kantelingshoek zien. Een betrouwbare parameter voor subtalaire instabiliteit lijkt de Brodén view dan ook niet te geven aangezien de niet afwijkende voet als vergelijk geen wezenlijk andere resultaten oplevert.

Radiologisch beleid en aanbevelingen van het inversieletsel van de enkel



In **Hoofdstuk zes** worden de resultaten van een stress-onderzoek van het onderste spronggewricht beschreven, verricht met conventioneel röntgenonderzoek en spiraal CT bij 10 patiënten. Met conventioneel stress-onderzoek werd in alle gevallen kanteling in het onderste spronggewricht gezien. Chronische inversieklachten en instabiliteit zijn zowel klinisch als radiologisch een moeilijk probleem. Het aantal publikaties over het bovenste spronggewricht is aanzienlijk groter dan over het onderste spronggewricht en dit gebied is wat betreft het instabiliteitsvraagstuk minder belicht. De exacte bewegingsvorm bij inversie van het onderste spronggewricht is door de sterk gekromde oppervlakken van dit gewricht radiologisch lastig te onderzoeken. Met de Brodén view is de mate van kanteling in het onderste spronggewricht een maat voor bandoverrekking of bandruptuur. Door middel van stress-onderzoek volgens Brodén werd conventionele röntgendiagnostiek met CT vergeleken. CT is zeer geschikt voor doorsnedetechnieken en kan hierdoor het onderste spronggewricht beter à vue brengen. Met dit onderzoek is aangetoond dat er geen evidente kanteling optreedt bij stress-onderzoek van het onderste spronggewricht. De kantelingshoeken, die wel gevonden werden met conventioneel röntgen stress-onderzoek zijn voornamelijk te verklaren door de moeilijke afbeeldingsvorm van het onderste spronggewricht met deze techniek.

Hoofdstuk zeven geeft het aantal gevallen van osteochondraal letsel weer die aan weerszijden van het enkelgewricht kunnen voorkomen na inversietrauma. Het MRI onderzoek is verricht bij 146 patiënten met éénmalige of recidiverende enkelverzwikkingen. Aantal en plaats van deze microfracturen werden vastgelegd en vergeleken met conventionele röntgenopnamen. Deze contusies komen op grote schaal voor na een inversietrauma, in onze serie in 18% van de gevallen. 'Kussende contusies' ("kissing" contusies, aan beide zijden van het gewricht) werden gezien in ruim de helft van deze 18%.

In **Hoofdstuk acht** wordt door vergelijking tussen dynamische botscentigrafie en dynamisch MRI onderzoek beoordeeld of het mogelijk is een uitspraak te doen over de doorbloeding van het osteochondraal defect in de talus. Met behulp van snelle MRI technieken en het intraveneus inbrengen van contrast (gadolinium) wordt getracht een indruk te krijgen van de doorbloeding van het OD letsel. Bij 9 patiënten werd er een verschil tussen de dynamische botscentigrafie en dynamisch MRI onderzoek vastgesteld. Met botscentigrafie is het door het lager oplossend vermogen het niet altijd mogelijk verminderde doorbloeding c.q. necrose waar te nemen. Hierdoor is dynamisch MRI onderzoek te prefereren boven dynamische botscentigrafie. Een bijkomend voordeel is dat het aansluitend op het conventionele MR onderzoek gedaan kan worden.

Hoofdstuk negen beschrijft de aangeboren afwijkingen in de vorm van fusie (coalitie) gevormd door vergroeiing van talus en calcaneus bij 14 patiënten. Deze coalitie beperkt de bewegingsmogelijkheden in het onderste spronggewricht en geeft pijnklachten en instabiliteit. Opvallend was hierbij het voorkomen van verhoogde signaal-intensiteit (oedeem, fibrose, en of arthrose) bij 86% van de patiënten op de T2 gewogen opname in het gebied rondom de coalitie. Door de sterk beperkte beweging in het onderste spronggewricht als gevolg van de coalitie, werd in een groot aantal gevallen oedeem en/of versterkte arthrose gezien. Dit verhoogde signaal in het onderste spronggewricht is een goede aanwijzing voor de mogelijke coalitie in het gewricht.

In **Hoofdstuk tien** wordt een overzicht gegeven van veel voorkomende overbelastingsbeelden met beschadiging van bot, pezen, kapsel, zenuwen en banden rondom het enkelgewricht. Sporten als hardlopen en aerobics zijn erg populair en hebben het aantal overbelastingsletsels in voet en enkel doen toenemen. MRI onderzoek is zeer belangrijk voor het diagnostiseren van deze afwijkingen en het bepalen van de juiste therapie.

Dankwoord

Achter de coulissen zijn een aantal mensen geweest die op een bijzondere manier een bijdrage hebben geleverd aan dit promotieonderzoek. Helaas kan ik deze niet allemaal voor het voetlicht brengen. Wel wil ik een aantal in het bijzonder bedanken.

Als eerste mijn co-promotor Dr. A.P.G. van Gils. Beste Ad het is een zeer groot genoegen geweest met je te werken. Vooral door je kennis, enthousiasme, toewijding en begeleiding is er uiteindelijk een promotie uit voortgekomen.

Hooggeachte promotor Prof. Dr. P.F.G.M. van Waes, beste Paul, je hebt me veel vrijheid gegeven om dit onderzoek uit te voeren. Het zijn soms hectische tijden geweest.

Via deze weg wil ik ook de radiologische staf in het AZU voor zijn inzet bedanken en mijn waardering uitspreken voor de vele mogelijkheden die mij gegeven zijn, mijn aanstelling en de uitstekende faciliteiten die door de afdeling radiologie geboden zijn voor het uitvoeren van wetenschappelijk onderzoek. Het was een groot voorrecht om als perifeer werkend radioloog ook nog in het AZU te werken en te promoveren.

Mijn zeergeleerde opleider, Dr. J.O. Op den Orth, in het St Elisabeth's of Groote Gasthuis te Haarlem. Van u heb ik niet alleen het vak geleerd maar vooral de bezieling voor de radiologie. Met name het feit dat artikelen schrijven en promoveren zeer veel inzet en grote inspanning vergt.

Hooggeleerde Prof. E.E. de Lange, beste Eddie, jouw hulp bij het structureren en bijschaven van de manuscripten bleek onontbeerlijk. Ik heb veel van je geleerd.

Van de leden van de beoordelingscommissie: Prof. Dr. P.M.T. Pattynama en Prof. Dr. M.A.M. Feldberg, beste Peter en Michiel, als radiologen in de commissie zijn jullie zeer waardevol voor me geweest. Hartelijk dank voor het beoordelen van dit proefschrift.

Van mijn klinische vrienden waar je als radioloog niet buiten kunt wil ik met name bedanken, Frank van Hellemond, (gezamenlijk zijn er heel wat militaire enkels gescand), Jan-Willem Louwerens, Henk Stevens en Ad Oostdijk,

Eric Tetteroo voor het in de avonduren lay-outen van het proefschrift. Ik ben onder de indruk van je inzet. Vooral op het laatst was deze steun zeer waardevol.

Verder nog hartelijke dank de medewerkers van de audiovisuele dienst Jan, Karin en Eugène voor de hulp bij de ontstellende hoeveelheid 'plaatjes'.

De bibliothecaresses in het Sophia ziekenhuis, Joke en Jolanda, dank voor het nimmer falende enthousiasme bij het opzoeken van alle literatuur.

Verder een ieder die de promovendus op de been gehouden heeft met name in het laatste te drukke jaar.

Curriculum Vitae

De auteur van dit proefschrift werd geboren op 15 april 1960 te Groningen. In 1979 behaalde zij het eindexamen Atheum-B aan de Rijksscholengemeenschap H. van der Vlist te Utrecht. In dat jaar begon zij met de studie geneeskunde aan de Rijksuniversiteit te Utrecht. Het artsexamen werd in 1986 behaald en in datzelfde jaar startte zij met de opleiding radiologie in het St Elisabeth's of Groote Gasthuis te Haarlem (opleider: Dr. J.O. Op den Orth). In 1991 volgde de inschrijving als radioloog en in hetzelfde jaar was zij hoofd van de afdeling radiologie in het Kamuzo Banda hospitaal in Lilongwe (Malawi). Vervolgens heeft zij van 1992 tot 1995 in het Academisch Ziekenhuis Utrecht gewerkt als fellow en in 1995 in het Refaja ziekenhuis te Dordrecht. Sinds 1996 is zij verbonden aan de Isala Klinieken (locatie Sophia) te Zwolle.

